LANGLEY GRANT
IN-71-CR
150136

Duke University
School of Engineering
DURHAM, NORTH CAROLINA 27706

DEPARTMENT OF MECHANICAL ENGINEERING
AND MATERIALS SCIENCE

TELEPHONE (919) 684-2832

P-110

July 28, 1988

Dr. Kevin Sheperd
Structural Acoustics Branch
Mail Stop 463
NASA
Langley Research Center
Hampton, VA 23665-5225

Dear Kevin:

Enclosed please find five copies of the Progress Report for NASA Research Grant NAG-1-709 -- Asymptotic Modal Analysis and Statistical Energy Analysis. Linda Peretti and I are enthusiastic about the results we have obtained and these are described in the Report.

With very best regards,

Sincerely,

Earl

Earl H. Dowell
J. A. Jones Professor and
Dean, School of Engineering

EHD:lh

Enclosures

cc: John F. Royal
University Grants Officer
Mail Stop 126
NASA
Langley Research Center
Hampton, VA 23665-5225
(1 copy with enclosure)

NASA Scientific and Technical
Information Facility
P. O. Box 8757
Baltimore and Washington
International Airport, MD
21240
(2 copies with enclosures)

(NASA-CR-183077) ASYMPTOTIC MODAL ANALYSIS AND STATISTICAL ENERGY ANALYSIS Progress Report, 15 Oct. 1987 - 14 Apr. 1988 (Duke Univ.) 110 p CSCL 20A
N88-29514
Unclas
G3/71 0150136

PROGRESS REPORT
FIVE COPIES REQUIRED

1. NASA Research Grant NAG-1-709

2. PERIOD COVERED BY REPORT: 15 October 1987 - 14 April 1988

3. TITLE OF GRANT: Asymptotic Modal Analysis and Statistical Energy Analysis

4. NAME OF INSTITUTION: Duke University

5. AUTHORS OF REPORT: Earl H. Dowell

6. LIST OF MANUSCRIPTS SUBMITTED OR PUBLISHED UNDER NASA SPONSORSHIP DURING THIS REPORTING PERIOD, INCLUDING JOURNAL REFERENCES:

   See attached

7. SCIENTIFIC PERSONNEL SUPPORTED BY THIS PROJECT AND DEGREES AWARDED DURING THIS REPORTING PERIOD:

   - Earl Dowell, Professor of Mechanical Engineering
   - Linda Peretti, Ph.D. student

Earl H. Dowell
Department of Mechanical Engineering
and Materials Science
Duke University
Durham, North Carolina 27706

## REFERENCES

1. Dowell, E. H., "Vibration Induced Noise in Aircraft: Asymptotic Modal Analysis and Statistical Energy Analysis of Dynamical Systems," R82-112447, United Technologies Research Center, January 1983.

2. Dowell, E. H., and Kubota, Y., "Asymptotic Modal Analysis and Statistical Energy Analysis of Dynamical Systems," ASME Journal of Applied Mechanics, Vol. 107, 1985, pp. 949-957.

3. Kubota, Y. and Dowell, E. H., "Experimental Investigation of Asymptotic Modal Analysis for a Rectangular Plate," Journal of Sound and Vibration, Vol. 106, No. 2, 1986, pp. 203-216.

4. Kubota, Y., Dionne, H. D., and Dowell, E. H., "Asymptotic Modal Analysis and Statistical Energy Analysis of an Acoustic Cavity," ASME Winter Annual Meeting, Boston, MA., December, 1987. Accepted for publication in the Journal of Vibration, Acoustics, Stress and Reliability in Design.

5. Peretti, L., "Asymptotic Modal Analysis of a Rectangular Acoustic Cavity", MSE Thesis, Duke University, 1988.

# ASYMPTOTIC MODAL ANALYSIS OF A RECTANGULAR ACOUSTIC CAVITY

by

Linda Franzoni Peretti

Department of Mechanical Engineering and Materials Science

Duke University

Date: 13 June 1988

Approved:

Earl Dowell

Dean Earl H. Dowell, Supervisor

Donald B. Bliss

Dr. Donald B. Bliss

E J Shaughnessy

Dr. Edward J. Shaughnessy

Senol Utku

Dr. Senol Utku

Thesis submitted in partial fullfillment of the requirements for the degree of Master of Science in the Department of Mechanical Engineering and Materials Science in the Graduate School of Duke University

1988

# ACKNOWLEDGEMENT

I would like to thank my advisor, Earl Dowell, for his support and encouragement. It is a rare person, who can be the Dean of an Engineering School and still manage to be a terrific advisor to his graduate students. He has been an inspiration to me, as well as a source of encouragement. I would also like to thank Professor Don Bliss, who taught the most interesting and the most relevant (to this thesis) class that I have ever taken - acoustics. Prof. Bliss is a gifted teacher and talented researcher, and I would also like to thank him for his constructive criticisms and instructive ideas, which were incorporated into this research in one way or another.

This work would not have been possible without the financial support of Langley Research Center. In particular, I would like to thank Kevin Sheppard and Andy Powell for believing in this project enough to recommend funding for it.

My parents have encouraged me, both, as examples and in more direct ways. I would like to thank them for their support (all kinds!), and mention that, from as far back as I can remember, my mother was always saying *"To whom much is given - much is expected!"* And she expected, expects, and will always expect ALOT! Thanks, Mom, I hope I can live up to your expectations.

Finally, but most importantly, I would like to thank my own family: my husband, Steve, for the endless hours of his time, which he has given selflessly, for his witty humor, which has saved me from insanity many times, and for believing in me - even when I didn't; and my children, Chris, Kate, Marc, and John, for their sacrifices (known & unknown), their encouragement, and when all else fails, their prayers.

## BRIEF OUTLINE OF RESEARCH FINDINGS

In relevant work accomplished prior to the NASA Grant and reported in Ref. 1-3, the results commonly referred to as Statistical Energy Analysis (SEA) have been rederived and generalized by considering the asymptotic limit of Classical Modal Analysis.. This approach is called Asymptotic Modal Analysis (AMA). The general approach is described in Ref. 1 for both structural and acoustic systems. The theoretical foundation is presented in Ref. 2 for structural systems and experimental verification is presented in Ref. 3 for a structural plate responding to a random force.

Work accomplished subsequent to the grant initiation has focussed on the acoustic response of an interior cavity (e.g. an aircraft or spacecraft fuselage) with a portion of the wall vibrating in a large number of structural modes. Ref. 4 describes our first results and has been presented at the ASME Winter Annual Meeting in December, 1987, and accepted for publication in the Journal of Vibration, Acoustics, Stress and Reliability in Design. Much of our work to date is summarized in Ref. 5. A copy of Ref. 5 is enclosed. A journal article based upon Ref. 5 is in preparation.

In Ref. 4 and 5 it is shown that asymptotically as the number of acoustic modes excited becomes large, the pressure level in the cavity becomes uniform except at the cavity boundaries. However the mean square pressure at the cavity corner, edge, and wall is, respectively, eight, four and two times the value in the cavity interior. Also it is shown that when the portion of the wall which is vibrating is near a cavity corner or edge, the response is significantly higher than when the portion of the wall which is vibrating is placed elsewhere.

One of the interesting issues is the distance over which the pressure level decays from a corner, edge or wall to the cavity interior. A preliminary analysis is given in Ref. 5. Further work is in progress.

TABLE OF CONTENTS

TABLE OF CONTENTS (CONT.)

LIST OF FIGURES

LIST OF FIGURES (CONT.)

LIST OF FIGURES (CONT.)

LIST OF FIGURES (CONT.)

## LIST OF SYMBOLS

| | |
|---|---|
| A | area |
| c | speed of sound |
| F | cavity acoustic modal function |
| H | acoustic modal transfer function |
| L | cavity dimension |
| M | generalized mass |
| $\Delta M$ | number of acoustic modes |
| $\Delta N$ | number of structural modes |
| p | pressure |
| Q | generalized force or acceleration |
| r | modal index |
| V | volume |
| w | displacement |
| x | spatial position coordinate |
| y | spatial position coordinate |
| z | spatial position coordinate |
| X | acoustic modal function component dependent on x |
| Y | acoustic modal function component dependent on y |
| Z | acoustic modal function component dependent on z |
| $\omega$ | frequency |

## LIST OF SYMBOLS (CONT.)

$\Phi$ power spectra

$\rho$ density

$\zeta$ damping

<> spatially averaged quantity

• time derivitive

## SUBSCRIPTS

c center frequency

f flexible

m structural modal index

r acoustic modal index

w pertaining to the flexible wall

o reference value

## SUPERSCRIPTS

A acoustic

E external

W pertaining to the flexible wall

## Introduction

Coupled structural-acoustic systems are encountered frequently in everyday life. Anytime a structure is used to attenuate or otherwise modify sound levels to a significant degree, the structural and acoustic properties of the system are effectively coupled. An auditorium, classroom, concert hall, theater, or the interior of either an automobile or an aircraft are all examples of such systems. Accurate, efficient means to analyze structural-acoustic systems are central to the design of structures with the desired sound transmittal properties. Two methods commonly used to solve three-dimensional acoustic problems are classical modal analysis (CMA) and statistical energy analysis (SEA). Recently, Dowell and his colleagues [1,2,3,4] have developed an additional method, asymptotic modal analysis (AMA), which can also be applied to structural-acoustic systems.

Classical modal analysis is a rigorous method, which produces an exact result. However, it requires extensive computation, since CMA takes the contribution of each mode into account. When there are a large number of modes, as in most practical 3-dimensional acoustic problems, CMA requires an equally large number of calculations. It is not uncommon to have on the order of 100,000 acoustic modes in a room acoustics problem.

Conversely, SEA, does not take the individual modal contributions into account, leading to a significant reduction in calculations required relative to CMA. Instead, quantities such as modal density, average modal damping and average modal impedance to sound sources are required. This is the advantage of SEA. The disadvantage is that, as a statistical method, it produces statistical results. The answers obtained are in terms of averages or means and deviations. Therefore, SEA results do not contain any local information.

The advantages of both these methods are incorporated in the AMA method. Providing there are a large number of modes, the CMA and the AMA results are nearly identical. But the computation cost of AMA is significantly less, since it does not take the individual modal contributions into account. An added advantage of AMA is that the degree of generality in the final result can be controlled by adjusting the types of assumptions and/or simplifications made in the derivation. This allows the use of AMA to obtain results identical to SEA, or to relax the averaging simplifications and obtain local results, of which SEA is not capable.

To explore the capabilities of AMA, a numerical study was done to analyze the interior sound field of a rectangular acoustic cavity. The ratio of response predicted by classical modal analysis to that predicted by asymptotic modal analysis was calculated either as a spatial average or at particular locations inside the cavity. Five of the cavity walls were rigid and therefore, did not allow the transmission of sound. A random "white noise" sound field passed through a portion of the sixth wall into the interior of the cavity. The flexible vibrating portion was varied in size and location, the resulting sound pressure levels in the interior were calculated using AMA and CMA, and compared.

Local response peaks or "intensification zones" were observed at boundary points, while the response in the interior region was nearly uniform. Finally, the "transition zone" which exists between an "intensification zone" and the nearly uniform interior response was closely examined.

## Background

Statistical energy analysis (SEA) has been used to study the high frequency interaction of large, complex, multimodal structures and acoustic spaces. The basic assumption underlying SEA is that the dynamic parameters in the system behave stochastically. SEA relates the power of the applied forces to the energy of the coupled systems and produces a set of linear equations that can be solved for the energy in each system. The energy in the system is the variable of primary interest, and other variables such as displacement, pressure, etc., are found from the energy of vibration. SEA has its advantages, as well as its limitations. The main advantage of SEA is its ability to describe the sound field without having to consider the individual modes. Statistical energy analysis also allows for a much simpler description of the system, requiring only parameters such as modal density, average modal damping, and certain averages of modal impedance to sound sources. The most significant disadvantage of using a statistical approach is that it is only valid for systems whose order is sufficiently high that the stochastic assumptions apply. Certain frequency bandwidths may not contain enough modes to allow the underlying assumptions to hold, rendering the SEA result unreliable. In addition, the local response information is lost in the SEA treatment. The text by Lyon [5] is the standard reference on SEA.

Dowell [1] has shown that results identical to those calculated using SEA can be obtained by studying the asymptotic behavior of classical modal analysis (CMA) for a general, linear (structural) system; this asymptotic approach is called asymptotic modal analysis (AMA). AMA is basically a modal sum method. It possesses all of the advantages of SEA, in that the individual modal characteristics do not play a role in the asymptotic analysis. Additionally, AMA has advantages which SEA does not. Since AMA results can be derived systematically from CMA, AMA allows an assessment of the assumptions and consequent simplifications which are made to obtain such results. Also, by using a combination of CMA and AMA, results can be obtained for all frequency bandwidths of interest, not just those with a sufficiently high number of modes. And finally, AMA has predicted local response peaks, or "intensification zones," results unobtainable using SEA [3,4].

Previous work has shown that the asymptotic behavior of AMA depends upon the number of modes in a frequency interval of interest and the location of point forces. In the limit of an infinite number of modes, all points on the structure have the same response except for some special areas. The exceptional areas ("intensification zones") are near the points of excitation and near the structural system boundary [3,4]. Numerical examples were presented for a beam in Ref. [2]. Crandall and his colleagues [6,7,8] experimentally found "intensification zones" in their work with structures. The response of a rectangular plate under a point random force was investigated by Kubota and Dowell [3], and AMA calculations were found to agree closely with experimental measurements.

Work has also been done using AMA for structural-acoustic systems. Kubota, Dionne, and Dowell [4] examined a rectangular acoustic cavity with one vibrating wall (the other five rigid). They assumed the vibrating wall had an infinite number of structural modes responding, and that the entire wall was oscillating. The results obtained from the numerical study indicated that the spatially averaged CMA response approaches the AMA response as the number of modes increases. The local asymptotic response revealed an almost uniform distribution in the cavity interior, with peaks at the boundaries (sides, edges, and corners) of the cavity.

The emphasis of this research is on developing Asymptotic Modal Analysis for structural-acoustic systems. Here, only a portion of the wall vibrates rather than the entire wall, and the size and location of the oscillating portion is varied. Also, the acoustic "intensification zones" at the cavity boundaries and their transition to the cavity interior are examined utilizing AMA techniques, for the one-dimensional case.

## Theory

Most coupled structural acoustic problems are modeled using either classical modal analysis, summing for the response of each mode, or statistical energy analysis which combines the predicted energies of the subsystems and coupling loss factors to obtain a final result. In this work, a comparison is made between the CMA result and the AMA result as the number of acoustic modes and the number of structural modes approach infinity. Note, that the spatially averaged AMA result is identical to the SEA result.

### Classical Modal Analysis

In order to calculate the response of the interior acoustic cavity to the transmission of noise through a structural wall on its boundary, both the structural modes of the wall and the acoustic modes of the interior must be considered.

The equation of motion describing the structural modes of the vibrating wall is

$$M_m\left[\ddot{q}_m + 2\,\zeta_m\omega_m\dot{q}_m + \omega_m^{2} q_m\right] = Q_m^E$$

where the modal expansion for the wall deflection is

$$w = \sum_m q_m(t)\Psi_m(x,y)$$

the structural generalized mass is

$$M_m \equiv \iint_{A_1} m_p\Psi_m^{2}\,dx\,dy$$

and the generalized force due to a given external pressure is

$$Q_m^E \equiv \iint_{A_1} p^E\Psi_m\,dx\,dy$$

The equation describing the acoustic modes of the cavity is:

$$\ddot{P}_r + 2\zeta_r^A \omega_r^A \dot{P}_r + \left(\omega_r^A\right)^2 P_r = Q_r^W$$

where the modal expansion for the acoustic cavity pressure is

$$p = \rho_o c_o^2 \sum_r \frac{P_r(t) F_r(x,y,z)}{M_r^A}$$

the acoustic generalized mass is

$$M_r^A \equiv \frac{1}{V} \iiint_V F_r^2(x,y,z)\, dx\, dy\, dz$$

and the generalized acceleration due to the structural wall is

$$Q_r^W \equiv -\frac{1}{V} \iint_{A_f} \ddot{w}\, F_r\, dx\, dy$$

Kubota, Dionne and Dowell [Ref.4] have simplified these equations using the following assumptions:

1. The number of structural modes is large, which implies that the power spectra of the wall response is uncorrelated in space. This assumption effectively removes the modal dynamics of the structure from the problem.

2. The power spectrum of wall response is slowly varying with respect to frequency relative to the rapidly varying transfer function. Therefore, the power spectrum of the wall response is treated as a constant, independent of frequency. This is often referred to as the "white noise assumption."

The result of applying these assumptions to the system of modal equations is the Classical Modal Analysis (CMA) result, and is expressed in terms of the non-dimensionalized cavity pressure $(p/\rho_o c_o^2)$ as:

$$\frac{\bar{p}^2}{\left(\rho_o c_o^2\right)^2} \equiv \frac{\pi}{4}\frac{A_f}{V^2}\Phi_{\ddot{w}}(\omega_c)\sum_r \frac{F_r^2(x,y,z)}{\left(M_r^A\right)^2\left(\omega_r^A\right)^3\zeta_r^A}\iint_{A_f} F_r^2(x,y,z_o)\,dx\,dy \qquad (1)$$

The step-by-step derivation is done in Reference [4] and is reproduced for convenience in the appendix.

Asymptotic Modal Analysis

To obtain the Asymptotic Modal Analysis (AMA) result, further assume the acoustic generalized mass squared $(M_r^A)^2$, the frequency of the acoustic mode cubed $(\omega_r^A)^3$, and the acoustic damping $(\zeta_r^A)$, do not vary rapidly with respect to modal number r and can therefore be replaced by their values at the center frequency, $(M_c^A)^2$, $(\omega_c^A)^3$, and $(\zeta_c^A)$. Moreover, the expression $\Sigma F_r^2(x,y,z) \iint F_r^2(x,y,z_o)\,dx\,dy$ is approximately equal to the average of $F_r^2(x,y,z)$ times $\Sigma\iint F_r^2(x,y,z_o)dxdy$ as $r \to \infty$, (i.e. a large number of acoustic modes).

$\Sigma\iint F_r^2(x,y,z_o)\,dx\,dy$ can be further simplified by:

$$\sum_r \iint_{A_f} F_r^2(x,y,z_o)\,dx\,dy = \sum_r A_f \left\langle X_r^2\right\rangle_{A_f}\left\langle Y_r^2\right\rangle_{A_f}\left\langle Z_r^2(z_o)\right\rangle_{A_f}$$

which reduces to:

$$A_f\,\Delta N^A \frac{\left\langle F_c^2\right\rangle}{\left\langle Z_c^2\right\rangle}$$

where $<Z_c^2> = <F_c^2>/<F_c^2>_{Af}$. $<F_c^2>$ is a volume average, and $<F_c^2>_{Af}$ is an average over the vibrating structural wall area.

Then,

$$\frac{\bar{p}^2}{\left(\rho_o c_o^2\right)^2} \cong \frac{\pi}{4}\frac{A_f}{V^2}\Phi_{\ddot{w}}(\omega_c)\frac{A_f\,\Delta N^A\left\langle F_c^2\right\rangle}{\left(M_c^A\right)^2\left(\omega_c^A\right)^3\zeta_c^A\left\langle Z_c^2\right\rangle}\sum_r\frac{F_r^2(x,y,z)}{\Delta N^A} \tag{2}$$

This is the AMA representation, which is derived in the appendix, following the AMA techniques of Ref. [4].

Comparisons of CMA & AMA

In order to separate the effects of position inside the cavity from position of the flexible portion ($A_f$) of the wall, two ratios are needed.

The ratio of the spatial average of CMA to the spatial average of AMA is

$$\frac{\langle CMA\rangle}{\langle AMA\rangle} = \sum_r \frac{\left\langle F_r^2(x,y,z)\right\rangle}{\left(M_r^A\right)^2\left(\omega_r^A\right)^3}\frac{\iint_{A_f} F_r^2(x,y,z_o)\,dx\,dy\left(\omega_c^A\right)^3\left\langle Z_c^2\right\rangle}{\Delta N^A\;A_f} \tag{3}$$

This is derived in Ref. 4 and can be obtained from equations (1) and (2).

Equation (3) was used in the first half of the analysis, to assess the intensification due to area change and position of the vibrating portion of the wall. The spatially averaged <AMA> result which comprises the denominator assumes that the vibrating portion was located at positions other than in a corner or on an edge.

The separate effect of interior position was studied by taking the ratio of the local response of CMA to the spatially-averaged AMA:

$$\frac{CMA}{\langle AMA \rangle} = \sum_r \frac{F_r^2(x,y,z)}{\left(M_r^A\right)^2 \left(\omega_r^A\right)^3} \iint_{A_f} \frac{F_r^2(x,y,z_o)\, dx\, dy \left(\omega_c^A\right)^3 \left\langle Z_c^2 \right\rangle}{\Delta N^A\ A_f} \quad (4)$$

Equations (1) through (4) hold for any cavity geometry.

Rectangular Cavity

Dowell, et.al. [9] have shown that the acoustic modal function for a rectangular cavity with a flexible wall (all others rigid) can be described by the well-known rigid wall expansion or "hard box modes" for the structure:

$$F_r(x,y,z) = \cos\left(\frac{r_x \pi x}{L_x}\right) \cos\left(\frac{r_y \pi y}{L_y}\right) \cos\left(\frac{r_z \pi z}{L_z}\right)$$

In this analysis, the flexible portion of the structural wall is allowed to vary both in size and position. Therefore, the integral $\iint F_r{}^2(x,y,z_o)\, dx\, dy$ in equations (3) and (4) becomes:

$$\int_0^{a_w}\int_0^{b_w} \cos^2\left(\frac{r_x \pi (x_{w_o} + x_w)}{L_x}\right) \cos^2\left(\frac{r_y \pi (y_{w_o} + y_w)}{L_y}\right) \cos^2\left(\frac{r_z \pi z_o}{L_z}\right) dx_w\, dy_w$$

where $r_x$, $r_y$, and $r_z$ are modal indicies, and $x_{w_o}$, $y_{w_o}$, $x_w$, $y_w$, $L_x$, and $L_y$ are defined in figure 1. This integral can then be solved analytically in terms of the parameters $x_{w_o}$, $y_{w_o}$ and $a_w$, $b_w$.

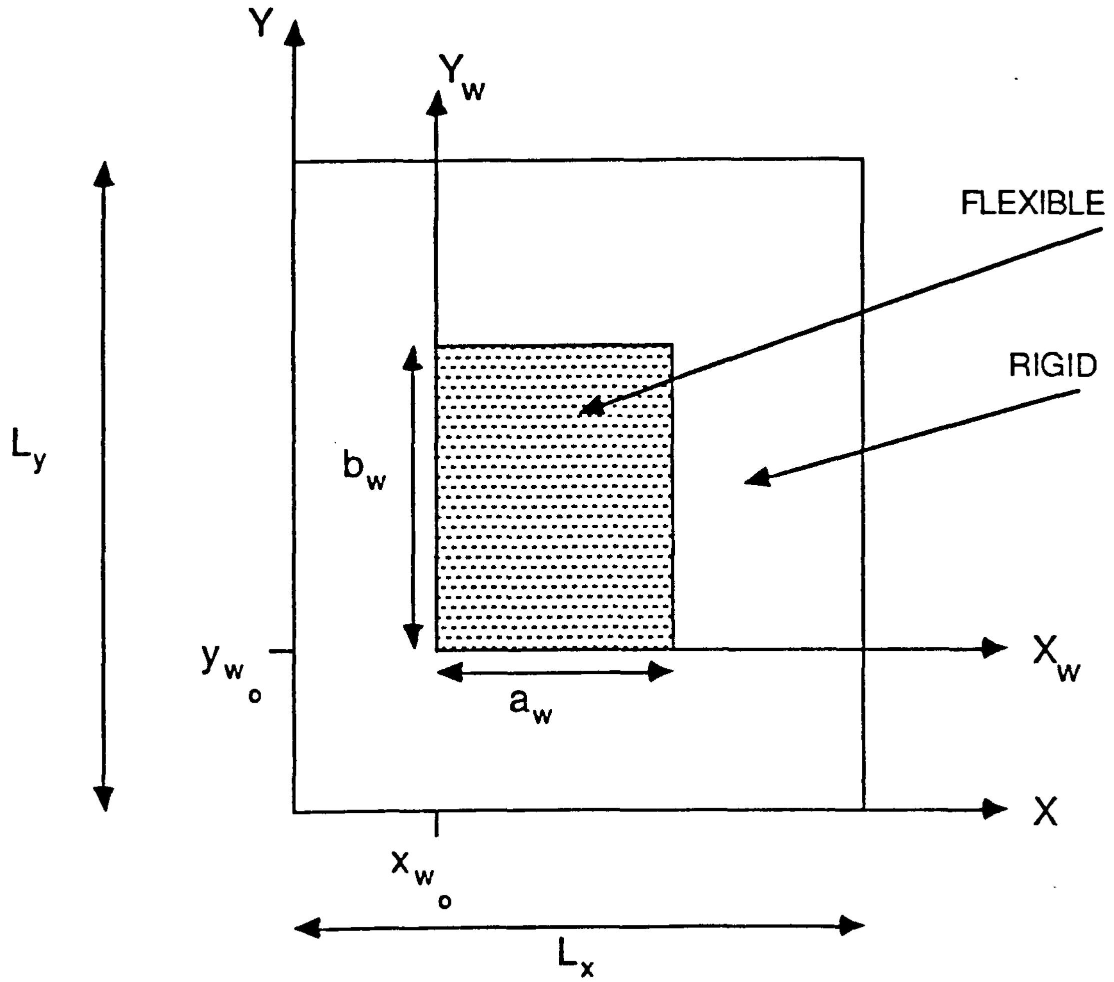


Figure 1. The flexible vibrating portion of one wall of cavity.

## Analysis

For the numerical study, a 2' X 3' X 7' rectangular acoustic cavity was considered (figure 2). One of the 2' X 3' walls, or a portion thereof, was assumed to vibrate in an infinite number of structural modes. The wall was driven with "white noise," which means all frequencies within a certain bandwidth were present and that the response was uniform with respect to frequency.

The effects of varying both the size and position of the vibrating portion of the wall were studied. The size of the flexible portion (plate) varied from full wall (100% wall area) down to a point (.004% wall area). Initially, two cases were evaluated, converging to a point in the center of the wall, and converging to a point in a corner of the wall (figure 3).

The quantities used in the study were the ratio of CMA to AMA as defined in the theoretical section. Initially, a spatial average of both CMA and AMA were taken in order to avoid introducing the location within the cavity as an additional parameter. Later, the local response of corner points, edge points, points on the face, and points in the interior were considered for the exceptional cases.

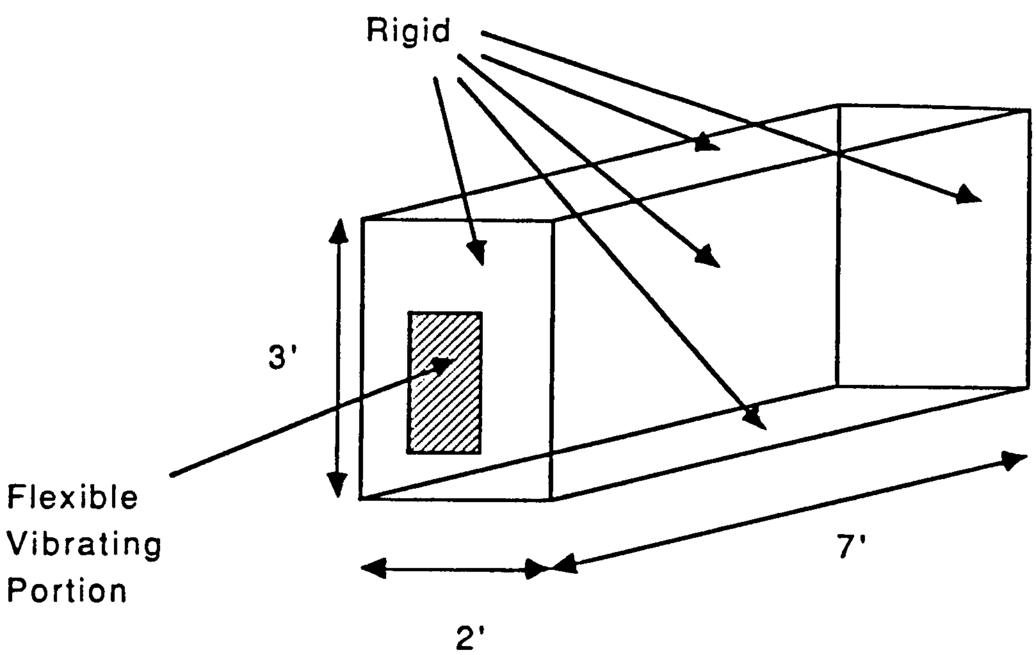


Figure 2. 2' X 3' X 7' Rectangular Acoustic Cavity with a portion of one wall flexible and vibrating.

- - - - - - - - - - - - - - - - - - - - - - - - - - - - - - - - - - - -

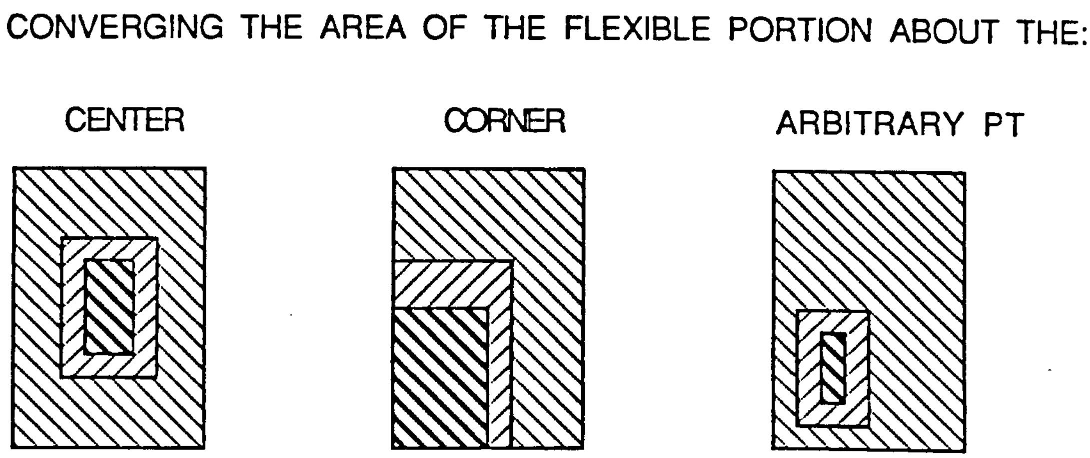


Figure 3: Flexible area on wall converges to a point at various locations on the wall.

## Results

Spatially Averaged Case:

The ratio of the spatial average of CMA to the spatial average of AMA (eqn. 3) for the case where the oscillating portion of the wall converges to a center point is shown in figures 4, 5, and 6. Each figure shows the spatially averaged CMA to spatially averaged AMA ratio for a different frequency bandwidth (200, 400, and 600 hz), as a function of center frequency. The bandwidth, $\Delta\omega$, is defined as, $\Delta\omega = \omega_{max} - \omega_{min}$, and the center frequency $\omega_c$, as $\omega_c = \sqrt{\omega_{max} * \omega_{min}}$ where $\omega_{max}$ and $\omega_{min}$ are the maximum and minimum frequencies of the frequency interval. All acoustic modes are assumed to have the same modal critical damping ratio, $\zeta$.

As can be seen from figures 4, 5, and 6, all results approach unity as the center frequency becomes large. The larger bandwidths yield smoother curves, and the smaller bandwidths approach the asymptote slightly more rapidly. These are expected results, and have already been discussed by Kubota in Ref. [9]. Kubota's work was done on a similar acoustic cavity, but with the entire wall oscillating. What was not expected was that departure from the entire wall oscillating, caused little change in the CMA/AMA ratio for the cavity. This may have been due to the fact that the oscillating "plate" was centered about the midpoint on the wall, and that all modes are symmetric or anti-symmetric about that point.

In figures 7, 8, and 9, the results of the spatially averaged CMA/AMA ratio (eqn. 3) for the oscillating plate of variable area and converging to a point in the corner are shown. Again, each plot corresponds to a different frequency bandwidth and the results are plotted as a function of center frequency. In this case, there are a family of curves which approach unity as center frequency (and therefore number of modes) increases, as expected. However, the asymptote is approached from above rather than below, for all plates smaller than the quarter wall. The quarter wall case is equivalent, in terms of the CMA/AMA ratio, to the full wall due to symmetry. The cases where the plate is larger than a quarter panel approach from below as did the center point cases. For those cases in which the vibrating wall is smaller than a quarter panel, not only does the curve approach the asymptote from above, but, as the oscillating portion of the wall better approximates a point, the peak of the curve approaches 4, and is slower to drop off to the asymptotic limit of 1. This region of elevated sound pressure level is similar to the "intensification" zones discussed in Crandall [6,7,8] and in Kubota, et al. [4]. However, the intensification is due to excitation location rather than response location.

In addition to these two extremes, the vibrating portion of the wall was centered around an intermediate point and varied in size. The results of the CMA/AMA ratio are shown in Figures 10, 11, and 12. Again, this is a spatial average of the response, which was calculated for three frequency bandwidths, and is plotted as a function of center frequency. This case illustrates that the limit can also be reached in an oscillatory manner, rather than strictly from above or below.

In addition to studying the effects of varying size and position of the oscillating portion of the wall in a spatially averaged sense, the local response was also calculated.

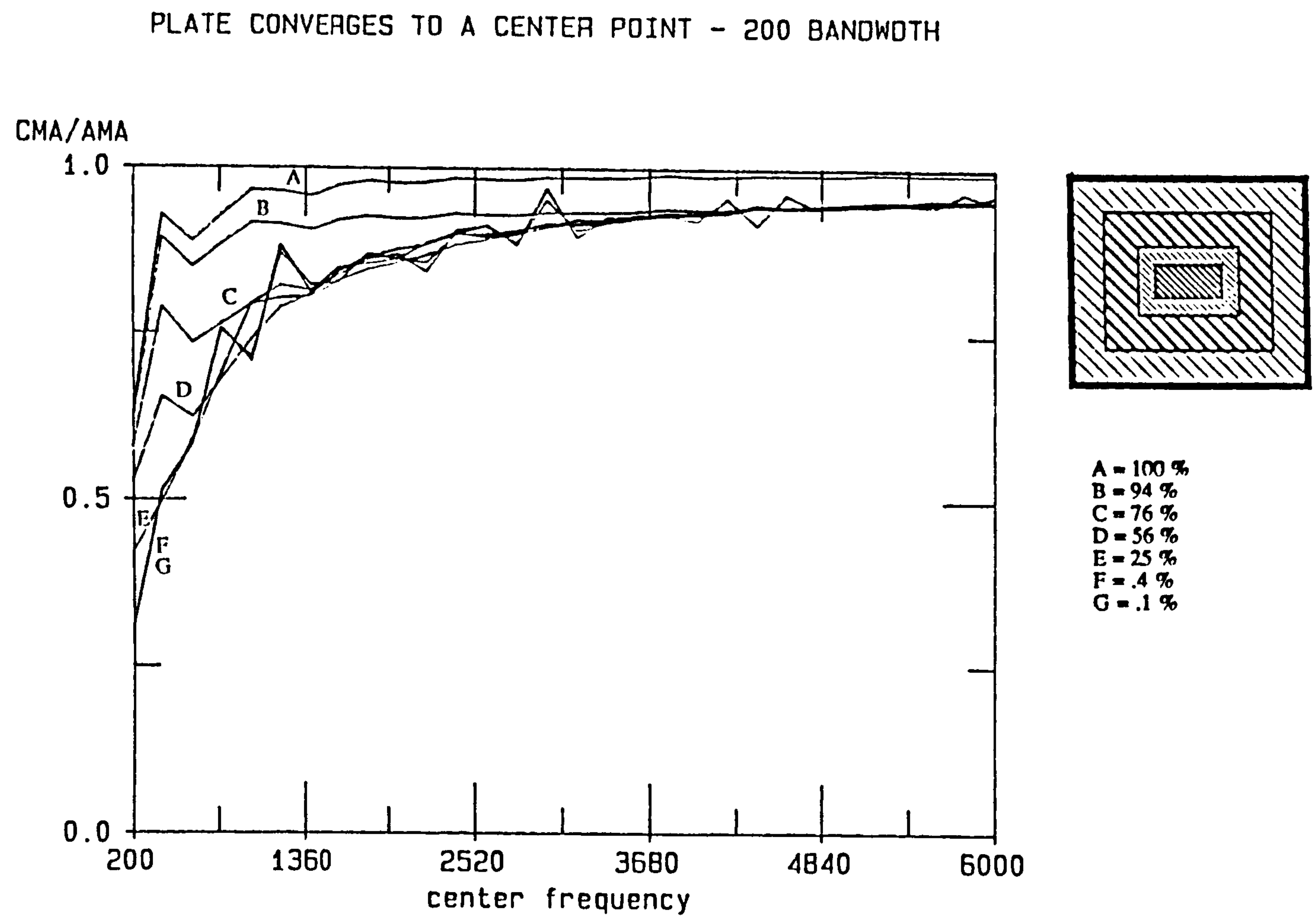


Figure 4. spatially averaged CMA to spatially averaged AMA ratio versus center frequency, with a fixed bandwidth of 200 hz, for the flexible area converging to a point in the center of the wall.

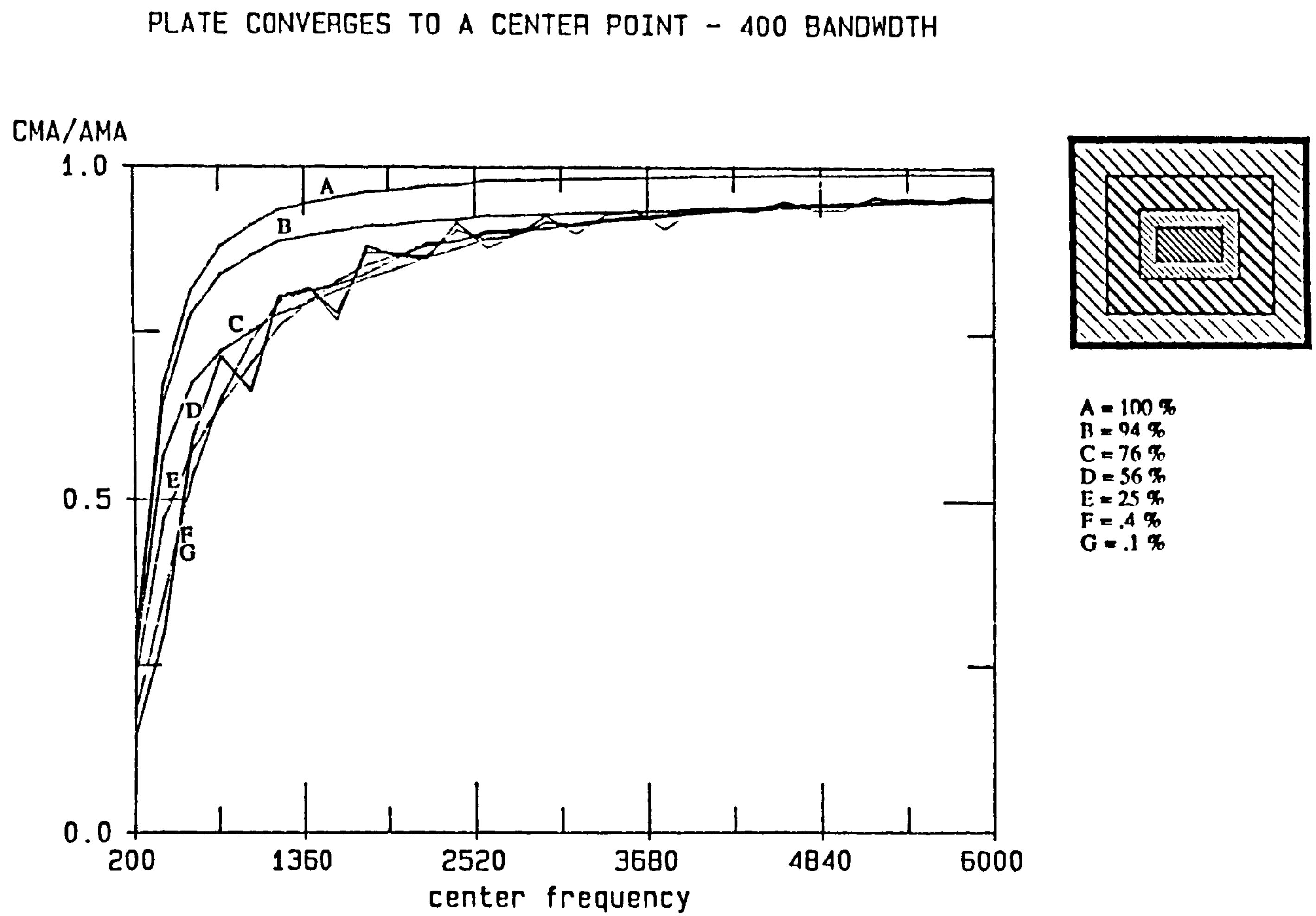


Figure 5. spatially averaged CMA to spatially averaged AMA ratio versus center frequency, with a fixed bandwidth of 400 hz, for the flexible area converging to a point in the center of the wall.

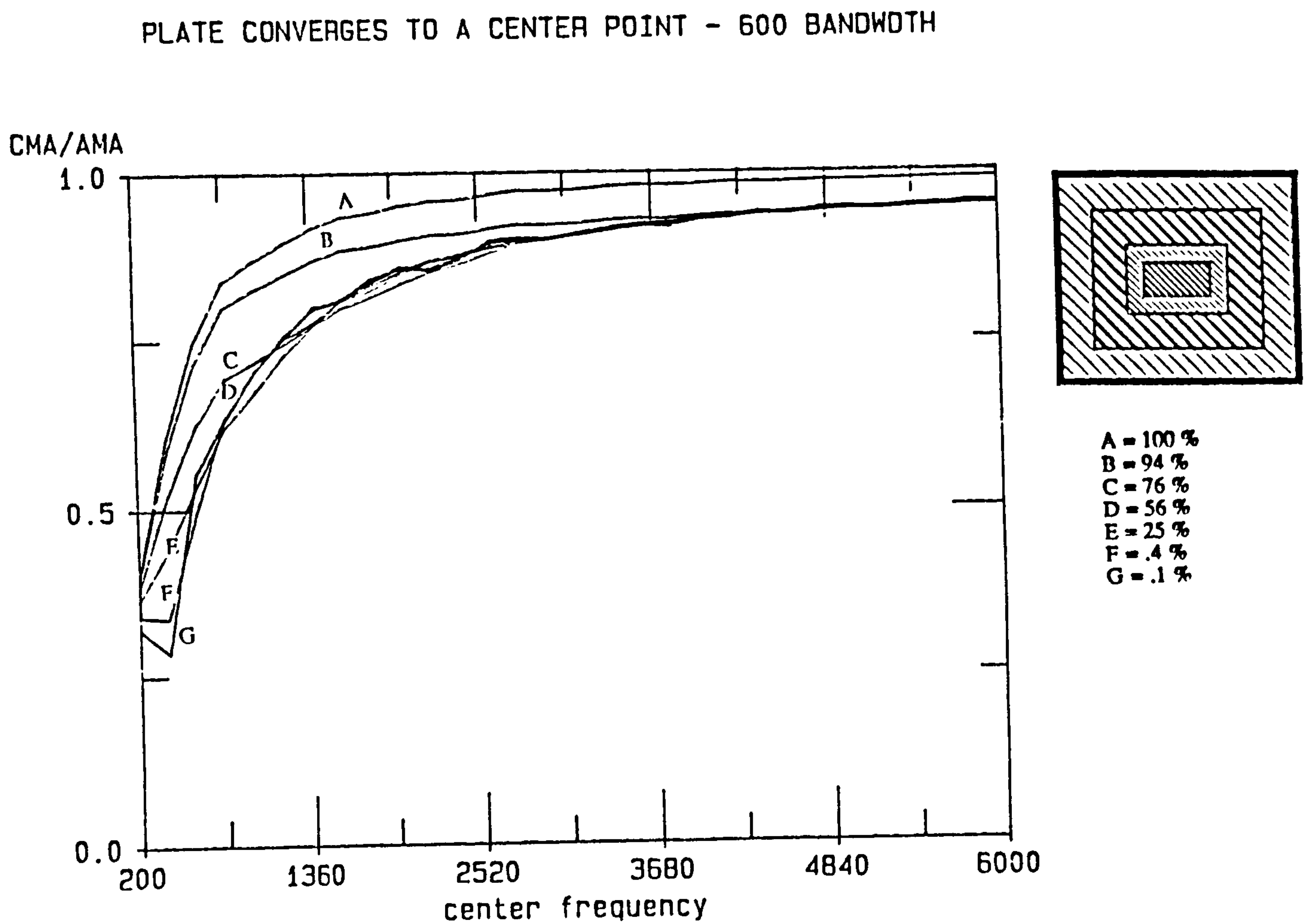


Figure 6. spatially averaged CMA to spatially averaged AMA ratio versus center frequency, with a fixed bandwidth of 600 hz, for the flexible area converging to a point in the center of the wall.

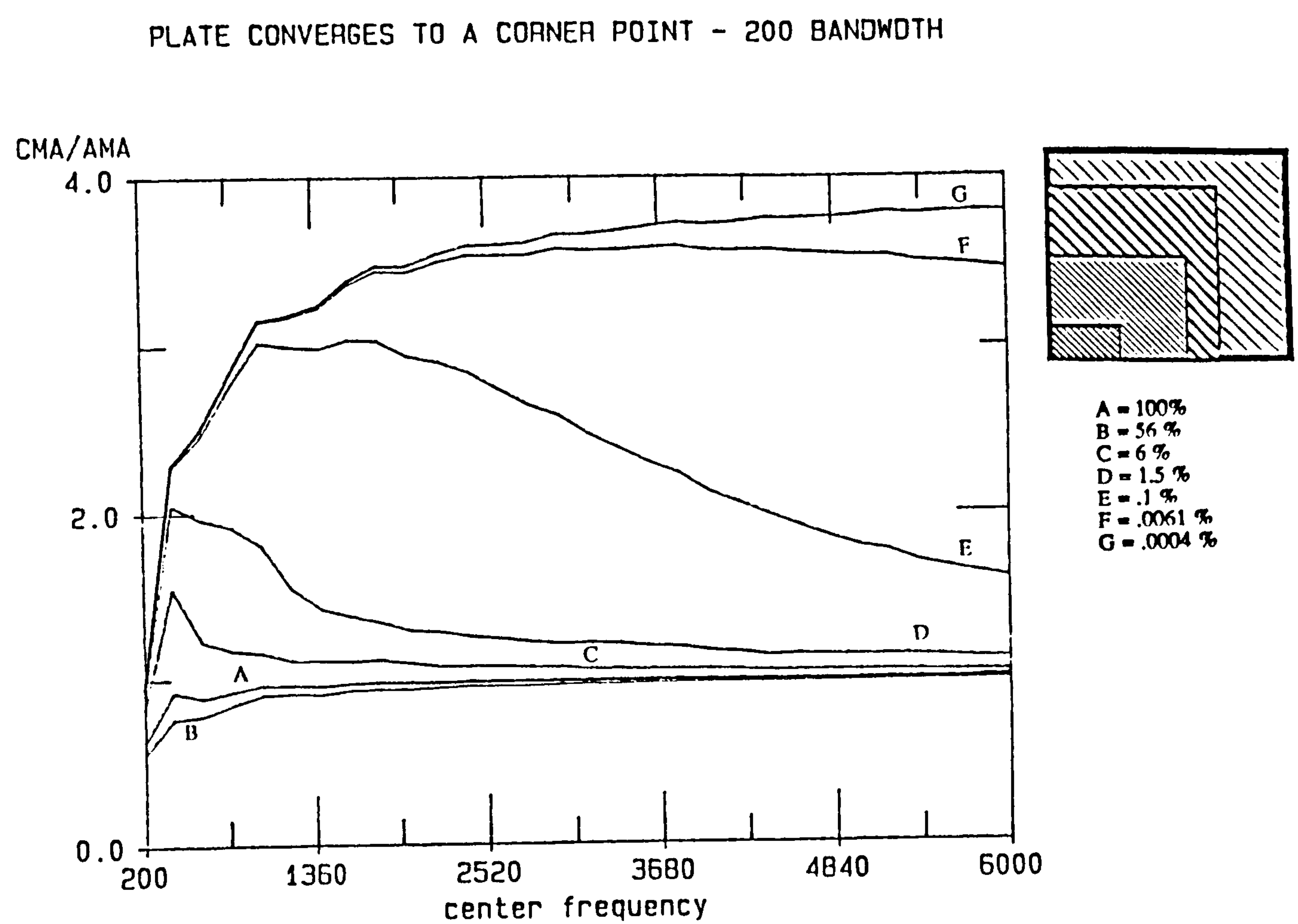


Figure 7. spatially averaged CMA to spatially averaged AMA ratio versus center frequency, with a fixed bandwidth of 200 hz, for the flexible area converging to a point in the corner of the wall.

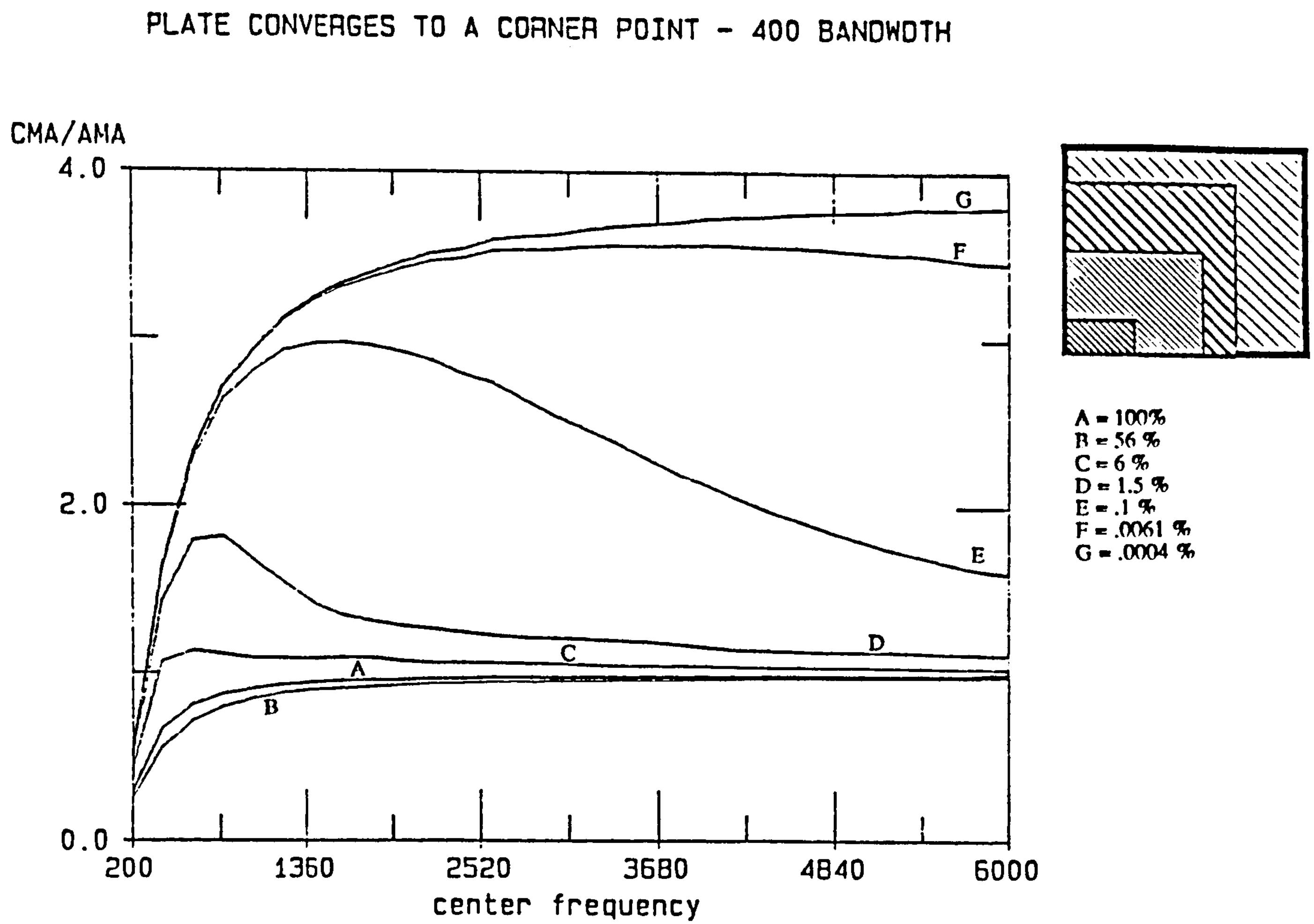


Figure 8. spatially averaged CMA to spatially averaged AMA ratio versus center frequency, with a fixed bandwidth of <u>400 hz</u>, for the flexible area converging to a point in the <u>corner</u> of the wall.

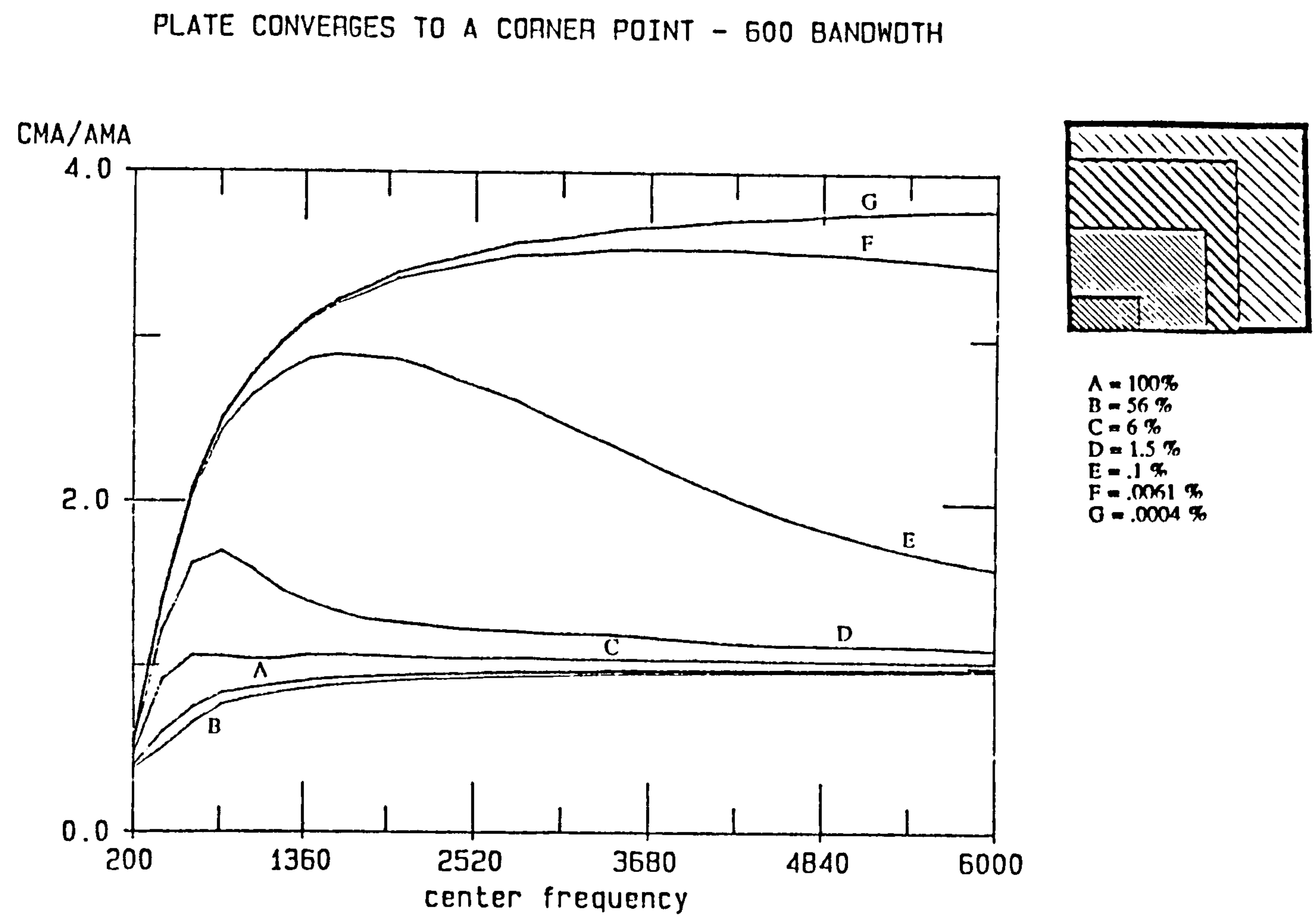


Figure 9. spatially averaged CMA to spatially averaged AMA ratio versus center frequency, with a fixed bandwidth of 600 hz, for the flexible area converging to a point in the corner of the wall.

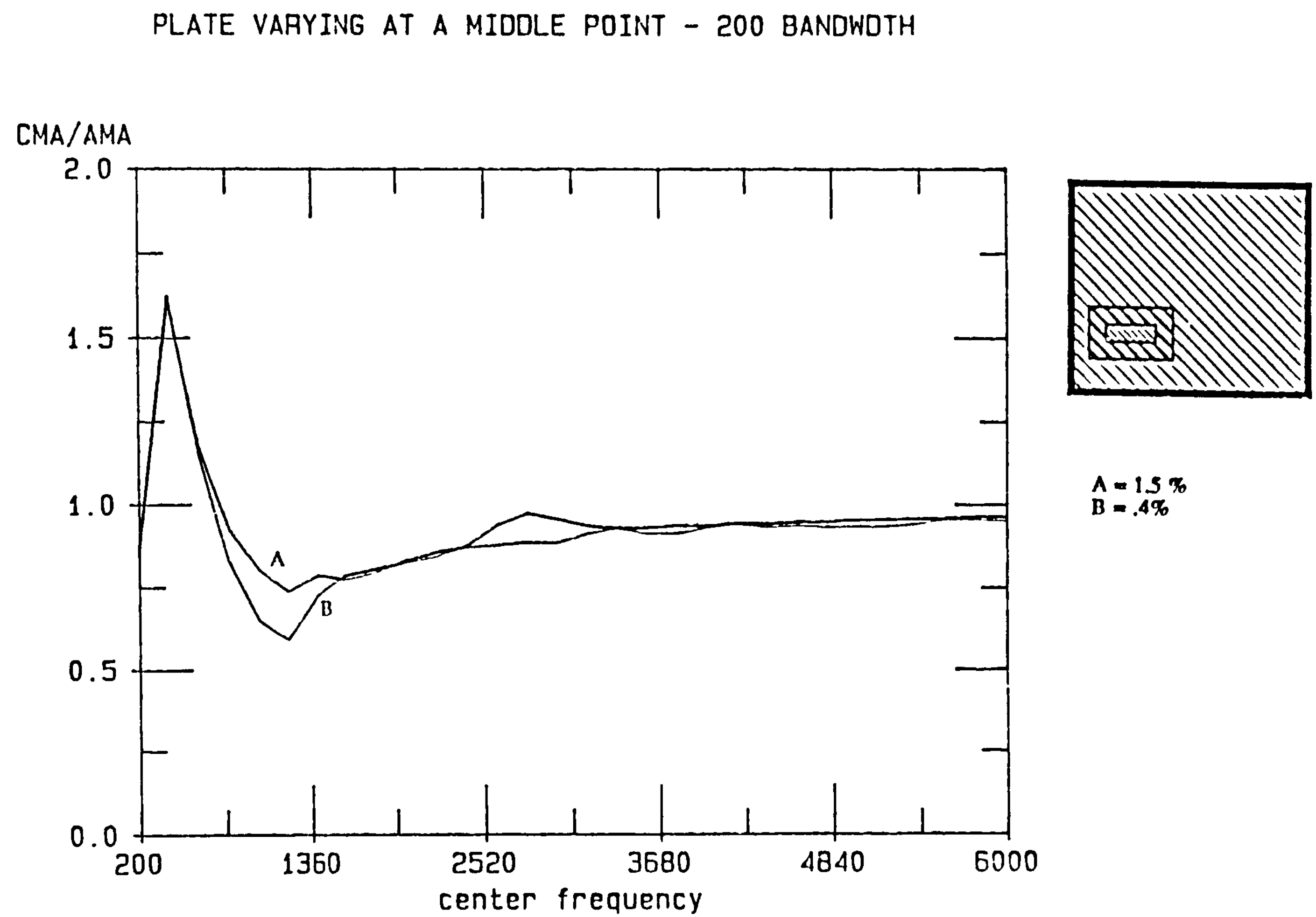


Figure 10. spatially averaged CMA to spatially averaged AMA ratio versus center frequency, with a fixed bandwidth of 200 hz, for the flexible area converging to a point other than the center or the corner of the wall.

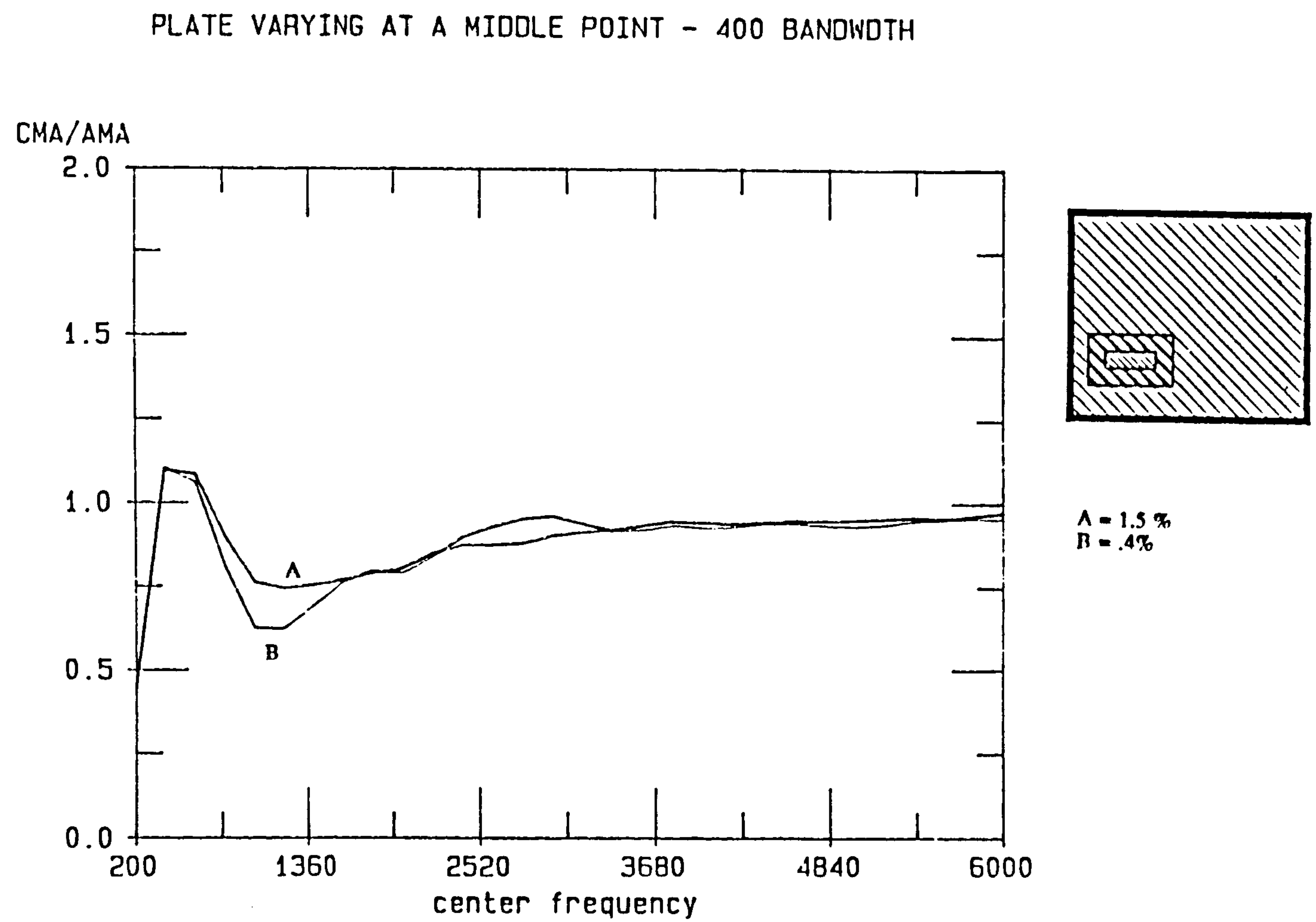


Figure 11. spatially averaged CMA to spatially averaged AMA ratio versus center frequency, with a fixed bandwidth of 400 hz, for the flexible area converging to a point other than the center or the corner of the wall.

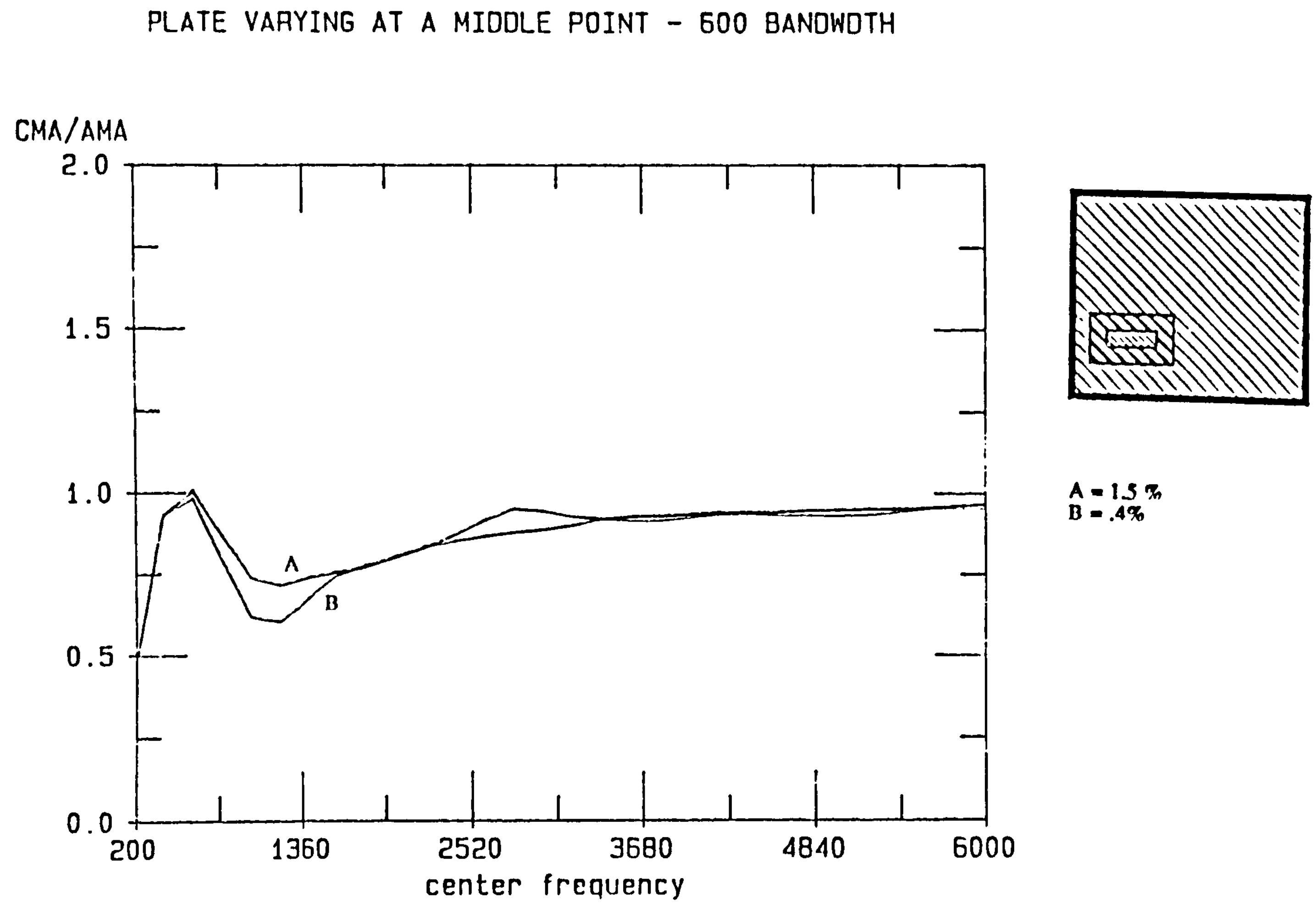


Figure 12. spatially averaged CMA to spatially averaged AMA ratio versus center frequency, with a fixed bandwidth of <u>600 hz</u>, for the flexible area converging to a point <u>other</u> than the center or the corner of the wall.

Local response:

The effect of position in the cavity was determined by considering the local response. This was again done for both convergence of the vibrating plate to the center and convergence to a corner. The results are presented as a ratio of CMA to spatially averaged AMA. (Were the AMA result not spatially averaged, this ratio would be 1.0 asymptotically for all positions. This will be discussed in further detail in the section which follows). The ratio was computed for many center frequencies at a constant bandwidth of 400 hz. There was no need to vary the bandwidth, since figures 4 through 12 show little variation with bandwidth. The result was computed for various center frequencies in 200 hz bandwidth increments up to a center frequency of 6000 hz. However, at 6000 hz there are over 5000 modes, and the number of modes increases as a function of the cube of the frequency. Therefore, it would be extremely time consuming to continue taking 200 hz bandwidth steps. Beyond 6000 hz, 1000 hz bandwidth increments were taken up to 11000 hz. This produces a smoother looking curve beyond 6000 hz, which is due to the larger frequency bandwidth increments.

Initially, four special response points were considered (see figure 13), the corner point (0.,0.,0.), the midpoint of the flexible wall, the midpoint of the entire cavity, and a point on the wall along the center line (1.8, 1.5, 0.). For these four points, the ratio of CMA to spatially averaged AMA was plotted as a function of center frequency in figures 14 through 17.

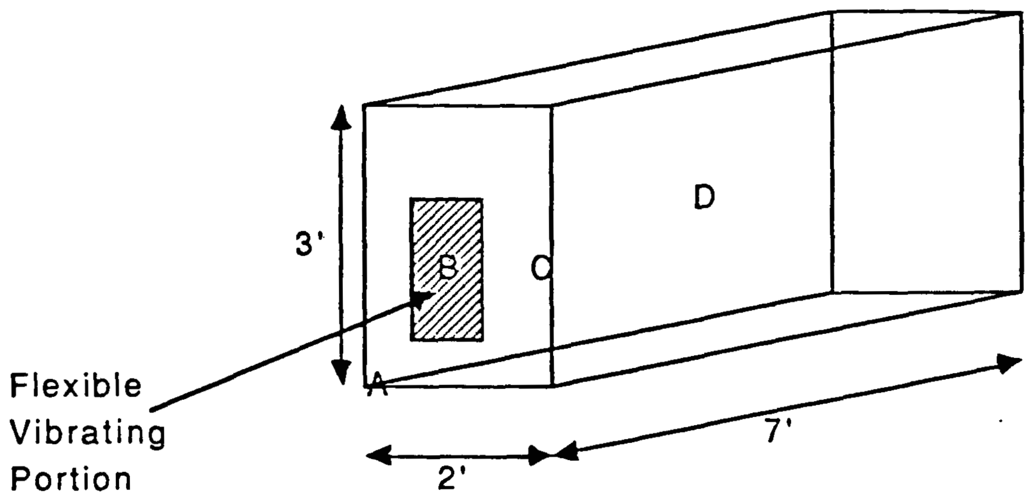


Four Particular Points of Interest - denoted by A, B, C, D

Figure 13. Points at which the local response was predicted

Taking the corner point first (point A in figure 13), figure 14 shows that as the plate converges to the center of the wall, the response of the corner approaches a "pseudo-asymptote" of 8, whereas, for convergence of the plate to the corner (figure 15) this same point has a pseudo-asymptote of 32, a factor of 4 times greater. The idea of a "pseudo-asymptote" will be discussed in the section which follows. This factor of 4 was seen in the spatially averaged cases as the ratio between center convergence versus corner convergence of the vibrating plate.

Figures 16 and 17 show that, at the mid point of the flexible wall (point B in figure 13), both types of convergence yield a pseudo-asymptote of 8. Since this point is on the wall, its expected pseudo-asymptote is 2. However, when the excitation is in the corner (figure 17), this is increased by a factor of 4, hence the value, 8. On the other hand, when the excitation location and the response location are at the center of the wall(figure 16), the response there is also increased by a factor of 4. This phenomena is similar to the "intensification" observed by Kubota in experiments where point loads are applied to a rectangular plate [3]. The effect of a point source is to divide the cavity into quadrants (defined by drawing perpendicular lines through the point source). In a newly defined sub-cavity this point where the source is located is now a corner point. The response at a corner point is eight-times greater than the interior region, so the pseudo-asymptote of 8 is appropriate for this case.

Kubota also found "hot lines" running perpendicularly through the point force. To test for these in this analysis, a point along one of the anticipated "hot lines" was studied. The values at this point (C in fig. 13) are depicted in figures 18 and 19. Since this point is on the face, it is expected to have a pseudo-asymptote of 2.0, which is indeed the case if the full wall is moving (dotted line on both plots). However, in the case of center convergence (i.e. analogous to a point load acting at the center of the wall), this point lies on a "hot line" and figure 18 shows a pseudo-asymptote of 4. Assuming the "hot lines" divide the cavity into subcavities, this point is an edge point of a sub-cavity. Therefore, the value of 4 is appropriate, since the response at an edge is 4-times greater than the interior. When the oscillating portion of the wall converges to the corner, the pseudo-asymptote is 8, which is a factor of 4 greater than if the whole wall is moving. This is consistent with previous findings for corner convergence.

Response at the mid point of the entire cavity (D in fig. 13) was also considered (figures 20 and 21). At an interior point such as this, the expected asymptote is 1.0. However, when the plate converges to the center of the wall (figure 20), this point lies in the line of action of the "point force," resulting in a factor of 4 increase, and therefore, a pseudo-asymptote of 4. Similar to the previous case, this point now lies on an edge point of a newly defined sub-cavity. Edge point response is 4-times greater than the interior.

When the plate converges to a corner of the wall, again a four-fold increase is expected, and the result is a pseudo-asymptote of 4, which is shown in figure 21.

In the corner convergence cases for the wall midpoint (B) and the cavity midpoint (D) (figures 17 and 21) five curves are actually plotted. Only the curves representing the smallest plate area (.01% and .004%) deviate significantly from the curve for the full wall.

The above points (A through D) were studied as the plate size was allowed to vary, for the two convergence cases and as a function of center frequency (for a fixed bandwidth). Next, the plate size was fixed at .004% of the wall area, which corresponds to a vibrating point. The center frequency was fixed at a value at which the pseudo-asymptotes had previously been reached (8000 hz), and the bandwidth was fixed at 400 hz. The distance into the cavity from the vibrating wall was varied, in figures 22 and 23 the trajectory is along an edge, while in figures 24 and 25 the trajectory is radial.

In figure 22, the sound source (vibrating point) is located in the center of the wall, and the response is plotted along an edge. The peak response in the corner is 8. Moving away from the corner, the response then oscillates before approaching the asymptote for an edge, which is 4.0. This region between the corner response peak and the almost flat response of the interior will later be referred to as the "transition zone." This same edge response is shown in figure 23, for the case when the sound source is located in the corner. The curves are basically the same shape, but the levels have increased by a factor of 4.0, which is due to the excitation (sound source) location. Both curves are symmetric in the z direction, which can be shown analytically, by substituting (z-d) in for (z) in the acoustic modal function, and using the trigonometric relations $\cos^2(z) = \cos^2(-z)$, and $\cos(a-b) = \cos(a)*\cos(b) + \sin(a)*\sin(b)$. Therefore, only half of the edge length is plotted (3.5 feet out of 7.0 feet).

Figures 24 and 25 are plots of the response in a radial direction away from the corner of the cavity, for the two different point sound source locations. The radial direction is defined by the line $x=y=z$, and the radial distance is equal to the square root of $(x^2 + y^2 + z^2)$. In figure 24, a point sound source (or vibrating point) is located in the center of the wall. Since the point source is in the center of the wall, "hot lines" exist which run down the center of the cavity. Due to these "hot lines," which redefine new effective boundary points, the cavity interior is no longer uniform, as is shown in figure 24. After the radial distance of 1.0, the response begins to increase, and approaches a value of 2.0, as if there were a wall or face there. This is not a physical boundary created by the cavity geometry, but rather an artificial boundary created by the point source. In figure 25, the same radial trajectory is taken. However, since the point source is located in the corner, the response of the interior is uniform. The peak value in the corner is 32 (corner response point, 8 X corner excitation point, 4 = 32). The response then oscillates, and eventually approaches a uniform interior value of 4.0.

In summary, for a vibrating point at the center of the wall, the asymptotic limit for points which do not lie on "hot lines" is: 1.0 for interior points, 2.0 for points on a face, 4.0 for points on an edge, and 8.0 for corner points. Also, the corner convergence cases yield the same relationships between locations but the magnitudes are increased by a factor of 4. "Hot lines" can be thought of as dividing the cavity into subcavities or quadrants. Each subcavity then, produces its own corner, edge and face points, redefining "effective" boundary points.

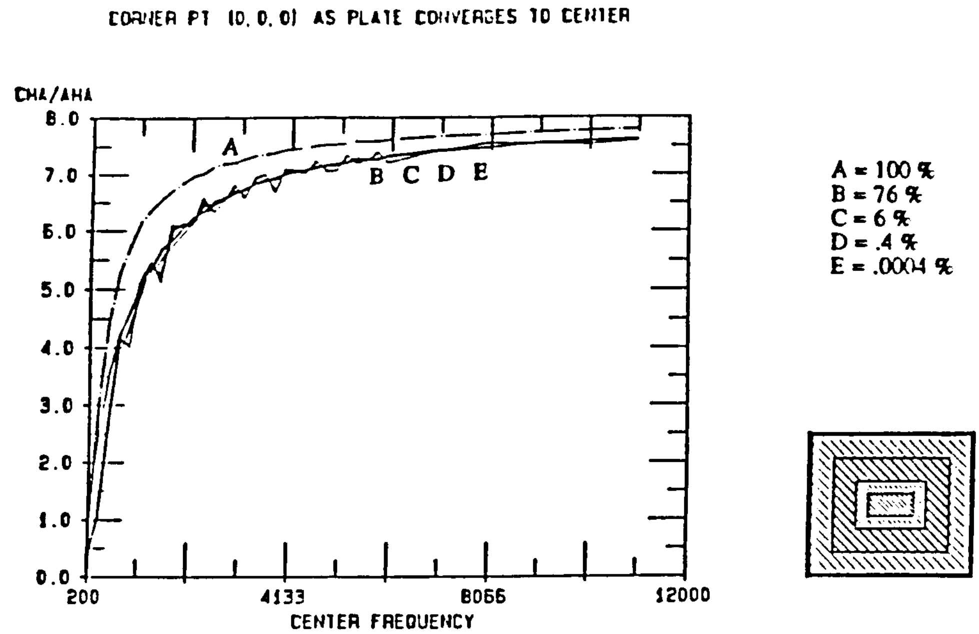


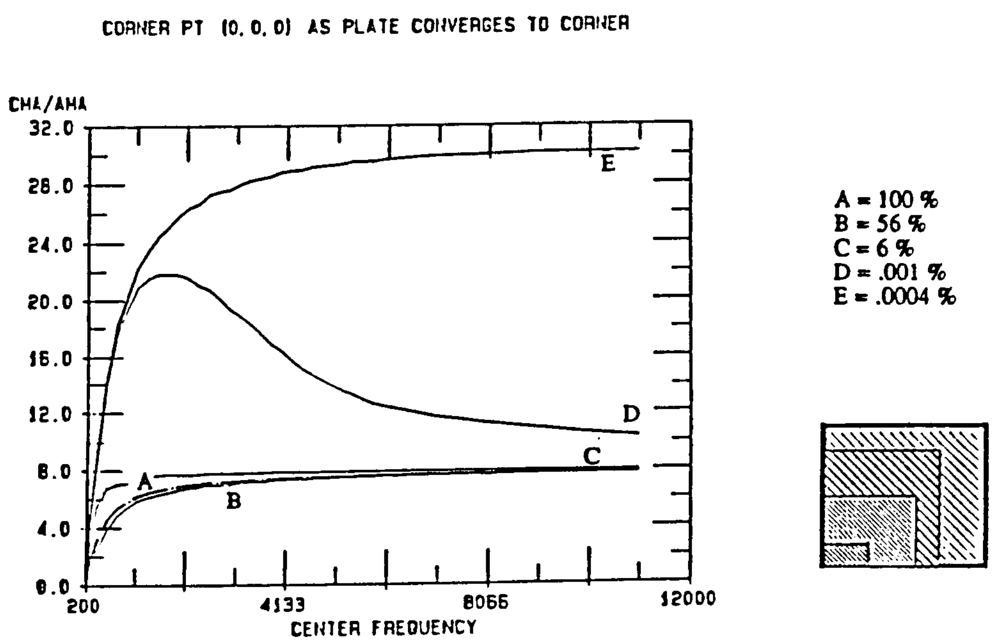


Figures 14 and 15. local CMA to spatially averaged AMA ratio versus center frequency for the corner point, for a fixed bandwidth of 200 hz (if center frequency < 6000 hz), and a fixed bandwidth of 1000 hz (if center frequency > 6000 hz), for the flexible plate area converging to a point in the center (top), and converging the plate area to a point in the corner (bottom).

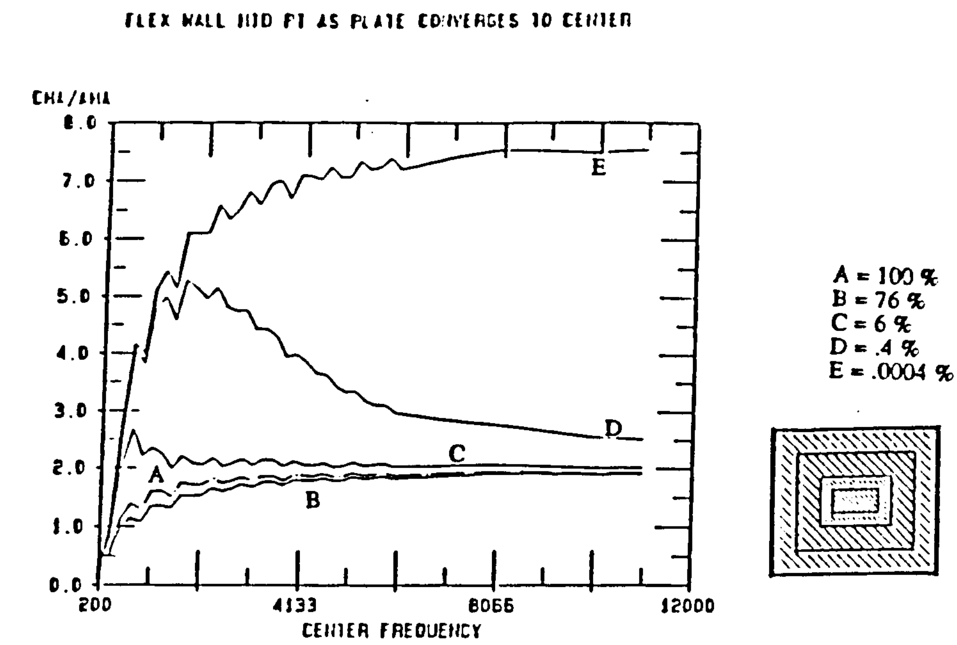


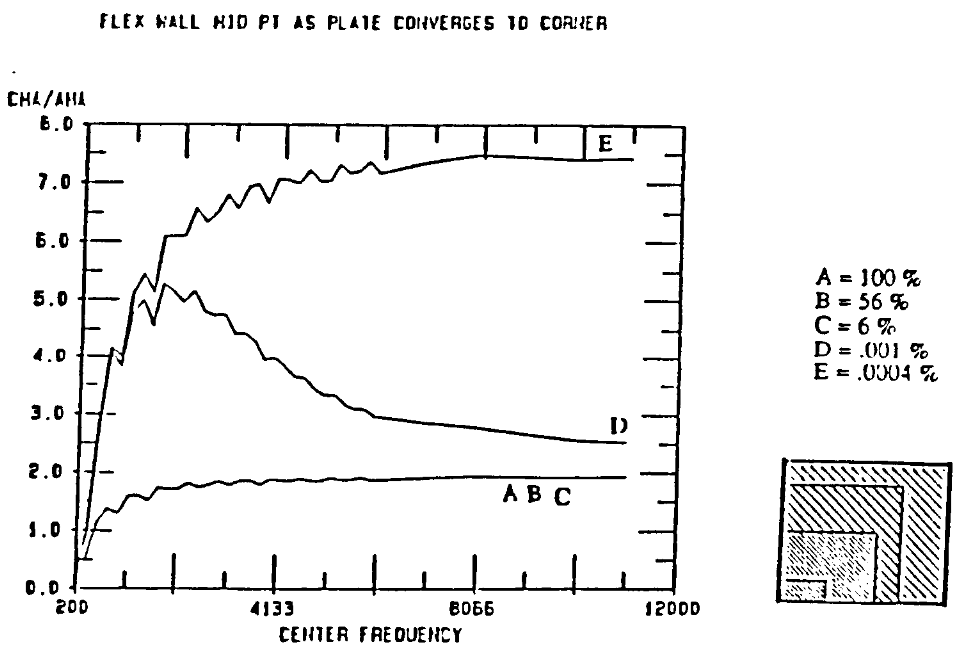


Figures 16 and 17. local CMA to spatially averaged AMA ratio versus center frequency for the flexible wall mid-point, for a fixed bandwidth of 200 hz (if center frequency < 6000 hz), and a fixed bandwidth of 1000 hz (if center frequency > 6000 hz), for the flexible plate area converging to a point in the center (top), and converging the plate area to a point in the corner (bottom).

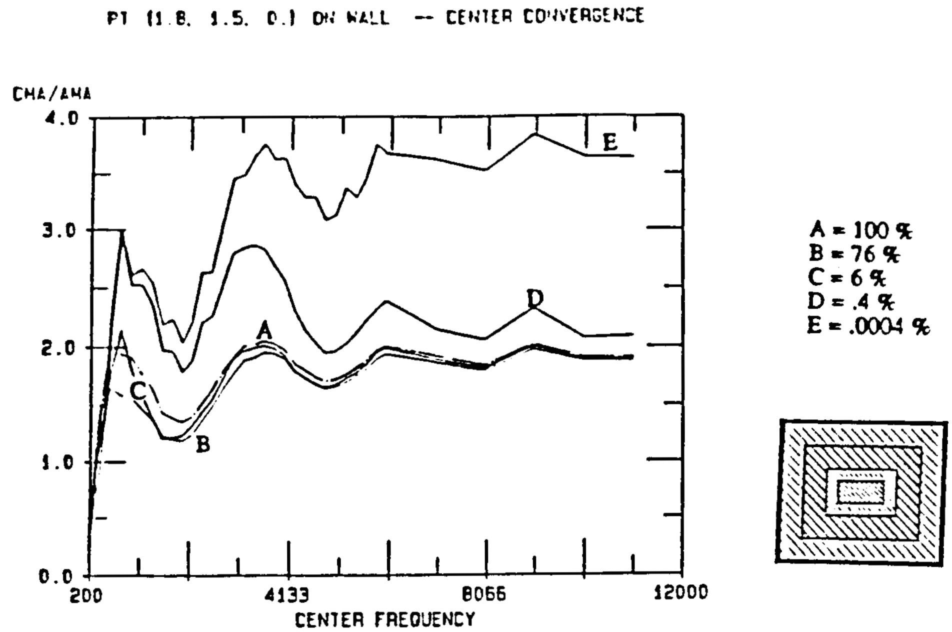


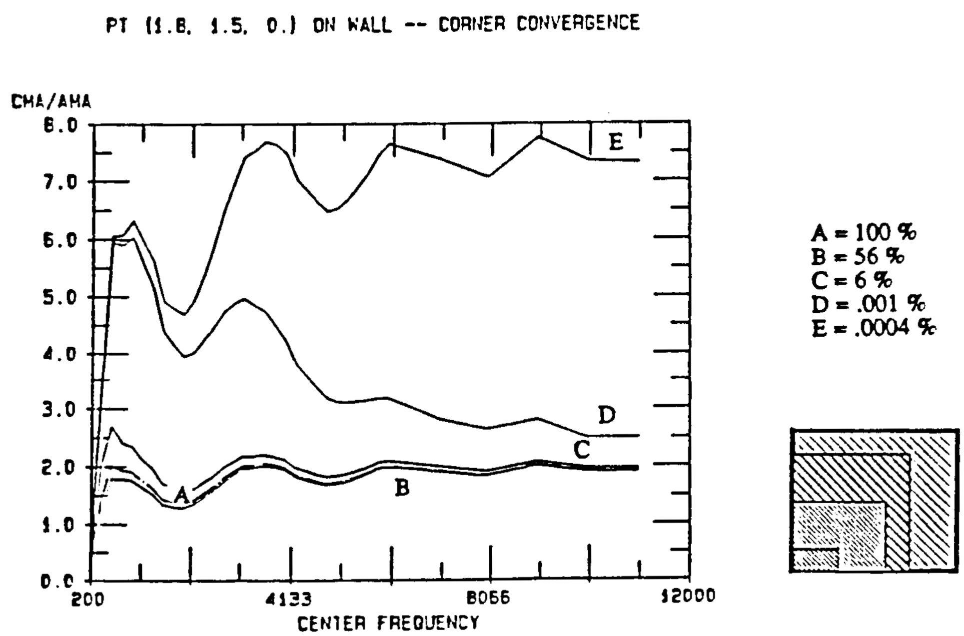


Figures 18 and 19. local CMA to spatially averaged AMA ratio versus center frequency for the point which lies on a "hot line", for a fixed bandwidth of 200 hz (if center frequency < 6000 hz), and a fixed bandwidth of 1000 hz (if center frequency > 6000 hz), for the flexible plate area converging to a point in the center (top), and converging the plate area to a point in the corner (bottom).

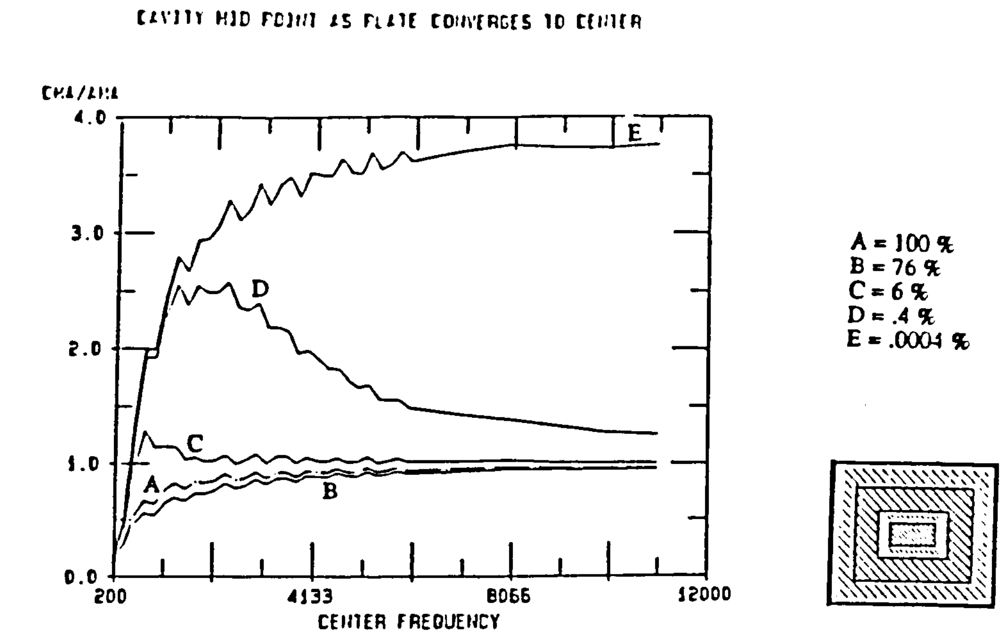


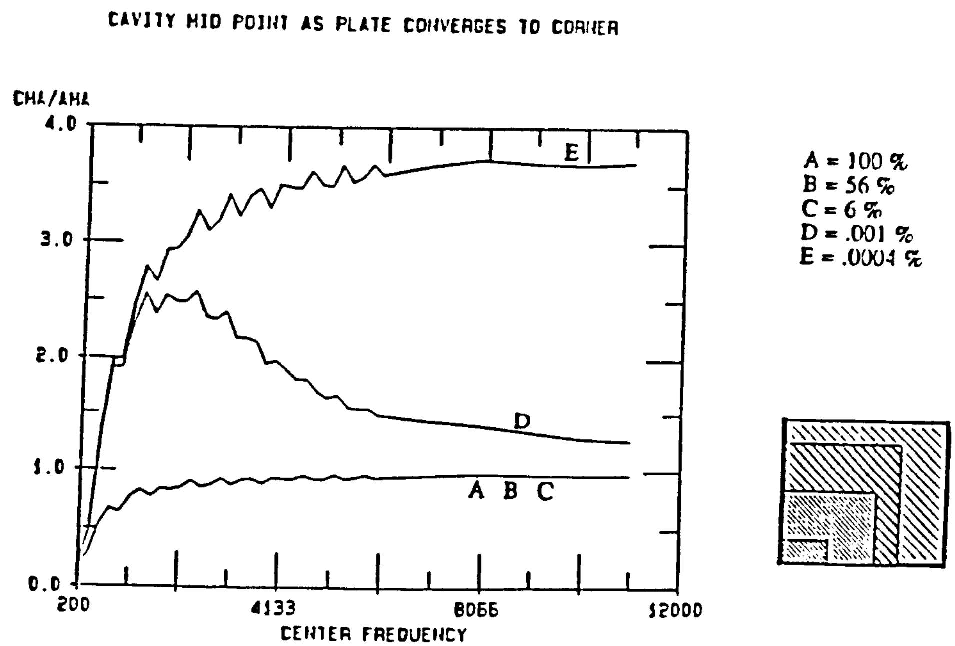


Figures 20 and 21. local CMA to spatially averaged AMA ratio versus center frequency for the cavity mid-point, for a fixed bandwidth of 200 hz (if center frequency < 6000 hz), and a fixed bandwidth of 1000 hz (if center frequency > 6000 hz), for the flexible plate area converging to a point in the center (top), and converging the plate area to a point in the corner (bottom).

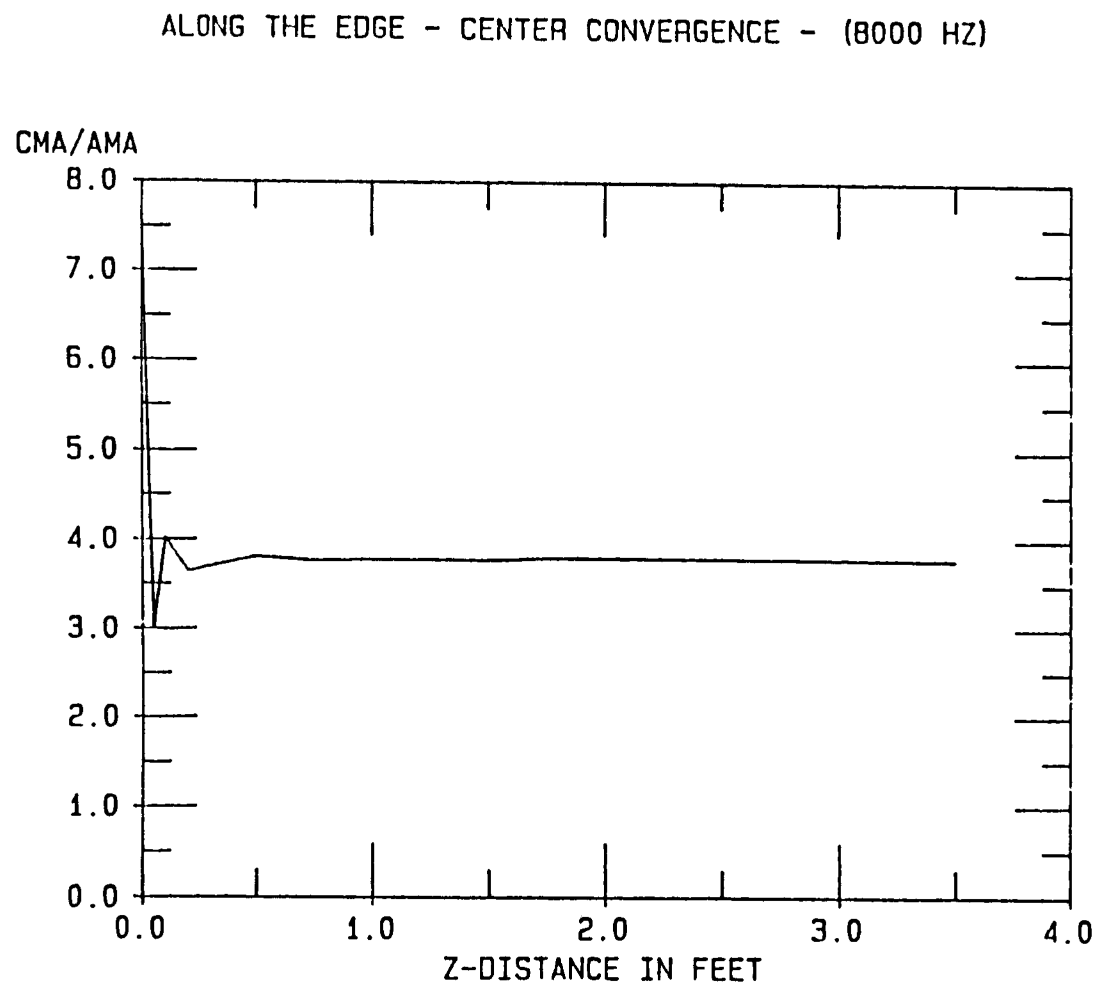


Figure 22. Local CMA to spatially averaged AMA ratio versus distance along an edge of the cavity away from a corner, (Center frequency is fixed at 8000 hz, and bandwidth is fixed at 400 hz), for a vibrating point sound source in the center of the wall.

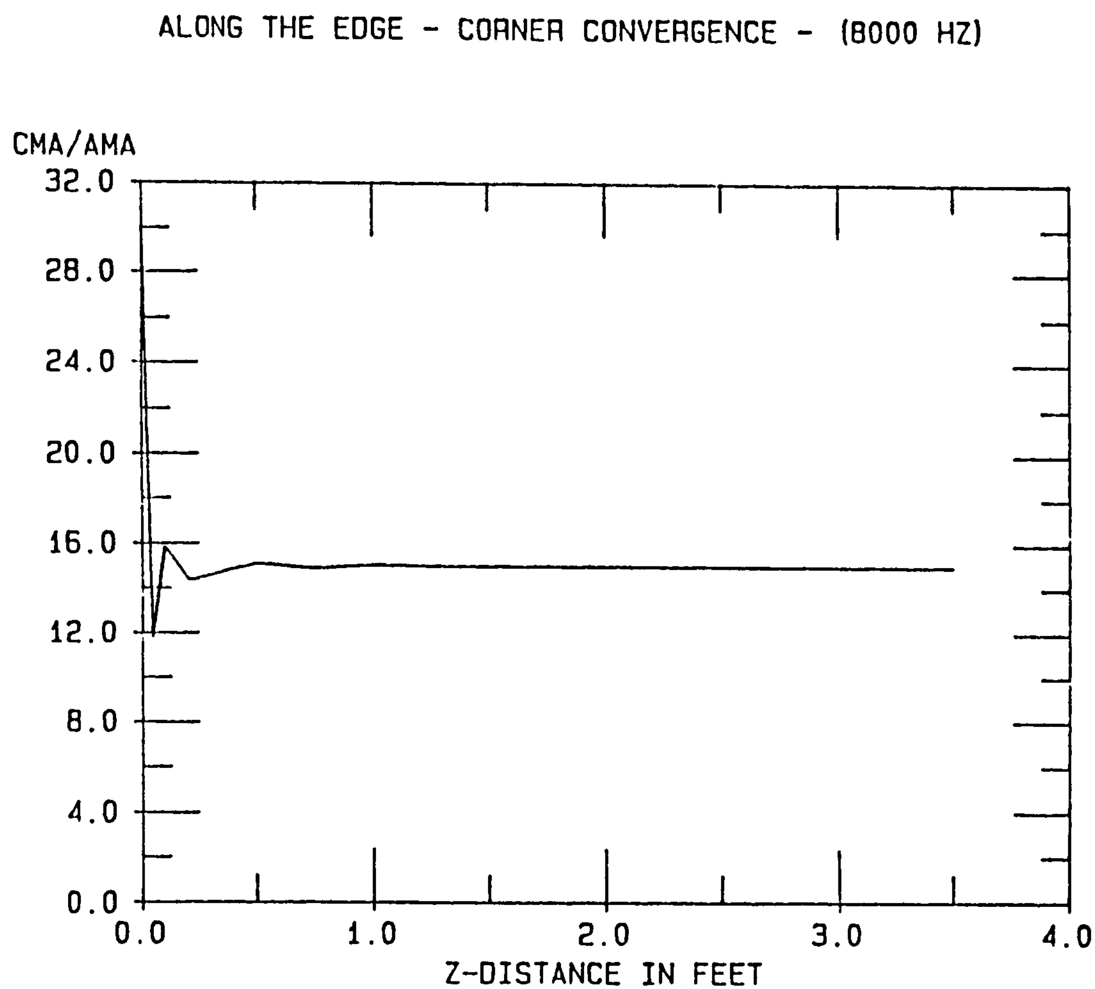


Figure 23. Local CMA to spatially averaged AMA ratio versus distance along an edge of the cavity away from a corner, (Center frequency is fixed at 8000 hz, and bandwidth is fixed at 400 hz), for a vibrating point sound source in the corner of the wall.

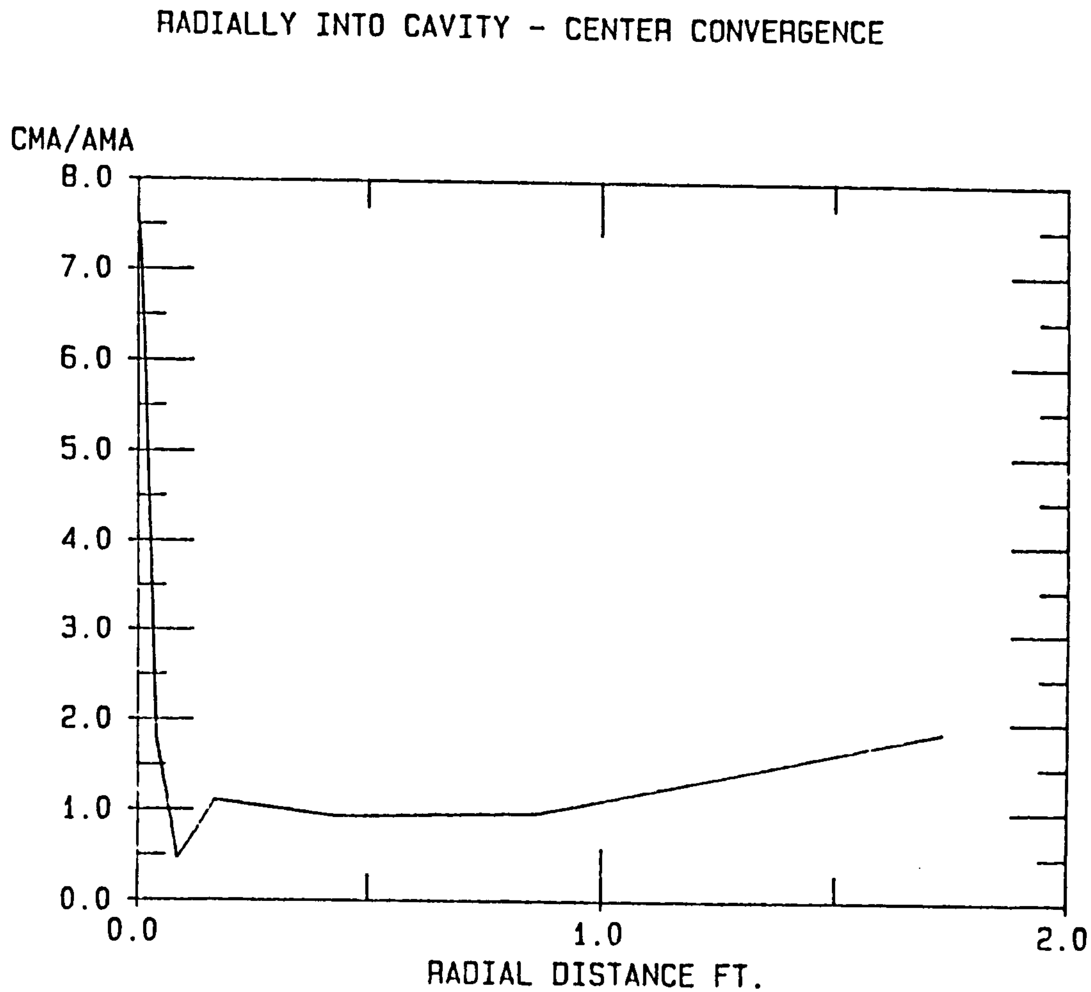


Figure 24. Local CMA to spatially averaged AMA ratio versus distance radially into the cavity away from a corner, (Center frequency is fixed at 8000 hz, and bandwidth is fixed at 400 hz), for a vibrating point sound source in the center of the wall.

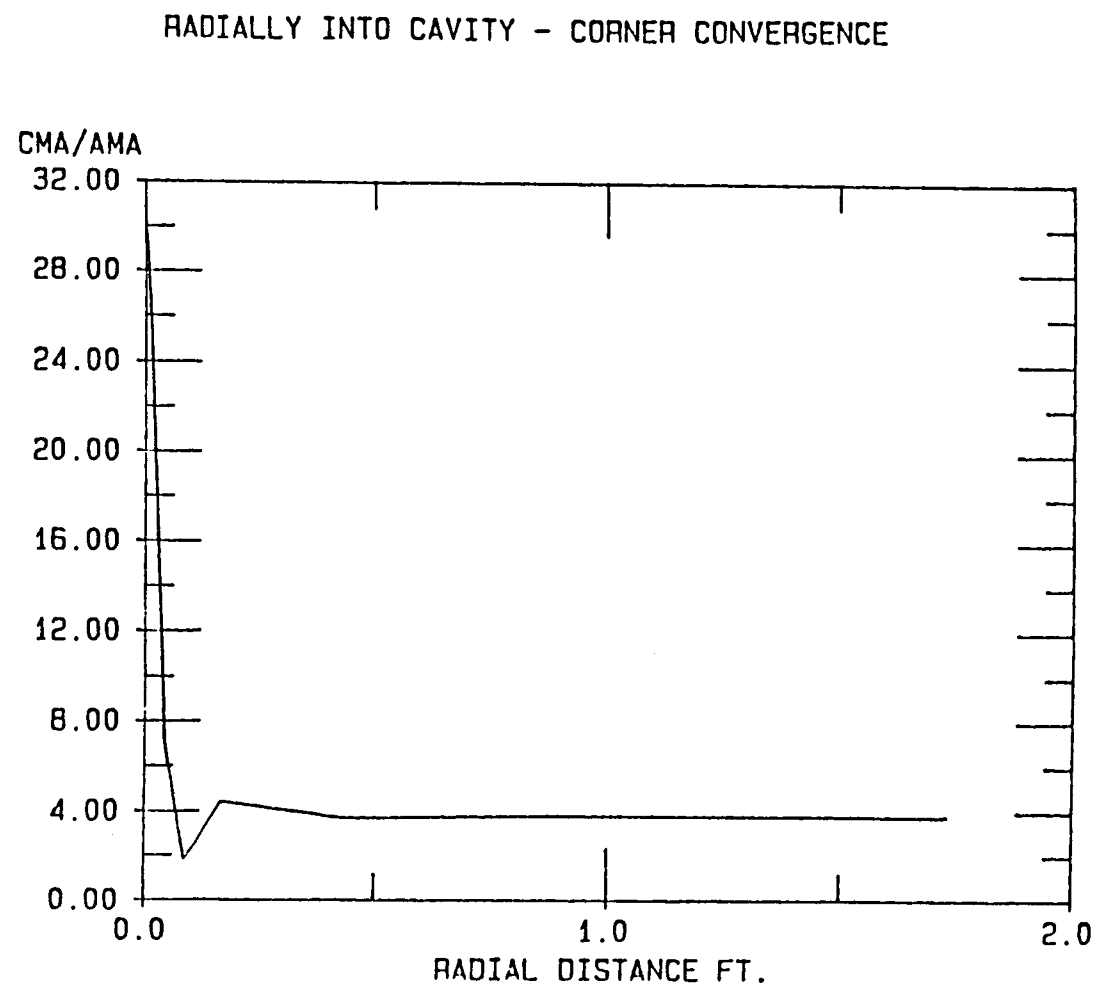


Figure 25. Local CMA to spatially averaged AMA ratio versus distance radially into the cavity away from a corner. (Center frequency is fixed at 8000 hz, and bandwidth is fixed at 400 hz), for a vibrating point sound source in the corner of the wall.

## Discussion

The term in the CMA/AMA equation (3 or 4) which is affected by changing the flexible area size and location of the flexible portion is $\iint F_r^2(x,y,z_0)\, dx\, dy / A_f$ . This can be thought of as a spatial average of the acoustic modal function in two dimensions (x and y). The expected result would be 1/4, unless the argument of one or both cosine functions (in $F_r$) is always zero. When the plate converges to a point in the corner, the x and y values are essentially zero, the value for the cosine is equal to one, and the "spatial average" above would then be 1.0 rather than 1/4. Therefore, the effect of shrinking the area down to the corner yields a four-fold increase.

However, one can imagine driving the frequency up so high that the approximated corner point no longer behaves like a point compared to an acoustic wavelength. It is for this reason, that this has been called a "pseudo-asymptote," rather than a true asymptote. As the center frequency becomes sufficiently large, the true asymptote will always be 1.0 for the spatially averaged CMA/AMA ratio.

The analysis has been done for the ratio of spatially averaged CMA [Spatial average denoted by < > ] to spatially averaged AMA : <CMA>/<AMA>, and for the local CMA response divided by spatially averaged AMA. If the local AMA to spatially averaged AMA (<AMA>) ratio were known, the local CMA to local AMA ratio could be deduced. This would (providing the result were 1.0 for a large number of modes) add to the credibility of AMA. Thus, consider the following.

The local AMA result is (equation 2):

$$\frac{\overline{p}^2}{\left(\rho_o c_o^2\right)^2} \cong \frac{\pi}{4} \frac{A_f}{V^2} \Phi_{\ddot{w}}(\omega_c) \frac{A_f\, \Delta N^A \left\langle F_c^2 \right\rangle}{\left(M_c^A\right)^2 \left(\omega_c^A\right)^3 \zeta_c^A \left\langle Z_c^2 \right\rangle} \sum_r \frac{F_r^2(x,y,z)}{\Delta N^A} \qquad (2)$$

whereas, the spatially averaged AMA result is: (derived in [Ref.4])

$$\frac{\bar{p}^2}{\left(\rho_o c_o^{\,2}\right)^2} \cong \frac{\pi}{4}\frac{\Delta N^A}{\Delta\omega^A}\left(\frac{A_f}{V}\right)^2 \frac{\Delta\omega\, \Phi_{\ddot{w}}(\omega_c)}{\left(\omega_c^A\right)^3 \zeta_c^A \left\langle Z_c^{\,2}\right\rangle} \quad (5)$$

Therefore, the ratio of local AMA to spatially averaged AMA is:

$$(AMA)_{local} \,/\, \langle AMA\rangle_{spatial\ average} = (\Sigma F_r^2(x,y,z)/\Delta N^A) \,/\, \langle F_c^2\rangle$$

The numerator, $(\Sigma F_r^2(x,y,z)/\Delta N^A)$, is equal to $1/2 \cdot 1/2 \cdot 1/2$ or $1/8$ when x, y, and z are not zero or $L_x$, $L_y$, $L_z$. It is equal to (1/2)*(1/2)*(1) or (1/4) when one of the values of x, y, or z are equal to 0 or the length of the cavity in the appropriate direction, which is true on any face.

For an edge, the numerator, $(\Sigma F_r^2(x,y,z)/\Delta N^A)$, is equal to (1/2)*(1)*(1) = (1/2), since two values of x, y, or z are equal to 0 or the length of the cavity in their direction. And $(\Sigma F_r^2(x,y,z)/\Delta N^A)$ is equal to (1)*(1)*(1) = (1) in a corner, since all three values of x, y, or z will either be 0 or $L_x$, $L_y$, $L_z$.

The spatially-averaged acoustic modal function evaluated at the center frequency, $\langle F_c^2\rangle$, which comprises the denominator of the $(AMA)_{local} \,/\, \langle AMA\rangle_{spatial\ average}$ ratio, is always equal to (1/2)*(1/2)*(1/2) or 1/8.

Therefore, the $(AMA)_{local}/\langle AMA\rangle_{spatial\ average}$ can be summarized in the following table. For a

| | | |
|---|---|---|
| corner | (1)/(1/8) | 8 |
| edge | (1/2)/(1/8) | 4 |
| face | (1/4)/(1/8) | 2 |
| interior | (1/8)/(1/8) | 1 |

Recall that local CMA to spatially averaged AMA for the center convergence case yields pseudo-asymptotes of :

8 in the corner
4 on an edge
2 on a face
1 in the interior

This indicates that for a large number of modes, the asymptotic modal analysis results agree locally with the exact results predicted by classical modal analysis when the oscillating wall is a full wall or converging toward the center. For corner convergence, the multiplicative factor of 4 must be accounted for as explained previously.

This factor of 4 is due to the fact that in deriving the AMA result used in this study it was assumed that the excitation occurs at a location other than in a corner or on an edge. It is possible to incorporate the excitation location effect into the AMA result, if it is desired.

## Intensification

Acoustic theory predicts, and the previous numerical work has shown, that there are local asymptotic response peaks or "intensification zones" in the acoustic field near the cavity boundary, and an otherwise uniform response in the interior region. In particular, for a rectangular acoustic cavity, the mean square pressure is eight-, four-, and two-times the uniform interior pressure levels at the corners, edges and faces, respectively.

In designing acoustic spaces, allowances must be made for these intensification zones. Therefore, it is important to determine the characteristic distance over which the response levels change from their peak values at the boundary to the uniform interior level. Parameters such as, cavity dimensions, frequency bandwidth, and center frequency may play a role in determining the size of this"transition zone," where the response levels are neither their peak values nor the uniform interior level. It is desirable to determine which parameters affect the transition zone, and which do not. This knowledge may allow the design of a cavity with rapidly decaying intensification zones.

As a first step, the one-dimensional case was considered. From the 1-d case, insight into the 2- and 3-d cases can be gained.

## Analysis

The non-dimensional pressure ratio which is used in the examination of the one-dimensional transition zone is derived from equation 1. A ratio is taken of the sound pressure level from equation 1 to its spatially-averaged value. After cancelling the like-terms, the result is:

$$\frac{\overline{p}^2}{\left\langle \overline{p}^2 \right\rangle} = \frac{\sum_r F_r^2(x,y,z) \Big/ \left(\omega_r^A\right)^3}{\sum_r \left\langle F_r^2(x,y,z) \right\rangle \Big/ \left(\omega_r^A\right)^3} \tag{6}$$

and considering only a 1-dimensional acoustic wave:

$$\frac{\overline{p}^2}{\left\langle \overline{p}^2 \right\rangle} = \frac{\sum_r \cos^2\left(\frac{n\pi x}{L_x}\right) \Big/ \left(\omega_r^A\right)^3}{\sum_r \left\langle \cos^2\left(\frac{n\pi x}{L_x}\right) \right\rangle \Big/ \left(\omega_r^A\right)^3} \tag{7}$$

Assuming a large number of acoustic modes allows the summation over n to be replaced by an integration (n is then treated as a continuous variable). Noting that the spatial average of cosine squared is 1/2 and that $\omega = n\pi c/L_x$ yields:

$$\frac{\int \cos^2\left(\frac{n\pi x}{L_x}\right) \Big/ \left(\frac{n\pi c}{L_x}\right)^3 dn}{\frac{1}{2} \int 1 \Big/ \left(\frac{n\pi c}{L_x}\right)^3 dn} \tag{8}$$

The variable n can be replaced by $\omega$ or f, in order to obtain a result in terms of frequency, by the relations:

$\omega = n\pi c/L_X$ , $f = 2\pi\omega$, which leads to $n = 2L_X f/c$

The final result in terms of frequency after doing the integration is:

$$1 + \frac{f_c^2}{f_u^2 - f_l^2}\left\{ \begin{array}{c} \frac{f_c^2}{f_l^2}\cos\theta_l - \frac{f_c^2}{f_u^2}\cos\theta_u + \frac{4\pi x f_c}{c}\left(\frac{f_c}{f_u}\sin\theta_u - \frac{f_c}{f_l}\sin\theta_l\right) + \\ \left(\frac{4\pi x f_c}{c}\right)^2 \left(Ci(\theta_l) - Ci(\theta_u)\right) \end{array} \right\}$$

(9)

where:

$f_c$ is the center frequency, and $f_b$ is the frequency bandwidth,

$f_l$ and $f_u$ are defined as the lower & upper frequencies of the frequency interval as follows:

$f_u - f_l = f_b$, and $f_c = \sqrt{f_l * f_u}$

and,

$\theta_l = 2 * k_c x * f_l / f_c$ $\qquad$ $k_c x = (2\pi f_c)x / c$

$\theta_u = 2 * k_c x * f_u / f_c$

Therefore, the ratios $f_l/f_c$, and $f_u/f_c$ can be obtained from $f_b/f_c$, using the above definitions. In fact, the entire expression (9), can be expressed in terms of $f_b/f_c$, and $k_cx$, where $k_cx$ is the wave number associated with the center frequency times the distance away from the end point. Therefore, knowing the ratio of frequency bandwidth to center frequency ($f_b/f_c$), the pressure function in the transition zone can be plotted as a function of distance away from the endpoint, $k_cx$. Note that the dimensions of the cavity do not appear in this result.

Results and Discussion

Plots are shown in figures 26 through 34 of non-dimensionalized pressure ratio versus $k_cx$ for various $f_b/f_c$ ratios. An $f_b/f_c$ ratio of .005 approximately simulates a tone, while an $f_b/f_c$ ratio of .239 corresponds to a 1/3 octave bandwidth, and $f_b/f_c$ = .500 represents an octave bandwidth.

The first three plots are for the "tone-like" case. It is "tone-like" because of the small $f_b/f_c$ ratio which corresponds to a narrow bandwidth at a high center frequency. However, it is not a "pure tone" because more than one frequency is present. Figure 26 shows the non-dimensionalized pressure ratio versus $k_cx$, where the pressure ratio is calculated using an integration (similar to an AMA-type calculation) rather than a summation over all the modes. For comparison, figures 27 and 28 show the same ratio calculated as a summation over all the modes (this is similar to a CMA type calculation). In figure 27, only 2 modes are summed. This response starts to decay around $k_cx$ = 25. Figure 28 shows the response when 26 modes are summed for the same $f_b/f_c$ ratio. This summation case more closely resembles the integration case, even though only 26 modes are included in the summation. Since the agreement is fairly good, at least to a $k_cx$ value of 50, between the integration (AMA-type) and the summation (CMA-type) results, this suggests that the integration is reasonably accurate even when a relatively few number of modes are present.

Results are shown for the 1/3 octave band case in the next three figures. Figure 29 is a plot of non-dimensionalized pressure ratio versus $k_c x$ calculated by integration rather than summation over all the modes. In figures 30 and 31, plots are shown of the summation over 15 modes and 479 modes. Agreement between integration and summation is best for the 479 mode summation. However, for the 15 mode summation plot the overall envelope of the function is still preserved.

Figures 32 through 34 are plots of the non-dimensionalized pressure ratio versus $k_c x$ for the octave band case. The results are similar to the 1/3 octave band case. The summation over the larger number of modes matches integration best, although the envelope of the function is still preserved for summation over relatively few modes.

Replacing the summation with an integration is only valid when n can be treated as a continuous variable, i.e. when there are a large number of acoustic modes. However, these plots indicate that even when there are only a few modes the overall envelope is still preserved. For most applications, it is actually the envelope which is important. Therefore, the integration does quite well even at low center frequencies (or frequency ranges with relatively few modes). Which also indicates that the AMA method may also be accurate when there are relatively few modes in a given frequency range.

Another interesting outcome of the 1-d transition zone study is that the parameters which determine the size of the transition zone and the shape of the pressure function are $k_c x$ and $f_b/f_c$. The cavity (in this case, 1-d) dimensions are not a factor. Therefore, the size of the transition zone does not depend upon the length of the 1-dimensional cavity. Extrapolating this result to the 3-d case, cavity dimensions are not the key parameters which determine the intensification area or "transition zone." The ratios of $L_x$, $L_y$, and $L_z$ to each other may be important. The one-dimensional case can not predict this. But, the actual size of the cavity does not enter into the problem directly.

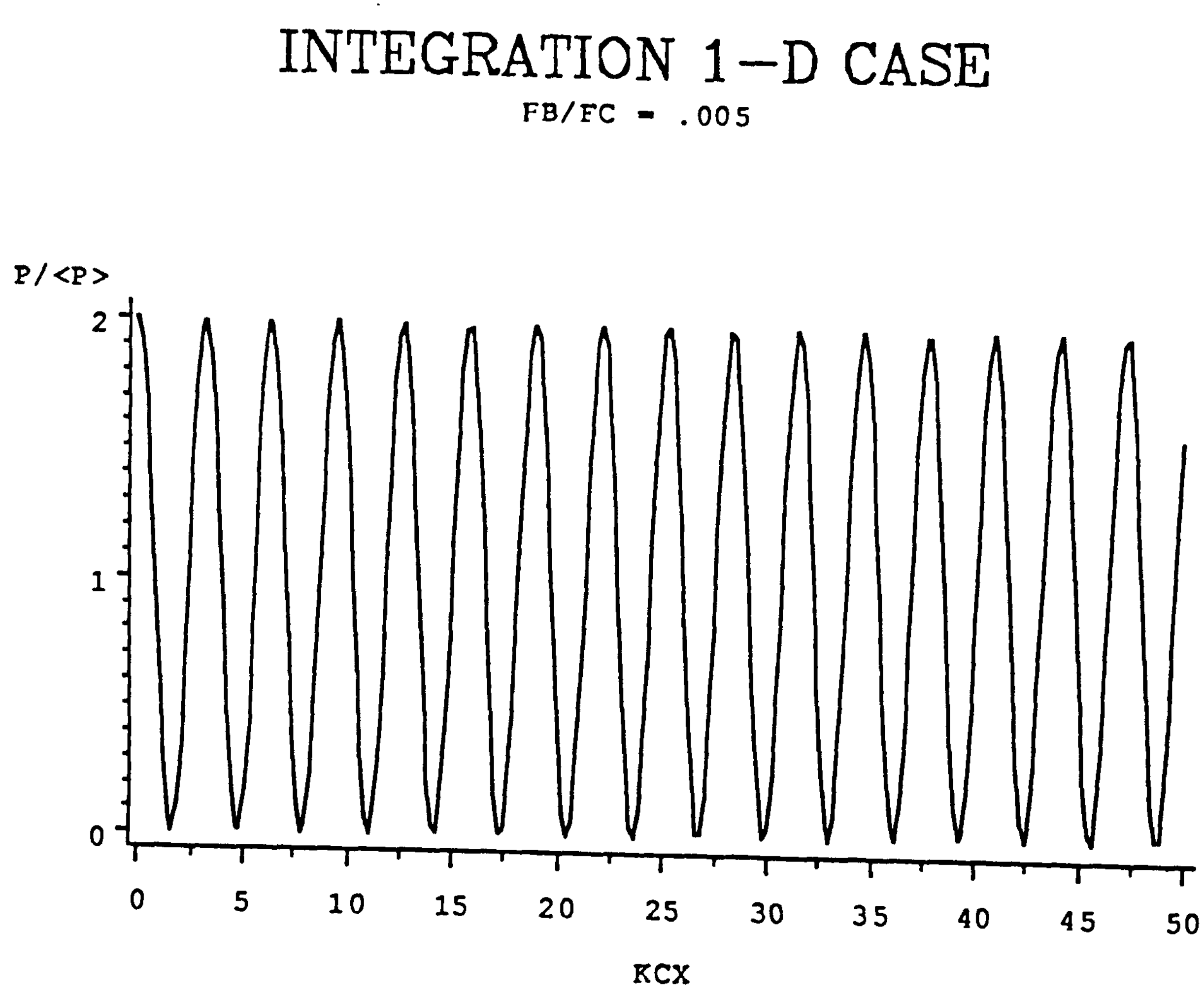


Figure 26. Non-dimensionalized pressure ratio versus $k_C x$ for the transition zone of a 1-dimensional cavity. Pressure calculation was made using integration. FB/FC = .005 which is similar to a tone.

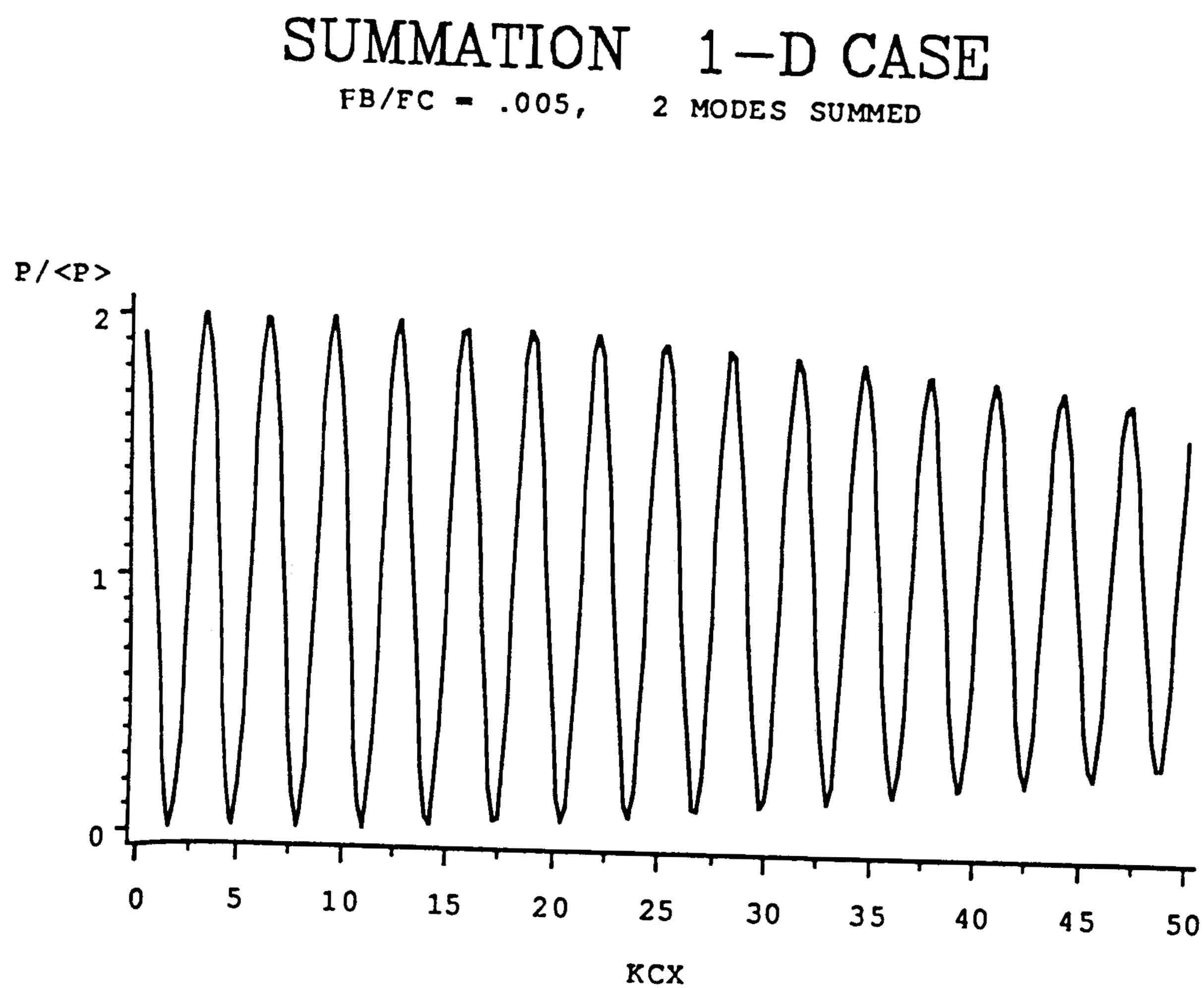


Figure 27. Non-dimensionalized pressure ratio versus $k_c x$ for the transition zone of a 1-dimensional cavity. Pressure calculation was made using summation. FB/FC = .005 which is similar to a tone. $Nref = \omega_c L_x / \pi c = 100$, which defines the summation over 2 modes.

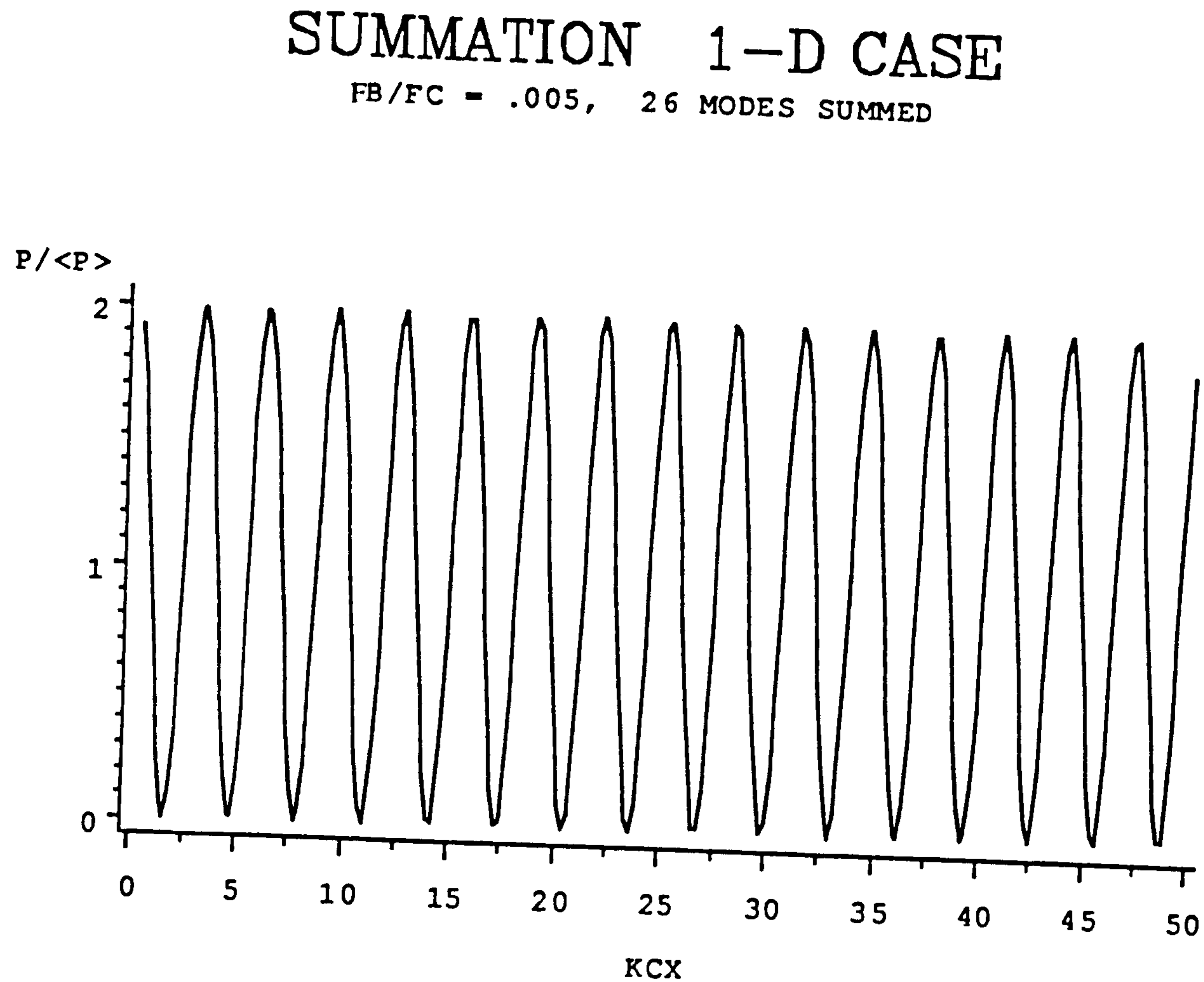


Figure 28. Non-dimensionalized pressure ratio versus $k_c x$ for the transition zone of a 1-dimensional cavity. Pressure calculation was made using summation. FB/FC = .005 which is similar to a tone. $Nref = \omega_c L_x / \pi c = 5000$, which defines the summation over 26 modes.

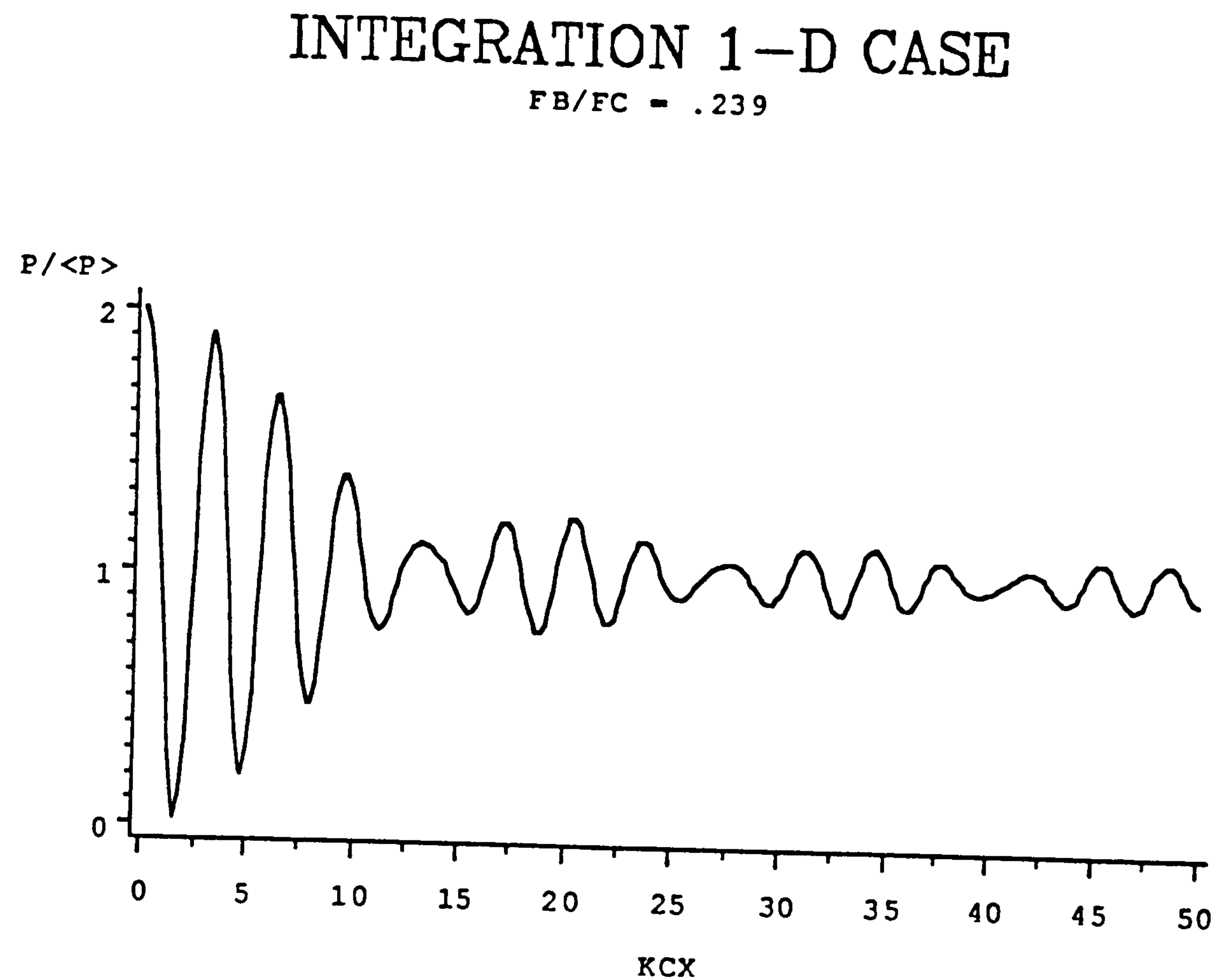


Figure 29. Non-dimensionalized pressure ratio versus $k_c x$ for the transition zone of a 1-dimensional cavity. Pressure calculation was made using integration. FB/FC = .239 which corresponds to a 1/3 octave band.

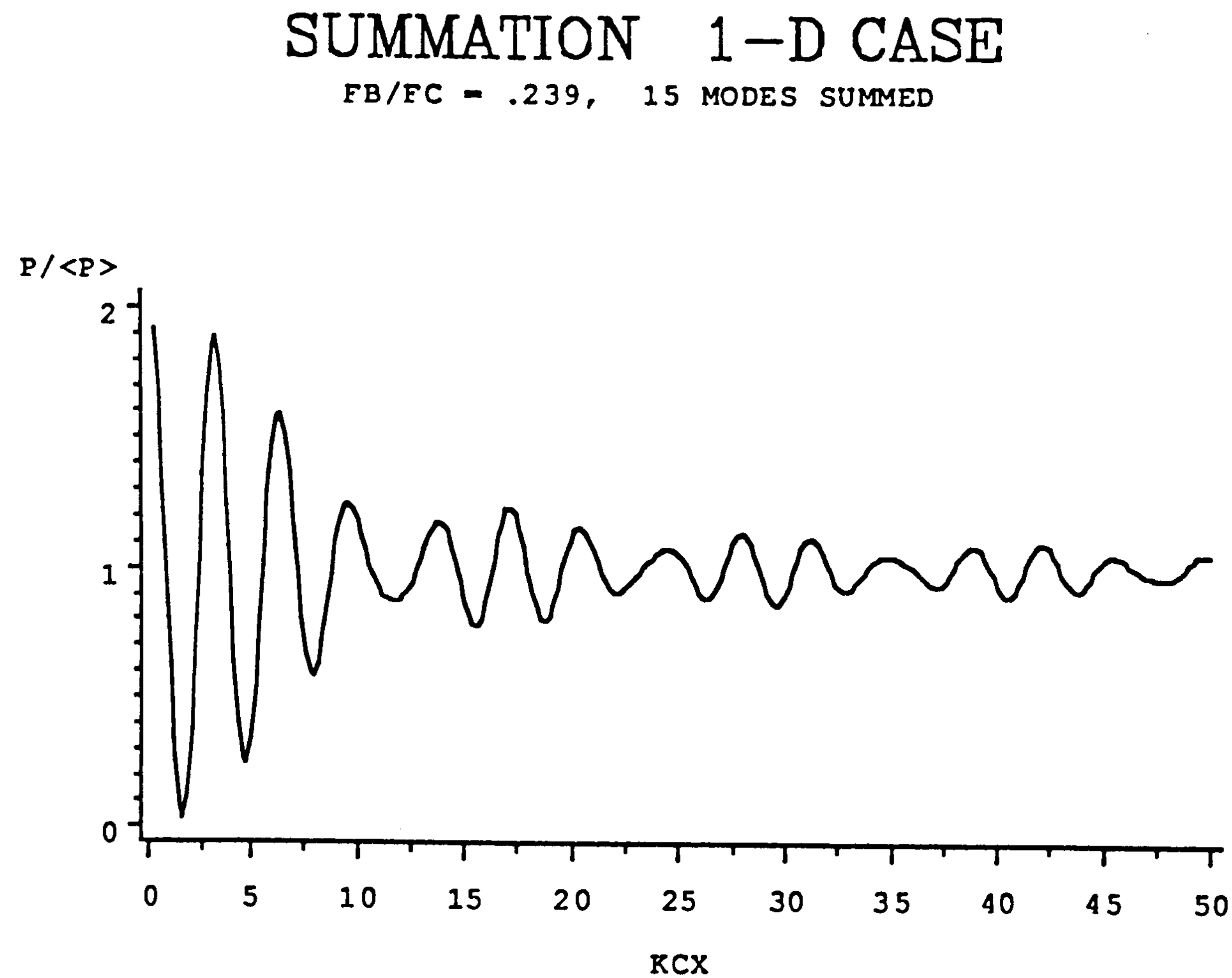


Figure 30. Non-dimensionalized pressure ratio versus $k_c x$ for the transition zone of a 1-dimensional cavity. Pressure calculation was made using summation. FB/FC = .239 which corresponds to a 1/3 octave band. Nref = $\omega_c L_x/\pi c$ = 60, which defines the summation over 15 modes.

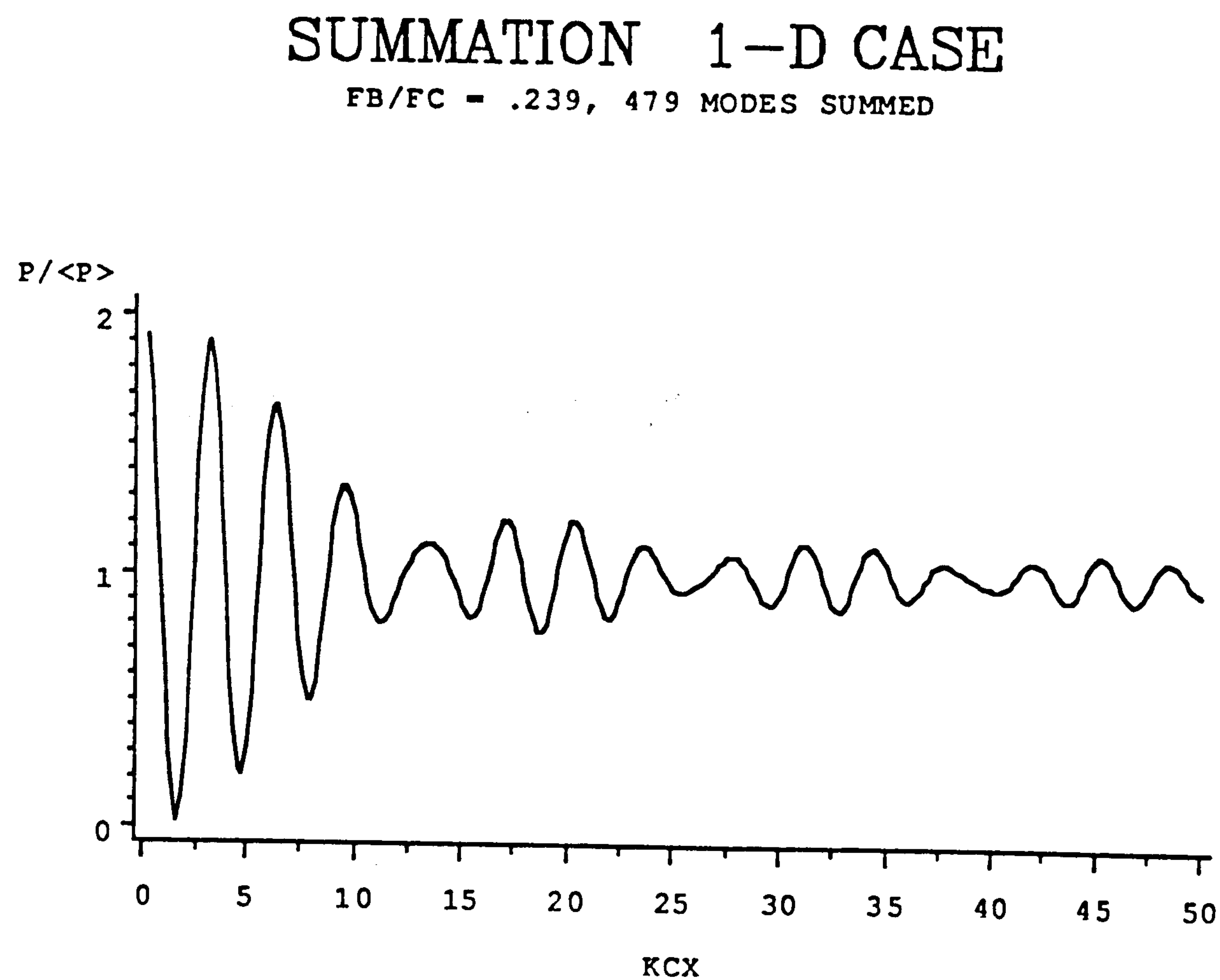


Figure 31. Non-dimensionalized pressure ratio versus $k_c x$ for the transition zone of a 1-dimensional cavity. Pressure calculation was made using summation. FB/FC = .239 which corresponds to a 1/3 octave band. Nref = $\omega_c L_x/\pi c$ = 2000, which defines the summation over 479 modes.

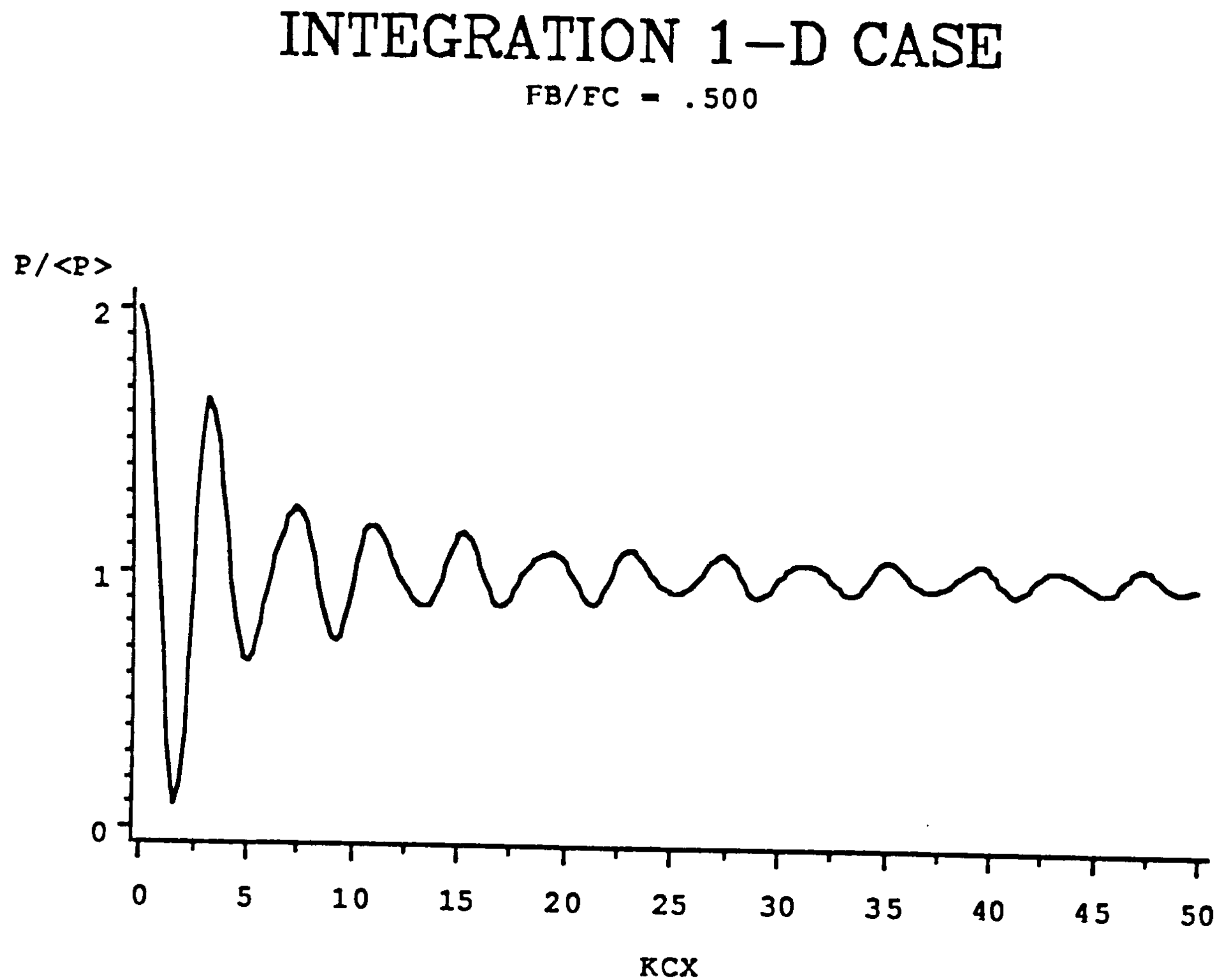


Figure 32. Non-dimensionalized pressure ratio versus $k_c x$ for the transition zone of a 1-dimensional cavity. Pressure calculation was made using integration. FB/FC = .500 which corresponds to an octave band.

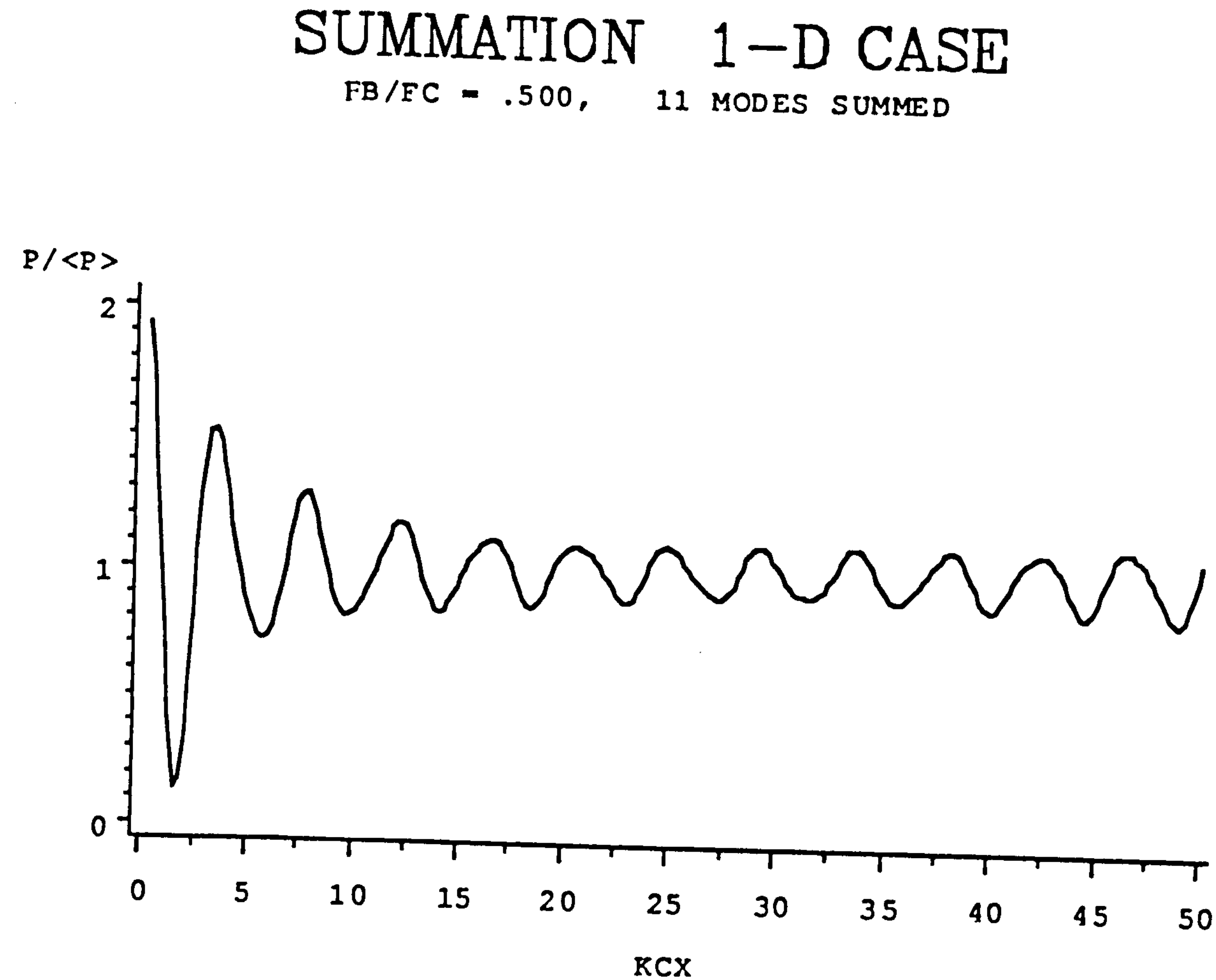


Figure 33. Non-dimensionalized pressure ratio versus $k_c x$ for the transition zone of a 1-dimensional cavity. Pressure calculation was made using summation. FB/FC = .500 which corresponds to an octave band. Nref = $\omega_c L_x/\pi c$ = 20, which defines the summation over 11 modes.

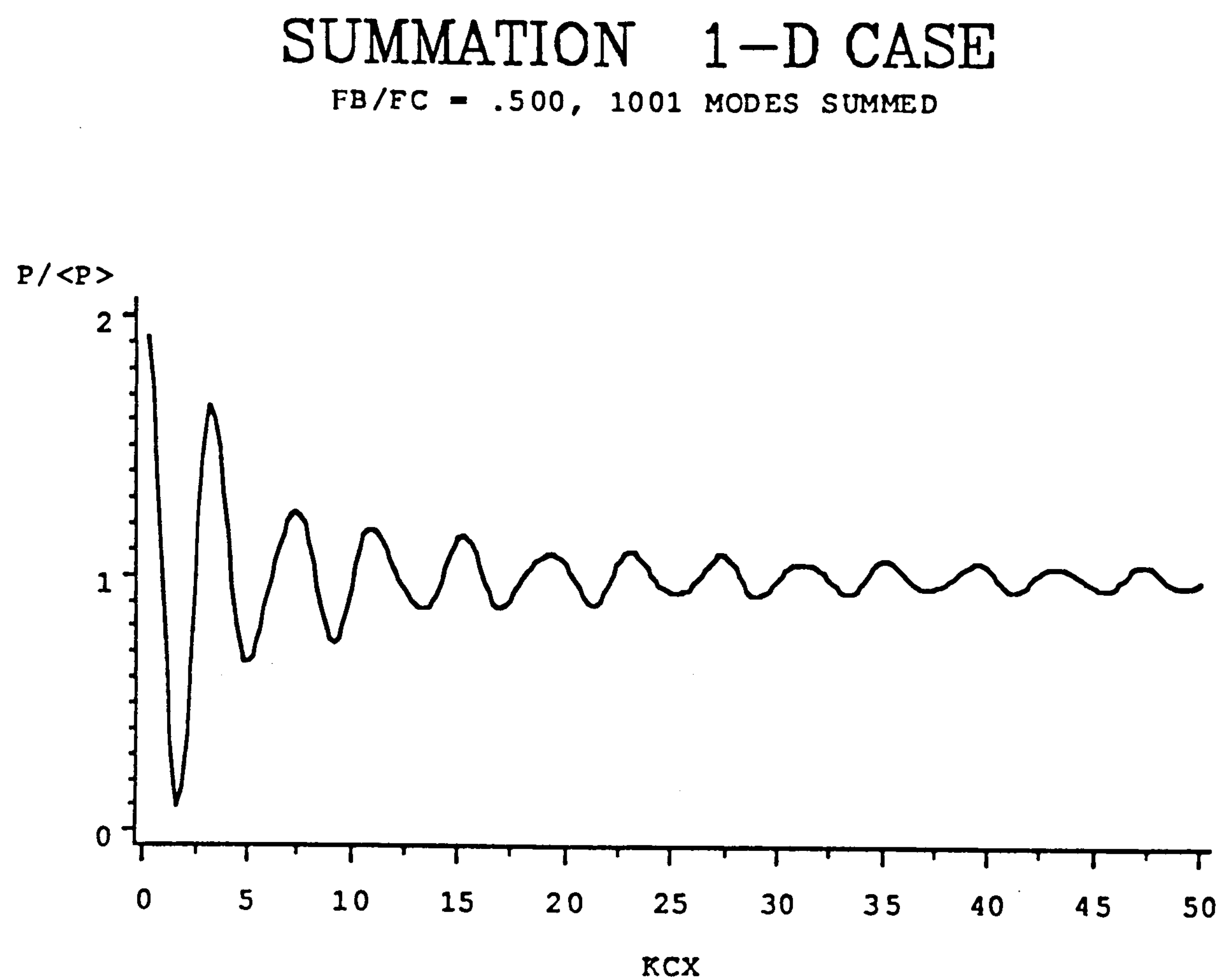


Figure 34. Non-dimensionalized pressure ratio versus $k_c x$ for the transition zone of a 1-dimensional cavity. Pressure calculation was made using summation. FB/FC = .500 which corresponds to an octave band. Nref = $\omega_c L_x / \pi c$ = 2000, which defines the summation over 1001 modes.

## Conclusion

An Asymptotic Modal Analysis approach has been developed and applied to a coupled structural-acoustic problem. It is broadly applicable to any linear dynamic system regardless of geometry. It is an extremely flexible approach, and can be developed in accord with the nature of the system under study through inclusion or exclusion of a series of simplifying assumptions. This technique can thereby bridge the gap between CMA and SEA in terms of computational requirements and predictive capability. Insofar as AMA is developed from Classical Modal Analysis, it retains the capability to predict spatial variations (intensification) in sound pressure levels or other relevant responses, something of which SEA is not capable. Simplifications arising from the nature of the forces and the number of structural and acoustic modes involved result in a process which does not require individual modal characteristics. This greatly reduces the number of calculations required relative to CMA.

A rectangular acoustic cavity, with five rigid walls, was chosen to investigate the capabilities of AMA. Spatial averages and local behavior for sound pressure levels were calculated for a number of cases involving the location and size of the sound source on the wall. For the spatially averaged cases, a strong effect of sound source location on average sound pressure levels in the cavity was noted. In particular, intensification due to source location was observed, such that, when a point sound source was located in the corner as opposed to the center of a wall, the spatially averged sound pressure ratio was increased by a factor of 4.

In addition to the spatial average, the local response was also calculated. Kubota, et.al. [4] found that the response of the cavity interior is nearly uniform, with the exception of points on the structural boundary (walls, edges, and corners), when one entire wall of the rectangular cavity is vibrating. However, when only a portion of one wall vibrates, and particularly when this portion approaches a vibrating point, there are further exceptions. Perpendicular lines ("hot lines") which run through the vibrating point were found to divide the cavity into sub-cavities, which have new corners, edges, and walls. On these newly defined sub-structural boundaries, the local response is also elevated. Such that, new corners, edges, and walls, exhibit the same relative increase as the original corners, edges and walls do, which is 8, 4 and 2 times greater than the interior, respectively. Kubota found similar "hot lines" in applying point forces to a rectangular plate [3].

The intensification zone for a 1-dimensional cavity was closely examined in the asymptotic limit. The shape of the sound pressure function, and therefore, the size of the intensification zone, were determined by a ratio of center frequency and frequency bandwidth. The length of the cavity did not play a role in determining the intensification zone. Extrapolating this result to the 2- and 3-dimensional cases, leads to the conclusion that the intensification zone is independent of the lengths (x, y, and z) of the cavity, and may therefore, be independent of the geometry of the cavity, as well.

## Future Work

The work which has been done, thus far, regarding the application of AMA to structural-acoustic systems, has assumed that the number of responding structural modes was infinite, i.e. AMA was invoked for the structural wall from the beginning. This allowed certain simplifications to be made in deriving the AMA result for the acoustic cavity, which would not be valid otherwise. Future work should include the derivation of an AMA result for the case of a finite number of responding structural modes, and an infinite number of acoustic modes. The case of a finite number of acoustic modes, and a finite number of structural modes is CMA for both the structural wall and the acoustic cavity.

The intensification zones are of importance for interior noise studies. Therefore, future work should include examination of the transition zone for the 2-dimensional and 3-dimensional cases, in addition to, the 1-dimensional case discussed in this thesis.

The previous work has been entirely theoretical and numerical. For verification of the AMA method, experiments should be performed and the results compared with the numerical results already obtained.

## References


1. Dowell, E.H., 1983 R82-112447, United Technologies Research Center. Vibration Induced Noise in Aircraft: Asymptotic Modal Analysis and Statistical Energy Analysis of Dynamical Systems.

2. Dowell, E.H., and Kubota, Y., 1985 ASME Journal of Applied Mechanics **107**, 949-957. Asymptotic Modal Analysis and Statistical Energy Analysis of Dynamical Systems.

3. Kubota,Y. and E. H. Dowell 1986 Journal of Sound and Vibration **106**, 203 - 216. Experimental investigation of asymptotic modal analysis for a rectangular plate.

4. Kubota, Y., H. D. Dionne and E. H. Dowell "Asymptotic Modal Analysis and Statistical Energy Analysis of an Acoustic Cavity," accepted for publication in Journal of Vibration, Acoustics, Stress and Reliablilty in Design .

5. Lyon, R.H., 1975 the MIT press, Cambridge, MA. Statistical Energy Analysis of Dynamical Systems: Theory and Applications.

6. S. H. Crandall 1979 in Developments in Statistics Volume 2 (editor P. R. Krishnaiah). New York: Academic Press, 1 - 82 . Random vibration of one- and two-dimensional structures.

7. K. Itao and S. H. Crandall 1978 American Society of Mechanical Engineers Journal of Mechanical Design **100**, 690 - 695. Wide-band random vibration of circular plates.

8. S. H. Crandall and A. P. Kulvets 1977 in Application of Statistics (editor P. R. Krishnaiah). North-Holand, 168 - 182. Source correlation effects on structural response.

9. Dowell, E. H., G. F. Gorman,III and D. A. Smith 1977 Journal of Sound and Vibration **52**, 519 - 542. Acoustoelasticity: General theory, acoustic natural modes and forced response to sinusoidal excitation, including comparisons with experiment.

# APPENDIX A: DERIVATION OF CMA AND AMA RESULTS FOR A RECTANGULAR ACOUSTIC CAVITY

The equation of motion describing the structural modes of the vibrating wall is (see Ref. 1, 2, and 3 for technical background).

$$M_m\left[\ddot{q}_m + 2\,\zeta_m\omega_m\dot{q}_m + \omega_m^{2} q_m\right] = Q_m^E \tag{1}$$

where the modal expansion for the wall deflection is

$$w = \sum_m q_m(t)\Psi_m(x,y) \tag{2}$$

the structural generalized mass is

$$M_m \equiv \iint_{A_f} m_p \Psi_m^{2}\, dx\, dy \tag{3}$$

and the generalized force due to a given external pressure is

$$Q_m^E \equiv \iint_{A_f} p^E \Psi_m\, dx\, dy \tag{4}$$

The acoustic cavity modal equation is:

$$\ddot{P}_r + 2\zeta_r^A \omega_r^A \dot{P}_r + \left(\omega_r^A\right)^2 P_r = Q_r^W \tag{5}$$

where the modal expansion for the acoustic cavity pressure is

$$p = \rho_o c_o^{2} \sum_r \frac{P_r(t) F_r(x,y,z)}{M_r^A} \tag{6}$$

the acoustic generalized mass is

$$M_r^A \equiv \frac{1}{V}\iiint_V F_r^{2}(x,y,z)\, dx\, dy\, dz \tag{7}$$

and the generalized acceleration due to the structural wall is

$$Q_r^W \equiv -\frac{1}{V}\iint_{A_f} \ddot{w}\, F_r\, dx\, dy \tag{8}$$

Define f, a non-dimensional cavity pressure,

$$f(t,x,y,z) \equiv \frac{p}{\rho_o c_o^2}$$

From (6) the auto-power spectrum of f may be determined as

$$\Phi_f(\omega,x,y,z) = \sum_r \sum_s \frac{F_r(x,y,z)}{M_r^A} \frac{F_s(x,y,z)}{M_s^A} \Phi_{P_r P_s} \tag{9}$$

where the cross-spectra are defined as

$$\Phi_{P_r P_s} \equiv \frac{1}{\pi} \int_{-\infty}^{\infty} R_{P_r P_s}(\tau)\, e^{iw\tau}\, d\tau \tag{10}$$

and the cross-correlations of the modal generalized pressure coordinates are

$$R_{P_r P_s} \equiv \lim_{T \to \infty} \frac{1}{2T} \int_{-T}^{T} P_r(t) P_s(t+\tau)\, dt \tag{11}$$

Similarly from (8) the cross-power spectra of $Q_r{}^W$ and $Q_s{}^W$ are

$$\Phi_{Q_r^w Q_s^w}(\omega) = \frac{1}{V^2} \iint_{Af} \iint_{Af} F_r\,(x,y,z)\, F_s\,(x^*,y^*,z^*)\, \Phi_{\ddot{w}}(w;x,y,z)\, dx\, dy\, dx^*\, dy^*$$

(12)

From (5) and standard random response theory, the relationship between $\Phi_{P_r P_s}$ and $\Phi_{Q_r{}^W Q_s{}^W}$ is

$$\Phi_{P_r P_s}(\omega) = H_r^A(\omega) H_s^A(-\omega)\, \Phi_{Q_r^w Q_s^w}(\omega) \tag{13}$$

where the modal transfer function is defined as

$$H_r^A(\omega) \equiv \frac{1}{\left[-\omega^2 + \left(\omega_r^A\right)^2 + 2i\zeta_r^A \omega_r^A \omega\right]} \tag{14}$$

From (9), (12), and (13)

$$\Phi_f(\omega;x,y,z) = \frac{1}{V^2} \sum_r \sum_s \frac{F_r(x,y,z)}{M_r^A} \cdot \frac{F_s(x,y,z)}{M_s^A} \cdot H_r^A(\omega) \cdot H_s^A(-\omega)$$

$$\cdot \iint_{Af} \iint_{Af} F_r(x,y,z_o) F_s(x^*,y^*,z_o^*)\, \Phi_{\ddot{w}}(\omega;x,y,x^*,y^*)\, dx dy dx^* dy^* \tag{15}$$

This is the basic expression for the power spectra of the cavity pressure in terms of the power spectra of the wall acceleration.

When the number of excited structural modes is large, $\Delta M \rightarrow \infty$, it can be shown that

$$\Phi_{\ddot{w}}(\omega;x,y,x^*,y^*) \cong A_f \Phi_{\ddot{w}}(\omega)\, \delta(x-x^*)\, \delta(y-y^*) \tag{16}$$

This means that the power spectra of the wall response is uncorrelated in space. This assumption is reasonable for large $\Delta M$, because

$$\frac{1}{\Delta M} \Phi_{\ddot{w}}(\omega;x,y,x^*,y^*) \rightarrow \frac{0 \qquad\qquad (x \neq x^*,\ y \neq y^*)}{\text{constant}\ (x = x^*,\ y = y^*)}$$

$$\text{as } \Delta M \rightarrow \infty \tag{17}$$

Recall, [Ref. 1,2]

$$\Phi_{\ddot{w}}(\omega;x,y,x^*,y^*) \cong \sum_m \sum_n \Psi_m(x,y) \Psi_n(x^*,y^*) \omega_m^2 H_m(\omega) H_n(-\omega)$$

$$\cdot \iint_{A_f} F_r(x,y,z_o) F_s(x,y,z_o)\, dx\, dy \tag{18}$$

(17) is readily derived from the above relationship and invoking the basic methods of AMA.

Also for a smoothly varying power spectrum, it is assumed that

$$\Phi_{\ddot{w}}(\omega) \cong \Phi_{\ddot{w}}(\omega_o) \tag{19}$$

This is just the usual white noise assumption. Thus, Eq. (15) becomes

$$\Phi_f(\omega;x,y,z) = \frac{A_f}{V^2} \cdot \Phi_{\ddot{w}}(\omega_o) \sum_r \sum_s \frac{F_r(x,y,z)}{M_r^A} \cdot \frac{F_s(x,y,z)}{M_s^A} \cdot H_r^A(\omega) \cdot H_s^A(-\omega)$$

$$\cdot \iint_{A_f} F_r(x,y,z_o) F_s(x,y,z_o)\, dx dy \tag{20}$$

The mean square response of the non-dimensional cavity pressure is

$$\overline{f}^2 \equiv \frac{\overline{p}^2(x,y,z)}{\left(\rho_o c_o^2\right)^2} = \int_0^\infty \Phi_f(\omega;x,y,z)\, d\omega$$

$$\cong \frac{\pi}{4}\frac{A_f}{V^2}\Phi_{\ddot{w}}(\omega_c) \sum_r \frac{F_r^2(x,y,z)}{\left(M_r^A\right)^2 \omega_r^{A^3} \zeta_r^A} \iint_{A_f} F_r^2\,(x,y,z_o)\, dxdy$$

(21)

This is the local CMA result which is referred to in this thesis. Note, that the structural wall is assumed to vibrate in an infinite number of modes, hence this result is AMA for the structural wall, but CMA for the acoustic cavity, (i.e. a finite number of acoustic modes).

Taking a spatial average of (21), and noting that $(M_r{}^A)^2$, $(\omega_r{}^A)^3$, $(\zeta_r{}^A)$, and $\langle F_r{}^2\rangle$ do not vary rapidly with respect to modal number, r, for large $\Delta N_A$, Eq. (21) becomes

$$\frac{\left\langle \overline{p}^2 \right\rangle}{\left(\rho_o c_o^2\right)^2} \cong \frac{\pi}{4}\frac{A_f}{V^2}\Phi_{\ddot{w}}(\omega_c)\frac{\left\langle F_c^2 \right\rangle}{M_c^{A^2}\,\omega_c^{A^3}\,\zeta_c} \sum_r \iint_{A_f} F_r^2(x,y,z_o)\, dxdy \qquad (22)$$

which is the spatially averaged CMA result referred to in the thesis.

Now consider a cavity acoustic modal function

$$F_r(x,y,z) = X_r(x)Y_r(y)Z_r(z) \qquad (23)$$

Take the plane at $z = z_o$ as the boundary of the acoustic cavity where the structural wall is vibrating. $Z_r(z_o)$ is usually independent of mode number r or it can be so normalized. Thus, for large $\Delta N^A$,

$$\sum_r \iint_{A_f} F_r^2(x,y,z_o)\, dx\, dy = \sum_r A_f \left\langle X_r^2 \right\rangle_{A_f} \left\langle Y_r^2 \right\rangle_{A_f} \left\langle Z_r^2(z_o) \right\rangle_{A_f}$$

which reduces to:

$$A_f \; \Delta N^A \frac{\langle F_c^2 \rangle}{\langle Z_c^2 \rangle}$$

where

$$\langle Z_c^2 \rangle \equiv \frac{\langle F_c^2 \rangle}{\langle F_c^2 \rangle_{A_F}}$$

and

$$M_c^A \equiv \langle F_c^2 \rangle$$

$$\langle \ddot{w}^2 \rangle_{\Delta\omega} \equiv \Delta\omega \, \Phi_{\ddot{w}}(\omega_c)$$

< . . . .> denotes spatial average. $<F_c^2>$ is a volume average of $F_c^2$, and $<F_c^2>_{Af}$ is an area average over the vibrating structural wall. Hence, eq.(22) becomes as $\Delta N^A \to \infty$,

$$\frac{\langle \overline{p}^2 \rangle}{\left(\rho_o c_o^2\right)^2} \cong \frac{\pi}{4} \frac{\Delta N^A}{\Delta\omega^A} \left(\frac{A_f}{V}\right)^2 \frac{\langle \ddot{w}^2 \rangle_{\Delta\omega}}{\omega_c^{A^3} \, \zeta_c^A \langle Z_c^2 \rangle} \tag{24}$$

Now $$\langle \ddot{w}^2 \rangle_{\Delta\omega} \cong \omega_c^4 \langle \overline{w}^2 \rangle_{\Delta\omega} \tag{25}$$

and from the AMA results for structural wall motion,

$$\langle \overline{w}^2 \rangle_{\Delta\omega} \cong \frac{\pi}{4} \frac{\Delta M}{\Delta\omega} \frac{\langle \overline{F}^2 \rangle_{\Delta\omega}}{M_p^2 \, \omega_c^3 \, \zeta_c} \tag{26}$$

Finally then, Eq. (24) becomes

$$\frac{\langle \overline{p}^2 \rangle}{\left(\rho_o c_o^2\right)^2} \cong \left(\frac{\pi}{4}\right)^2 \frac{\Delta M}{\Delta\omega} \frac{\Delta N^A}{\Delta\omega^A} \left(\frac{A_f}{V}\right)^2 \frac{\Delta\omega^A}{\Delta\omega} \frac{\omega_c \langle \overline{F}^2 \rangle_{\Delta\omega}}{\omega_c^{A^3} \, \zeta_c^A \, \zeta_c \, M_p^2 \langle Z_c^2 \rangle} \tag{27}$$

This is the spatially averaged AMA result, which is used in the denominator of the non-dimensionalized pressure ratios throughout this thesis. (AMA is applied to both the structural wall and the acoustic cavity).

To obtain the local Asymptotic Modal Analysis (AMA) result from the local CMA result (equation (21)), further assume the acoustic generalized mass squared $(M_r^A)^2$, the frequency of the acoustic mode cubed $(\omega_r^A)^3$, and the acoustic damping $(\zeta_r^A)$, do not vary rapidly with respect to modal number r and can therefore be replaced by their values at the center frequency, $(M_c^A)^2$, $(\omega_c^A)^3$, and $(\zeta_c^A)$. Moreover, the expression $\sum F_r^2(x,y,z) \iint F_r^2(x,y,z_0)\,dx\,dy$ is approximately equal to the average of $F_r^2(x,y,z)$ times $\sum\iint F_r^2(x,y,z_0)dxdy$ as $r \rightarrow \infty$, (i.e. a large number of acoustic modes):

$$\sum_r F_r^2(x,y,z)\iint_{A_f} F_r^2(x,y,z_0)dxdy \cong \frac{\sum_r F_r^2(x,y,z)}{\Delta N^A}\sum_r\iint_{A_f} F_r^2(x,y,z_0)dxdy$$

$\sum\iint F_r^2(x,y,z_0)\,dx\,dy$ can be further simplified by:

$$\sum_r\iint_{A_f} F_r^2(x,y,z_0)\,dx\,dy = \sum_r A_f \left\langle X_r^2\right\rangle_{A_f}\left\langle Y_r^2\right\rangle_{A_f}\left\langle Z_r^2(z_0)\right\rangle_{A_f}$$

which reduces to:

$$A_f\ \Delta N^A\frac{\left\langle F_c^2\right\rangle}{\left\langle Z_c^2\right\rangle}$$

where $\langle Z_c^2 \rangle = \langle F_c^2 \rangle / \langle F_c^2 \rangle_{Af}$. $\langle F_c^2 \rangle$ is a volume average, and $\langle F_c^2 \rangle_{Af}$ is an average over the vibrating structural wall area.

Then,

$$\frac{\overline{p}^2}{\left(\rho_o c_o^2\right)^2} \cong \frac{\pi}{4} \frac{A_f}{V^2} \Phi_{\ddot{w}}(\omega_c) \frac{A_f \, \Delta N^A \left\langle F_c^2 \right\rangle}{\left(M_c^A\right)^2 \left(\omega_c^A\right)^3 \zeta_c^A \left\langle Z_c^2 \right\rangle} \sum_r \frac{F_r^2(x,y,z)}{\Delta N^A}$$

This is the AMA representation for the local response.

# APPENDIX B: COMPUTER PROGRAMS

MAIN PROGRAM

```
C   CALCULATES CMA TO AMA RATIO FOR CAVITY X_LENGTH
C   BY Y_LENGTH BY Z_LENGTH
C   FLEXIBLE PLATE ON ONE WALL VARIABLE
C
C   ASSUMES ACOUSTICAL AND STRUCTURAL DAMPING ARE EQUAL
C
C
C   INPUT:  STORED IN FILE CAVITY.IN,  FREE FORMAT
C       SPEED OF SOUND
C       X_LENGTH, Y_LENGTH, Z_LENGTH
C
C       ALSO, NEEDED FOR PART OF WALL FLEXIBLE:
C       XW0, YW0   THE X & Y COORDINATES OF FLEX PART
C       AW, BW     THE X & Y DIMENSIONS OF FLEX PART
C
C       number of locations - as well as the x,y,z components
C
    REAL*8      BANDWIDTH
C                   DIFFERENCE IN UPPER AND LOWER
C                   FREQUENCY BOUNDS
C
    INTEGER*4   BW_LOOP
C                   LOOP INDEX FOR BANDWIDTH
C
    REAL*8      C
C                   SPEED OF SOUND
C
C
    REAL*8      CENTER_FREQ
C                   CENTER FREQUENCY OF BANDWIDTH
C                   DEFINED AS SQUARE ROOT OF THE
C                   PRODUCT OF THE UPPER AND LOWER
C                   FREQUENCY BOUNDS
C
    INTEGER*4   CFREQ_LOOP
C                   LOOP INDEX FOR CENTER FREQUENCY
C
    REAL*8      CMA_TO_AMA_RATIO
C                   RATIO OF MEAN SQUARE RESPONSE OF
C                   CAVITY PRESSURE OBTAINED FROM
C                   CLASSICAL MODAL ANALYSIS TO THAT
```

```
C                   DERIVED FROM ASYMPTOTIC MODAL
C                    ANALYSIS
C
   INTEGER*2    INPUT_UNIT1
C                    INPUT UNIT
C                    READS FROM "CAVITY.IN"
C
   INTEGER*4    INDEX
C                    VALUE OF INDEXING LOOP PASSED
C                    TO SUBROUTINE VARFREQ
C
   REAL*8      LOWER_FREQ
C                    LOWER FREQUENCY IN BANDWIDTH
C
   LOGICAL     MODE_CHECK
C                    ERROR CODE FROM SUBROUTINE MODES
C                    TRUE IF MODES EXIST IN SPECIFIED
C                    BANDWIDTH, FALSE IF NO MODES ARE
C                    FOUND
C
   INTEGER*4    NUMBER_OF_MODES
C                    NUMBER OF MODES IN BANDWIDTH
C
   INTEGER*2    OUTPUT_UNIT1
C                    OUTPUT UNIT FOR PLOTTING DATA
C                    WRITES TO "CARAT.PLT"
C
   INTEGER*2    OUTPUT_UNIT2
C                    OUTPUT UNIT FOR ERROR MESSAGES
C                    WRITES TO "CARAT.ERR"
C
C
   INTEGER*2    OUTPUT_UNIT3
C                    OUTPUT UNIT FOR PRINTED OUTPUT
C                    WRITES TO "CARAT.OUT"
C
   REAL*8      UPPER_FREQ
C                    UPPER FREQUENCY IN BANDWIDTH
C
   REAL*8      X_LENGTH, Y_LENGTH, Z_LENGTH
C                    ROOM DIMENSIONS
C
```

```
      REAL*8      XW0, YW0
C                     COORDINATES OF FLEX PART
C
      REAL*8      AW, BW
C                     DIMENSIONS OF THE FLEXIBLE PART
C
      integer*2   num_loc
c                     number of locations
c
      integer*2   restart
c                     Restart = 1 (restarting from a previous run)
c                     Restart = 0  Fresh start : everything new
c
      integer*2   BWopt
c                     BWopt = 1  user specifies the bandwidth
c                     BWopt = 0  200, 400, 600 bandwidths done
c                            for 30 center frequencies
c
      integer     count
c
      INPUT_UNIT1 = 50
      OUTPUT_UNIT1 = 55
      OUTPUT_UNIT2 = 56
      OUTPUT_UNIT3 = 57
C
      BANDWIDTH  = 0.0
      LOWER_FREQ = 0.0
      UPPER_FREQ = 0.0
C
      MODE_CHECK = .TRUE.
C
      FREQ_COUNT = 0
      CMA_TO_AMA_RATIO = 0.0
C
C     READ IN SIZE OF ROOM AND SPEED OF SOUND
C
      OPEN(UNIT=INPUT_UNIT1,ERR=300,FILE="CAVITY.IN",STATUS='OLD')

      READ(INPUT_UNIT1,*) C
      READ(INPUT_UNIT1,*) X_LENGTH, Y_LENGTH, Z_LENGTH
      read(input_unit1,*) xw0, yw0
      read(input_unit1,*) aw, bw
```

```
      read(input_unit1,*) num_loc
      read(input_unit1,*) restart
      read(input_unit1,*) BWopt
      CLOSE(UNIT=INPUT_UNIT1)
C
       OPEN(UNIT=OUTPUT_UNIT1,ERR=310,FILE="space.out",STATUS='NEW')


c
OPEN(UNIT=OUTPUT_UNIT2,ERR=320,FILE="CARAT.ERR",STATUS='NEW')

c
OPEN(UNIT=OUTPUT_UNIT3,ERR=330,FILE="CARAT.OUT",STATUS='NEW')

      if(restart.eq.1) then
        open(unit=53, file = "weights.out", status = 'old')
      else
        open(unit=54, file = "weights.out", status = 'new')
      endif
C
      WRITE(OUTPUT_UNIT1,FMT=500) C
      WRITE(OUTPUT_UNIT1,FMT=501) X_LENGTH, Y_LENGTH, Z_LENGTH

      WRITE(OUTPUT_UNIT1,FMT=555) XW0, YW0, AW, BW
      write(output_unit1,fmt=551) num_loc,restart,bwopt
C
c     User may just be interested in one bandwidth
c
      if (bwopt.eq.1) then
        open (51, file="inputbw.dat", status = 'old')
       read (51, *) upper_freq, lower_freq
         count = 1
         CALL MODES(UPPER_FREQ,LOWER_FREQ,X_LENGTH,Y_LENGTH,
     &        Z_LENGTH,count,xw0,yw0,aw,bw,C,num_loc,restart,
     &        CMA_TO_AMA_RATIO,MODE_CHECK,NUMBER_OF_MODES)

       write (6,*) num_loc,restart,c
         go to 100
     else
c
     DO CFREQ_LOOP = -2,27
       CENTER_FREQ = 600. + FLOAT(CFREQ_LOOP) * 200.
```

```
      WRITE(OUTPUT_UNIT1,FMT=502) CENTER_FREQ
c     WRITE(OUTPUT_UNIT2,FMT=400) CENTER_FREQ
c     WRITE(OUTPUT_UNIT3,FMT=502) CENTER_FREQ
c     WRITE(OUTPUT_UNIT3,FMT=550)
c     WRITE(OUTPUT_UNIT3,FMT=505)
c     WRITE(OUTPUT_UNIT3,FMT=550)
C
c      DO BW_LOOP = 1,5,2
      do bw_loop = 3,3
       INDEX = BW_LOOP
       CALL VARBW(INDEX,CENTER_FREQ,UPPER_FREQ,LOWER_FREQ,
     &              BANDWIDTH)
       if (center_freq.eq.200.) then
         count = 1
         else
         count = 0
       endif
       CALL MODES(UPPER_FREQ,LOWER_FREQ,X_LENGTH,Y_LENGTH,
     &       Z_LENGTH,count,xw0,yw0,aw,bw,C,num_loc,restart,
     &         CMA_TO_AMA_RATIO,MODE_CHECK,NUMBER_OF_MODES)

      ENDDO
    ENDDO
    endif
C
 100  CLOSE(UNIT=OUTPUT_UNIT1)
c   CLOSE(UNIT=OUTPUT_UNIT2)
c   CLOSE(UNIT=OUTPUT_UNIT3)
C
    WRITE(6,FMT=800)
C
    GO TO 1000
C
 200 FORMAT(2(F10.4,5X))
C
 300 WRITE(6,301)
 301 FORMAT(5X,'***ERROR ENCOUNTERED ACCESSING INPUT FILE
CAVITY.IN')
    GO TO 1000
 310 WRITE(6,311)
 311 FORMAT(5X,'***ERROR ENCOUNTERED ACCESSING OUTPUT FILE
CARAT.PLT')
```

```
   GO TO 1000
 320 WRITE(6,321)
 321 FORMAT(5X,'***ERROR ENCOUNTERED ACCESSING OUTPUT FILE
CARAT.ERR')
   GO TO 1000
 330 WRITE(6,331)
 331 FORMAT(5X,'***ERROR ENCOUNTERED ACCESSING OUTPUT FILE
CARAT.OUT')
   GO TO 1000
C
 400 FORMAT(2X,'ERROR MESSAGES FOR CARCF WITH CENTER FREQUENCY
= ',
   &      F10.3,' HZ')
 420 FORMAT(2X,'NO MODES FOUND IN BANDWIDTH OF ',F10.3,' HZ')
C
 500 FORMAT(2X,'SPEED OF SOUND IS ',F10.2)
 501 FORMAT(2X,'CAVITY IS ',F10.3,' FT BY ',F10.3, ' FT BY ',F10.3,' FT

   &')
 502 FORMAT(2X,'CENTER FREQUENCY IS ',F10.3,' HZ')
 505 FORMAT(5X,'   BANDWIDTH    ',4X,'CMA TO AMA RATIO',4X,
   &       'NUMBER OF MODES IN BAND')
 510 FORMAT(5X,F10.2,18X,F8.5,10X,I5)
 550 FORMAT(5X,' ')
 551 format(5x,'number of points =',1x,i3,5x,'options are:'/,
   *      45x,'restart opt - ',i2,/,45x,'bandwidth opt - ',i2,/)
 555 FORMAT(2X,'FLEXIBLE PART BEGINS AT   X =',F10.3,'Y =',F10.3,
   &/,2X,'FLEXIBLE DIMENSIONS ARE: ',F10.3,'BY',F10.3,/)
C
 800 FORMAT(2X,'OUTPUT IS IN CARAT.OUT, POINTS FOR PLOTTING ARE IN
CARA
   &T.PLT')
C
 1000 CONTINUE
C
   STOP
   END
```

USED FOR SPATIALLY AVERAGED CMA/SPATIALLY AVERAGED AMA RATIO

```
      SUBROUTINE MODES(UPPER_BOUND,LOWER_BOUND,
     &            X_LENGTH,Y_LENGTH,Z_LENGTH,
     &             xw0, yw0, aw, bw, C,
     &            CMA_TO_AMA_RATIO,ERROR_CODE,
     &            FREQ_COUNT)
C
C     CALCULATES NATURAL FREQUENCIES OF ROOM
C     X_LENGTH BY Y_LENGTH BY Z_LENGTH
C
C
      REAL*8      BANDWIDTH
C                       DIFFERENCE BETWEEN UPPER AND
C                       LOWER FREQUENCY LIMITS
C
      REAL*8      C
C                       SPEED OF SOUND
C
C
      REAL*8      CENTER_FREQ
C                       CENTER FREQUENCY OF BANDWIDTH
C                       DEFINED AS SQUARE ROOT OF THE
C                       PRODUCT OF THE UPPER AND LOWER
C                       FREQUENCY BOUNDS
C
      REAL*8      CMA_TO_AMA_RATIO
C                       RATIO OF MEAN SQUARE RESPONSE OF
C                       CAVITY PRESSURE OBTAINED FROM
C                       CLASSICAL MODAL ANALYSIS TO THAT
C                       DERIVED FROM ASYMPTOTIC MODAL
C                       ANALYSIS
C
      LOGICAL     ERROR_CODE
C                       .TRUE. RETURNED IF MODES ARE FOUND
C                       WITHIN THE SPECIFIED BANDWIDTH
C                       .FALSE. RETURNED IF NO MODES
C                       ARE FOUND
C
      INTEGER*4   FREQ_COUNT
C                       COUNTS NUMBER OF ACOUSTICAL
C                       MODES IN SPECIFIED BANDWIDTH
C
```

```
      REAL*8      FREQUENCY
C                     NATURAL FREQUENCY OF MODE
C
      INTEGER*2   I
C                     INDEXING PARAMETER
C
      INTEGER*4   INTEGRAL_WEIGHT(10000)
C
C
      REAL*8      LOWER_BOUND
C                     LOWER FREQUENCY IN BANDWIDTH
C
C
      REAL*8      SORTMAT(10000)
C                     MATRIX OF FREQUENCY VALUES
C
      REAL*8      UPPER_BOUND
C                     UPPER FREQUENCY IN BANDWIDTH
C
      REAL*8      X_LENGTH, Y_LENGTH, Z_LENGTH,a,b,l,m
C                     ROOM DIMENSIONS
C
      real*8      fintegral(10000)
c                     vector of integral of modal function
c                     of flexible wall over the flex portion
c
      INTEGER*2   XMODE,YMODE,ZMODE
C                     INDEXING PARAMETER FOR MODES
C
      INTEGER*2   XMODEMAX,YMODEMAX,ZMODEMAX
C                     MAXIMUM MODE INDEX
C
C   INITIALIZE SORTMAT TO ZERO, INTEGRAL_WEIGHT TO 2
C
      REAL*8      XW0, YW0
C                     COORDINATES OF FLEX PART OF WALL
      REAL*8      AW, BW
C                     DIMENSIONS OF FLEX PART OF WALL
C
C
      real*8      f1, f2, f3, f4, f5, f6, f7, f8, f9
c                     separate terms in integral
```

```
c
      pi = 3.1415925
      a = x_length
      b = y_length
      X0 = XW0/A
      Y0 = YW0/B
      AWA = AW/A
      BWB = BW/B
C
      DO I = 1,10000
        SORTMAT(I) = 0.0
        INTEGRAL_WEIGHT(I) = 2
      ENDDO
C
      FREQ_COUNT = 0
      ERROR_CODE = .TRUE.
C
      CENTER_FREQ = DSQRT(LOWER_BOUND * UPPER_BOUND)
      BANDWIDTH = UPPER_BOUND - LOWER_BOUND
C
C   CALCULATE MAXIMUM MODE INDICIES FOR SPECIFIED BAND
C
      XMODEMAX = INT(UPPER_BOUND * 2.0 * X_LENGTH / C ) + 2
      YMODEMAX = INT(UPPER_BOUND * 2.0 * Y_LENGTH / C ) + 2
      ZMODEMAX = INT(UPPER_BOUND * 2.0 * Z_LENGTH / C ) + 2
C
      DO XMODE = 0, XMODEMAX
        DO YMODE = 0, YMODEMAX
          DO ZMODE = 0, ZMODEMAX
           if (freq_count.gt.10000) go to 200
             FREQUENCY = .5 * C * DSQRT((XMODE/X_LENGTH)**2.0
     &                   + (YMODE/Y_LENGTH)**2.0
     &                   + (ZMODE/Z_LENGTH)**2.0)
             IF ((FREQUENCY .GE. LOWER_BOUND ) .AND.
     &             (FREQUENCY .LE. UPPER_BOUND)) THEN
                 FREQ_COUNT = FREQ_COUNT + 1
                 SORTMAT(FREQ_COUNT) = FREQUENCY
                 IF (ZMODE .EQ. 0) THEN
                    INTEGRAL_WEIGHT(FREQ_COUNT) = 1
                 ELSE
                    CONTINUE
                 ENDIF
```

```
C     for portion of wall flexible the following has been added:
      L = XMODE * 2 * PI
      M = YMODE * 2 * PI
C
      F1 = AW * BW
c
         if (xmode.eq.0) then
           f2 = AW * BW
           f3 = 0.
           go to 60
         endif
c
      F2 = BW * (A/L) * COS(L*X0) * SIN(L*AWA)
      F3 = BW * (A/L) * SIN(L*X0) * (COS(L*AWA) -1)
c
 60      if (ymode.eq.0) then
           f4 = AW * BW
           f5 = 0.
           go to 70
         endif
c
      F4 = AW * (B/M) * COS(M*Y0) * SIN(M*BWB)
      F5 = AW * (B/M) * SIN(M*Y0) * (COS(M*BWB) - 1)
C
 70      if ((xmode.eq.0).and.(ymode.eq.0)) then
           f6 = aw * bw
           f7 = 0.
           f8 = 0.
           f9 = 0.
           go to 100
         endif
c
         if (xmode.eq.0) then
           f6 = f4
           f7 = f5
           f8 = 0.
           f9 = 0.
           go to 100
         endif
c
         if (ymode.eq.0) then
           f6 = f2
```

```
          f7 = 0.
          f8 = f3
          f9 = 0.
          go to 100
        endif
c
c
     F6 = (A/L) * (B/M) * COS(L*X0) * COS(M*Y0) * SIN(L*AWA) *
   *     SIN(M*BWB)
     F7 = (A/L) * (B/M) * COS(L*X0) * SIN(M*Y0) * SIN(L*AWA) *
   *     (COS(M*BWB) - 1)
     F8 = (A/L) * (B/M) * COS(M*Y0) * SIN(L*X0) * SIN(M*BWB) *
   *     (COS(L*AWA) - 1)
     F9 = (A/L) * (B/M) * SIN(L*X0) * SIN(M*Y0) * (COS(L*AWA)
   *     - 1) * (COS(M*BWB) - 1)
 100   FINTEGRAL(freq_count) = F1 + F2 + F3 + F4 + F5 + F6 + F7
   *                  + F8 + F9
C
c  Now we need to divide by whole wall moving integral -
c    since original program was for whole wall moving.
c
        fintegral(freq_count) = fintegral(freq_count)/(a*b)
c
c       special consideration given to the case(s) where xmode,
c               ymode are zero!
c
        if ((xmode.eq.0).and.(ymode.eq.0)) then
                fintegral(freq_count) = fintegral(freq_count)*.25
                go to 120
        endif
c
        if ((xmode.eq.0).or.(ymode.eq.0)) then
                fintegral(freq_count) = fintegral(freq_count)*.50
                go to 120
        endif
c
 120    continue
c
              ELSE
C                THE MODE IS NOT WITHIN THE DESIRED BANDWIDTH

                     CONTINUE
```

```
              ENDIF
C
            ENDDO
          ENDDO
        ENDDO
C
C
        IF (FREQ_COUNT .GT. 0) THEN
200       CALL
RATIO(CENTER_FREQ,FREQ_COUNT,SORTMAT,INTEGRAL_WEIGHT,
     &           fintegral, x_length,y_length, aw, bw,
     &           CMA_TO_AMA_RATIO)
        ELSE
          ERROR_CODE = .FALSE.
        ENDIF
C
        RETURN
        END
```

```
USED FOR LOCAL CMA/SPATIALLY AVERAGED AMA RATIO
    SUBROUTINE MODES(UPPER_BOUND,LOWER_BOUND,
   &            X_LENGTH,Y_LENGTH,Z_LENGTH,count,
   &            xw0, yw0, aw, bw, C,num_loc,restart,
   &            CMA_TO_AMA_RATIO,ERROR_CODE,
   &            FREQ_COUNT)
C
c
c   this version is designed to be compatible with 6-24-87 version
c      of CARCF
c
C   CALCULATES NATURAL FREQUENCIES OF ROOM
C   X_LENGTH BY Y_LENGTH BY Z_LENGTH
C
C
    integer    count
    REAL*8     BANDWIDTH
C                   DIFFERENCE BETWEEN UPPER AND
C                   LOWER FREQUENCY LIMITS
C
    REAL*8     C
C                   SPEED OF SOUND
C
C
    REAL*8     CENTER_FREQ
C                   CENTER FREQUENCY OF BANDWIDTH
C                   DEFINED AS SQUARE ROOT OF THE
C                   PRODUCT OF THE UPPER AND LOWER
C                   FREQUENCY BOUNDS
C
    REAL*8     CMA_TO_AMA_RATIO
C                   RATIO OF MEAN SQUARE RESPONSE OF
C                   CAVITY PRESSURE OBTAINED FROM
C                   CLASSICAL MODAL ANALYSIS TO THAT
C                   DERIVED FROM ASYMPTOTIC MODAL
C                   ANALYSIS
C
    LOGICAL    ERROR_CODE
C                   .TRUE. RETURNED IF MODES ARE FOUND
C                   WITHIN THE SPECIFIED BANDWIDTH
C                   .FALSE. RETURNED IF NO MODES
C                   ARE FOUND
```

```
C
      INTEGER*4    FREQ_COUNT
C                      COUNTS NUMBER OF ACOUSTICAL
C                      MODES IN SPECIFIED BANDWIDTH
C
      REAL*8       FREQUENCY
C                      NATURAL FREQUENCY OF MODE
C
      INTEGER*2    I
C                      INDEXING PARAMETER
C
C
C
      REAL*8       LOWER_BOUND
C                      LOWER FREQUENCY IN BANDWIDTH
C
C
C
      REAL*8       UPPER_BOUND
C                      UPPER FREQUENCY IN BANDWIDTH
C
       REAL*8       X_LENGTH, Y_LENGTH, Z_LENGTH,a,b,l,m,x0,y0,awa,bwb

C                      ROOM DIMENSIONS
C
      real*8      fintegral
c                      integral of modal function
c                      of flexible wall over the flex portion
      real*8      flex_int(10000)
c                      storage of fintegral
      real*8      wt(10000)
c                      storage of weight
c
      INTEGER*2    XMODE,YMODE,ZMODE
C                      INDEXING PARAMETER FOR MODES
C
      INTEGER*2    XMODEMAX,YMODEMAX,ZMODEMAX
C                      MAXIMUM MODE INDEX
C
C   INITIALIZE SORTMAT TO ZERO, INTEGRAL_WEIGHT TO 2
C
      REAL*8       XW0, YW0
```

```
C                   COORDINATES OF FLEX PART OF WALL
      REAL*8      AW, BW
C                   DIMENSIONS OF FLEX PART OF WALL
C
C
C
      real*8      f1, f2, f3, f4, f5, f6, f7, f8, f9
c                   separate terms in integral
c
C     NOT SPATIALLY AVERAGED
C
C
      REAL*8      ARGX,ARGY,ARGZ
C
C
      INTEGER*2   INPUT_UNIT1
C                   READS FROM CAVITY.IN
C
      INTEGER*2   LOCATION
C                   INDEXING PARAMETER
C
      INTEGER*2   LOOP
C                   INDEXING PARAMETER
C
C
C
C
      REAL*8      MODE(10000)
C                   MATRIX OF FREQUENCY VALUES
C
      REAL*8      MODE_CONTRIB
C
      REAL*8      MODE_SUM
C
      INTEGER*2   NUM_LOC
C
      INTEGER*2   OUTPUT_UNIT1, OUTPUT_UNIT2, OUTPUT_UNIT3
C
      REAL*8      PI
C
      REAL*4      PLT_VAR
C
      REAL*8      SHAPE
C
```

```
C
      REAL*4        SPRAT,SPX,SPY,SPZ
C                        SINGLE PRECISION VARIABLES FOR
C                        PLOTTING
C
C
      REAL*8        WEIGHT
C
      INTEGER*4     X_INDEX(10000),Y_INDEX(10000),Z_INDEX(10000)
C
C
      real*8        xx(100),yy(100),zz(100)
      REAL*8        X_LOC, Y_LOC, Z_LOC
C                        POSITION IN CAVITY
C
      integer*2     restart
c                     (see main program CARCF for explanation)
C
C     INITIALIZE ARRAYS AND COUNTERS
C     DEFINE CONSTANTS
C
      PARAMETER (PI = 3.141592)
      output_unit1 = 55
C
      DO I = 1,2500
         X_INDEX(I) = 0
         Y_INDEX(I) = 0
         Z_INDEX(I) = 0
         MODE(I) = 0
      ENDDO
C
      write (6,*) numloc
      write (6,*) restart
      WRITE (6,*) NUM_LOC
      WRITE (6,*) XW0,YW0,AW,BW
      FREQ_COUNT = 0
C
       OPEN(UNIT=52,ERR=1000,STATUS='OLD',FILE="locations.in")
C
C
C
      a = x_length
```



C-2

```
      b = y_length
      X0 = XW0/A
      Y0 = YW0/B
      AWA = AW/A
      BWB = BW/B
C
C
      ERROR_CODE = .TRUE.
C
      CENTER_FREQ = DSQRT(LOWER_BOUND * UPPER_BOUND)
      BANDWIDTH = UPPER_BOUND - LOWER_BOUND
C
C     CALCULATE MAXIMUM MODE INDICIES FOR SPECIFIED BAND
C
      XMODEMAX = INT(UPPER_BOUND * 2.0 * X_LENGTH / C ) + 2
      YMODEMAX = INT(UPPER_BOUND * 2.0 * Y_LENGTH / C ) + 2
      ZMODEMAX = INT(UPPER_BOUND * 2.0 * Z_LENGTH / C ) + 2
C
C
      DO XMODE = 0, XMODEMAX
        DO YMODE = 0, YMODEMAX
          DO ZMODE = 0, ZMODEMAX
             FREQUENCY = .5 * C * DSQRT((XMODE/X_LENGTH)**2.0
     &                   + (YMODE/Y_LENGTH)**2.0
     &                   + (ZMODE/Z_LENGTH)**2.0)
             IF ((FREQUENCY .GE. LOWER_BOUND ) .AND.
     &               (FREQUENCY .LE. UPPER_BOUND)) THEN
                  FREQ_COUNT = FREQ_COUNT + 1
                  MODE(FREQ_COUNT) = FREQUENCY
                  X_INDEX(FREQ_COUNT) = XMODE
                  Y_INDEX(FREQ_COUNT) = YMODE
                  Z_INDEX(FREQ_COUNT) = ZMODE
             ELSE
C               THE MODE IS NOT WITHIN THE DESIRED BANDWIDTH

                  CONTINUE
             ENDIF
C
          ENDDO
        ENDDO
      ENDDO
c
```

```
      if (restart.eq.1) then
        do j=1,freq_count
          read(53,*) wt(j), flex_int(j), mode(j)
        enddo
      endif
c
C
C
      IF (FREQ_COUNT .GT. 0) THEN
c          OPEN(UNIT=OUTPUT_UNIT1,ERR=1010,STATUS='NEW',
c   &         FILE="SPOTS.DAT")
          WRITE(OUTPUT_UNIT1,100) X_LENGTH,Y_LENGTH,Z_LENGTH
          WRITE(OUTPUT_UNIT1,10)
          WRITE(OUTPUT_UNIT1,110) CENTER_FREQ,BANDWIDTH
          WRITE(OUTPUT_UNIT1,10)
          WRITE(OUTPUT_UNIT1,115) FREQ_COUNT
          WRITE(OUTPUT_UNIT1,10)
          WRITE(OUTPUT_UNIT1,10)
          WRITE(OUTPUT_UNIT1,120)
          WRITE(OUTPUT_UNIT1,121)
          WRITE(OUTPUT_UNIT1,10)
C
          WRITE(6,*) CENTER_FREQ,BANDWIDTH
          WRITE(6,*)FREQ_COUNT
C
c
c          OPEN(UNIT=OUTPUT_UNIT2,ERR=1030,STATUS='NEW',
c   &         FILE="CONTOUR.PLT")
c          OPEN(UNIT=OUTPUT_UNIT3,ERR=1020,STATUS='NEW',
c   &         FILE="SURFACE.PLT")
C
        DO LOCATION = 1,NUM_LOC
       if (count.eq.1) then
         read(52,*) xx(location),yy(location),zz(location)
       endif
        x_loc = xx(location)
        y_loc = yy(location)
        z_loc = zz(location)
            MODE_SUM = 0.0
            DO LOOP = 1, FREQ_COUNT
               ARGX =  FLOAT(X_INDEX(LOOP)) * PI * X_LOC/X_LENGTH
               ARGY = FLOAT(Y_INDEX(LOOP)) * PI * Y_LOC/Y_LENGTH
```

```
      ARGZ =  FLOAT(Z_INDEX(LOOP)) * PI * Z_LOC/Z_LENGTH
      SHAPE = DCOS(ARGX) * DCOS(ARGY) * DCOS(ARGZ)
c
c     need not do the rest of the calculations for every location
c     once is enough!
c
      if ((location.gt.1).or.(restart.eq.1)) go to 1210
c
       IF ( (X_INDEX(LOOP) .NE. 0 ) .AND.
   &        (Y_INDEX(LOOP) .NE. 0 ) .AND.
   &        (Z_INDEX(LOOP) .NE. 0 ) ) THEN
          WEIGHT = 16.0
       ELSEIF ( (X_INDEX(LOOP) .NE. 0 ) .AND.
   &         (Y_INDEX(LOOP) .NE. 0 ) .AND.
   &         (Z_INDEX(LOOP) .EQ. 0 ) ) THEN
           WEIGHT = 4.0
       ELSEIF ( (X_INDEX(LOOP) .NE. 0 ) .AND.
   &         (Y_INDEX(LOOP) .EQ. 0 ) .AND.
   &         (Z_INDEX(LOOP) .NE. 0 ) ) THEN
           WEIGHT = 8.0
       ELSEIF ( (X_INDEX(LOOP) .EQ. 0 ) .AND.
   &         (Y_INDEX(LOOP) .NE. 0 ) .AND.
   &         (Z_INDEX(LOOP) .NE. 0 ) ) THEN
           WEIGHT = 8.0
       ELSEIF ( (X_INDEX(LOOP) .NE. 0 ) .AND.
   &         (Y_INDEX(LOOP) .EQ. 0 ) .AND.
   &         (Z_INDEX(LOOP) .EQ. 0 ) ) THEN
           WEIGHT = 2.0
       ELSEIF ( (X_INDEX(LOOP) .EQ. 0 ) .AND.
   &         (Y_INDEX(LOOP) .NE. 0 ) .AND.
   &         (Z_INDEX(LOOP) .EQ. 0 ) ) THEN
           WEIGHT = 2.0
       ELSEIF ( (X_INDEX(LOOP) .EQ. 0 ) .AND.
   &         (Y_INDEX(LOOP) .EQ. 0 ) .AND.
   &         (Z_INDEX(LOOP) .NE. 0 ) ) THEN
           WEIGHT = 4.0
       ELSEIF ( (X_INDEX(LOOP) .EQ. 0 ) .AND.
   &         (Y_INDEX(LOOP) .EQ. 0 ) .AND.
   &         (Z_INDEX(LOOP) .EQ. 0 ) ) THEN
           WEIGHT = 1.0
      ELSE
          WRITE(6,800)
```

```
              ENDIF
c
c
C   for portion of wall flexible the following has been added:
      xmode = x_index(loop)
      ymode = y_index(loop)
      L = XMODE * 2 * PI
      M = YMODE * 2 * PI
C
      F1 = AW * BW
c
        if (xmode.eq.0) then
          f2 = AW * BW
          f3 = 0.
          go to 60
        endif
c
      F2 = BW * (A/L) * COS(L*X0) * SIN(L*AWA)
      F3 = BW * (A/L) * SIN(L*X0) * (COS(L*AWA) -1)
c
 60     if (ymode.eq.0) then
          f4 = AW * BW
          f5 = 0.
          go to 70
        endif
c
      F4 = AW * (B/M) * COS(M*Y0) * SIN(M*BWB)
      F5 = AW * (B/M) * SIN(M*Y0) * (COS(M*BWB) - 1)
C
 70     if ((xmode.eq.0).and.(ymode.eq.0)) then
          f6 = aw * bw
          f7 = 0.
          f8 = 0.
          f9 = 0.
          go to 1005
        endif
c
        if (xmode.eq.0) then
          f6 = f4
          f7 = f5
          f8 = 0.
          f9 = 0.
```

```
          go to 1005
        endif
c
        if (ymode.eq.0) then
          f6 = f2
          f7 = 0.
          f8 = f3
          f9 = 0.
          go to 1005
        endif
c
c
      F6 = (A/L) * (B/M) * COS(L*X0) * COS(M*Y0) * SIN(L*AWA) *
     *     SIN(M*BWB)
      F7 = (A/L) * (B/M) * COS(L*X0) * SIN(M*Y0) * SIN(L*AWA) *
     *     (COS(M*BWB) - 1)
      F8 = (A/L) * (B/M) * COS(M*Y0) * SIN(L*X0) * SIN(M*BWB) *
     *     (COS(L*AWA) - 1)
      F9 = (A/L) * (B/M) * SIN(L*X0) * SIN(M*Y0) * (COS(L*AWA)
     *     - 1) * (COS(M*BWB) - 1)
 1005 FINTEGRAL = F1 + F2 + F3 + F4 + F5 + F6 + F7
     *                + F8 + F9
C
c  Now we need to divide by whole wall moving integral -
c    since original program was for whole wall moving.
c
      fintegral = fintegral/(a*b)
c
c      special consideration given to the case(s) where xmode,
c              ymode are zero!
c
      if ((xmode.eq.0).and.(ymode.eq.0)) then
              fintegral = fintegral*.25
              go to 1205
      endif
c
      if ((xmode.eq.0).or.(ymode.eq.0)) then
              fintegral = fintegral*.50
              go to 1205
      endif
c
 1205 continue
```

```
c
c
c  At this point fintegral is now the ratio of
c    Flexible integral for the partial wall to
c    Flexible integral for the whole wall moving,
c    where a factor of 1/4 cosine(z_index*pi*z/z_length) has
c    been factored out of both the top and bottom.
C
C
 1210  if ((restart.ne.1).and.(location.eq.1)) then
        wt(loop) = weight
        flex_int(loop) = fintegral
c       write(54,*) wt(loop),flex_int(loop),mode(loop)
      endif
c
        MODE_CONTRIB = SHAPE ** 2.0 * wt(loop)*
    &              flex_int(loop)*(mode(loop)**(-3.0))
            MODE_SUM = MODE_SUM + MODE_CONTRIB
          ENDDO
C
C
          CMA_TO_AMA_RATIO =0.5 *(CENTER_FREQ**3.0) * MODE_SUM /

    &               (FREQ_COUNT*((aw*bw)/(x_length*y_length)))
          WRITE(OUTPUT_UNIT1,200)
X_LOC,Y_LOC,Z_LOC,CMA_TO_AMA_RATIO
          WRITE(6,*) X_LOC,Y_LOC,Z_LOC,CMA_TO_AMA_RATIO
C
c          SPX = X_LOC
c          SPY = Y_LOC
c          SPZ = Z_LOC
c          SPRAT = CMA_TO_AMA_RATIO
c          PLT_VAR = SQRT(SPZ**2.0 + SPY**2.0)
c          WRITE(OUTPUT_UNIT3,*) PLT_VAR,SPRAT,SPX
C          WRITE(OUTPUT_UNIT2,*) SPRAT
C
C
      ENDDO
C
      ELSE
        WRITE(OUTPUT_UNIT1,900)
      ENDIF
```

```
C
c    CLOSE(OUTPUT_UNIT1)
c    CLOSE(OUTPUT_UNIT2)
c    CLOSE(OUTPUT_UNIT3)
C
     WRITE(6,2000)
C
     GO TO 1100
C
   10 FORMAT(2X,' ')
  100 FORMAT(2X,'CAVITY IS ',F8.3,' FT BY ',F8.3,' FT BY ',F8.3,' FT')
  110 FORMAT(2X,'CENTER FREQUENCY: ',F9.2,' HZ,  BANDWIDTH: ',F9.2,

    &          ' HZ')
  115 FORMAT(2X,'NUMBER OF MODES IN THIS BAND: ',I8)
  120 FORMAT(4X,'X LOCATION',3X,'Y LOCATION',3X,'Z LOCATION',
    &      7X,'CMA TO AMA RATIO')
  121 FORMAT(4X,'----------',3X,'----------',3X,'----------',
    &      7X,'----------------')
  200 FORMAT(3(5X,F8.4),10X,F15.6)
  300 FORMAT(2X,F10.6)
  800 FORMAT(2X,'PROBLEM WITH WEIGHT')
  900 FORMAT(2X,'NO MODES IN THIS BAND')
 1000 WRITE(6,1001)
 1001 FORMAT(2X,'ERROR ENCOUNTERED ACCESSING CAVITY.IN')
     GO TO 1100
 1010 WRITE(6,1011)
 1011 FORMAT(2X,'ERROR ENCOUNTERED ACCESSING SPOTS.DAT')
     GO TO 1100
 1020 WRITE(6,1021)
 1021 FORMAT(2X,'ERROR ENCOUNTERED ACCESSING CONTOUR.DAT')
     GO TO 1100
 1030 WRITE(6,1031)
 1031 FORMAT(2X,'ERROR ENCOUNTERED ACCESSING CONTOUR.PLT')
 1100 CONTINUE
C
 2000 FORMAT(2X,'OUTPUT IN SPOTS.DAT,CONTOUR.PLT AND
SURFACE.PLT')
C
     return
     END
```

```
      SUBROUTINE VARBW(INDEX,CENTER_FREQ,UPPER_FREQ,LOWER_FREQ,
     &          BANDWIDTH)
C
C   ROUTINE TO FIND UPPER AND LOWER FREQUENCIES AND BANDWIDTH

C   FOR SPECIFIED CENTER FREQUENCY
C
      REAL*8 BANDWIDTH
      REAL*8 CENTER_FREQ
      REAL*8 UPPER_FREQ
      REAL*8 LOWER_FREQ
      INTEGER*4 INDEX
C
C
        BANDWIDTH  = 100. + FLOAT(INDEX) * 100.0
        UPPER_FREQ = .5 * (BANDWIDTH + DSQRT( (BANDWIDTH**2.0)
     &             + 4.0 * CENTER_FREQ ** 2.0))
        LOWER_FREQ = UPPER_FREQ - BANDWIDTH
C
C
      RETURN
      END
```

INTEGRATION USED TO CALCULATE THE NON-DIMENSIONAL PRESSURE RATIO FOR THE 1-DIMENSIONAL CASE

```
  integer numratio
   real fbfcratio, kcx(101), press(4,101)
   write(*,999)
999    format(2x,'enter endkcx')
   read(*,*) endkcx
   deltakcx=endkcx/100
   open(52, file="data")
   read(52,*) numratio
    do i=1,numratio
    read(52,*) fbfcratio
     fubyfc=.5*(fbfcratio+sqrt((fbfcratio**2)+4))
     flbyfc=.5*(-fbfcratio+sqrt((fbfcratio**2)+4))
     b=1/(fbfcratio*sqrt((fbfcratio**2)+4))
     kcx(1)=0.
c
     do j=1,100
      thetafl=(kcx(j)*2*flbyfc)
      thetafu=(kcx(j)*2*fubyfc)
      c = (cos(thetafl))/((flbyfc)**2)
      d = (cos(thetafu))/((fubyfc)**2)
      e = (2*kcx(j)*sin(thetafu))/(fubyfc)
      f = (2*kcx(j)*sin(thetafl))/(flbyfc)
      g = (4*kcx(j)*kcx(j)*ci(thetafl))
      h = (4*kcx(j)*kcx(j)*ci(thetafu))
       if(kcx(j).eq.0) write(*,*) c,d,e,f,g,h,b
c
      press(i,j) = 1 + b*(c-d+e-f+g-h)
      if (kcx(j).eq.0) write(*,*) press(i,j)
c
     kcx(j+1)=kcx(j)+deltakcx
     end do
c
   end do
c
   open (unit=53,file="output")
   write(53,111)
   do i=1,100
      If(i.eq.1) write(*,*) press(i,1)
    write(53,110) kcx(i),(press(j,i),j=1,numratio)
```

```
        If(i.eq.1) write(*,*) press(i,1)
      end do
 110   format (3x,1pe13.6,3x,4((1pe13.6),3x))
 111    format (8x,'kcx',11x,'ratio1',10x,'ratio2',10x,'ratio3',10x,'ratio4')

      end
c
c
      Function ci(x)
      Real x, numerator, denominator, f, g
c
      if (x.ge.1) then
       a1 = 38.027264
       a2 = 265.187033
       a3 = 335.677320
       a4 = 38.102495
       b1 = 40.021433
       b2 = 322.624911
       b3 = 570.236280
       b4 = 157.105423
c
       numerator = x**8 + a1*(x**6) + a2*(x**4) + a3*(x**2) + a4
       denominator = x**8 + b1*(x**6) + b2*(x**4) + b3*(x**2) + b4
c
       f = (numerator)/(denominator*x)
c
       a1 = 42.242855
       a2 = 302.757865
       a3 = 352.018498
       a4 = 21.821899
       b1 = 48.196927
       b2 = 482.485984
       b3 = 1114.978885
       b4 = 449.690326
c
      numerator = x**8 + a1*(x**6) + a2*(x**4) + a3*(x**2) + a4
      denominator = x**8 + b1*(x**6) + b2*(x**4) +b3*(x**2) + b4
c
      g = (numerator)/(denominator*x*x)
c
      ci = f*sin(x) - g*cos(x)
c
```

```
      elseif (x.gt.0) then
c
        sum = -(x**2)/4 + (x**4)/96. - (x**6)/4320. + (x**8)/322560.
     &        - (x**10)/36288000.
        ci = .577215665 + log(x) + sum
c
      else
c
        ci = 0.
      endif
      return
      end
c
```